DEVELOPMENT OF A RAPID DETECTION SYSTEM FOR THE FOOT AND MOUTH DISEASE VIRUS

THESIS

submitted for the degree of

DOCTOR OF PHILOSOPHY

in

Organic / Biological Chemistry

at

KINGSTON UNIVERSITY

by

Samerah Malik

School of Pharmacy and Chemistry
Kingston University
Penrhyn Road,
KT1 2EE

2019

DECLARATION

This thesis entitled **"**Development of a rapid detection system for the foot and mouth disease virus**"** is based upon work conducted by the author in the School of Pharmacy and Chemistry at Kingston University London between October 2014 and December 2017. All of the work described herein is original unless otherwise acknowledged in the text or by references. None of the work has been submitted for another degree in this or any other universities.

_____

Samerah Malik

ACKNOWLEDGEMENTS

First and foremost, I would like to thank my now director of studies Dr. Adam Le Gresley for his continuous support, motivation and valuable feedback throughout this project. I am also grateful to being a part of his bright, young research group, a special thanks to group members Luke Bywaters and Alex Fudger for always being there to bounce ideas off and to solve problems with.

I'd like to thank the following academics and technical staff - Prof. Mark Fielder for his invaluable expertise and advice in the area of pathogens and also like to thank Dr. Ali Ryan for training me to run all the biochemical testing completed in this project under his supervision in his laboratories. I am also very grateful to the NMR support and research guidance provided by Dr. Jean-Marie Peron throughout my research project journey.

I'd also like to acknowledge the great friendships I've made over the years with past and present members of the research offices EM 2008-10. In particular a special thanks to Syedah Shah, Paddy Melia, Ummara Butt, Zara Kassam, Negeen Kargar, Sarah Fawaz, Cameron Robertson, Tomris Coban, for listening to my synthetic woes and organising or joining me on much needed lunches / coffee breaks.

Finally, I wish to thank my loving family 'the Maliks' for supporting my research interests, especially my husband Amar, for being my rock throughout this process, that has been filled with ups and downs and always supporting my professional and personal developments. I'd also like to mention the new additions to my family; my baby girls: Sehar and Zahra and a special thanks to my sisters Farha and Flona for their unconditional love, support and kindness throughout my whole PhD journey.

ABSTRACT

The total syntheses of BocAL(Z)QAMC (i) and BocAL(Boc)Q(Trt)AMC (ii) have been accomplished. Synthesis of compound (i) was achieved by initially coupling the amino acid adjacent to the fluorophore, AMC, using selenocarboxylate / azide amidation coupling conditions, followed by the dipeptide coupling on to the third amino acid in the sequence Q using the coupling reagent HATU, under optimised conditions.[1] Synthesis of compound (ii) was achieved using automated peptide synthesis of the protected tripeptide sequence and the final coupling to the fluorophore; AMC was achieved using HATU, under optimised conditions.

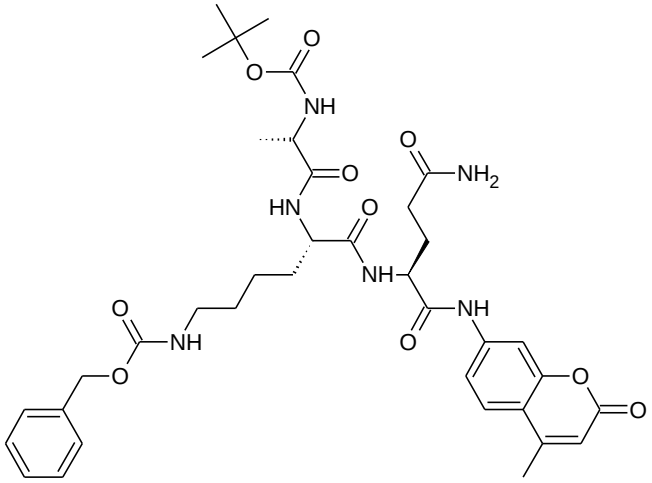

(i)

Figure i – Structure of BocAL(Z)QAMC

[1]X. Wu and L. Hu. (2007). Efficient Amidation from Carboxylic Acids and Azides via Selenocarboxylates: Application to the Coupling of Amino Acids and Peptides with Azides. *Journal of Organic Chemistry*.72, p765-774.

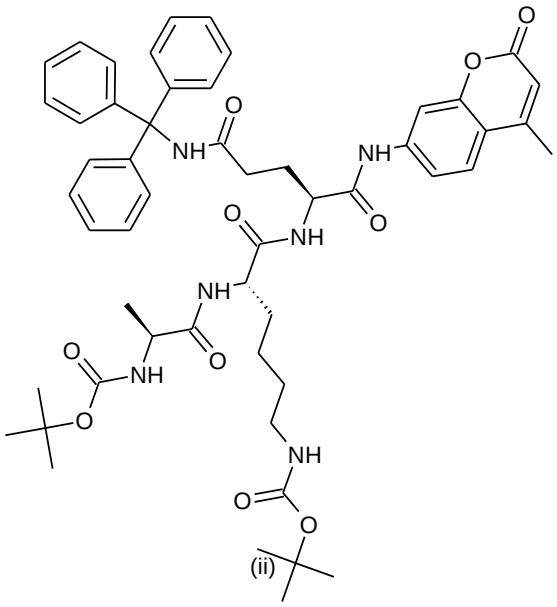

Figure ii - Structure of BocAL(Boc)Q(Trt)AMC

The integrity of compound (i) and its fragment Q-AMC was found to be compromised during purification steps and storage, by spontaneous decomposition resulting in the premature, non-enzyme assisted cleavage of the fluorophore, AMC. This decomposition was minimised by the addition of the bulky trityl protecting group, therefore compound (ii) was used for biochemical testing.

Successful deprotection of compound (ii) was accomplished prior to the enzymatic assay, with the target enzyme $3C^{pro}$. Importantly, the proof of concept has been gained through evidence of enzyme assisted breakdown of the detection probe by fluorescence measurements. Also the deprotected version of compound (ii) was found to show selectivity towards the target enzyme FMDV $3C^{pro}$ over other enzymes potentially also present in clinical samples. These enzymes include chymotrypsin, thrombin and trypsin in FMDV clinical samples and the carefully selected TEV protease due to its reported cleavage after amino acid Q in peptide sequences.[2] However, problems with the stability of the detection probe after deprotection were still apparent, resulting in a very short shelf-life of the probe. Further work is to be done in the stability of the probe but this project has proved $3C^{pro}$ recognises and processes shorter peptide fragments, previously reported not to be the case.

[2]J. R. Birtley, S. R. Knox, A. M. Jaulent, P. Brick, R. J. Leatherbarrow, and S. Curry. (2004). Crystal Structure of Foot-and-Mouth Disease Virus 3C Protease New insights into catalytic mechanism and cleavage specificity.*The Journal of Biological Chemistry*.280 (12), p11520-11527.

LIST OF ABBREVIATION

$3C^{pro}$	3C protease
$3D^{pol}$	3D polymerase
A	Ala
ACN	Acetonitrile
ACC	7-amino-4-carbamoylmethyl coumarin
AFC	7-amino-4-trifluoromethyl coumarin
AMC	7-amino-4-methyl coumarin
Boc	*tert*-butoxycarbonyl protecting group
CFT	Complement fixation test
COMU	1-Cyano-2-ethoxy-2-oxoethylidenaminooxy)dimethylamino-morpholino-carbenium hexafluorophosphate
DABCYL	4-((4-(dimethylamino)phenyl)azo)benzoic Acid
DCM	Dichloromethane
DIEA	*N*,*N*-Diisopropylethylamine
DIVA	Differentiate between infected and vaccinated animals
DNA	Deoxyribonucleic acid
DSF	Differential scanning fluorimetry
DTT	Dithiothreitol
E	Glutamic acid
EDANS	5-((2-Aminoethyl)amino)naphthalene-1-sulfonic acid
EDC	1-Ethyl-3-(3-dimethylaminopropyl)carbodiimide
EDTA	Ethylenediaminetetraacetic acid

EEDQ	Ethyl 1,2-dihydro-2-ethoxyquinoline-1-carboxylate
ELISA	Enzyme linked immunosorbent assay
Eq.	Equivalents
ES	Electrospray
EU	European union
F*	Fluorophore
FMD	Foot and mouth disease
FMDV	Foot and mouth disease virus
FT-IR	Fourier-transform infrared spectroscopy
GC/MS	Gas chromatography mass spectrometry
HATU	1-[Bis(dimethylamino)methylene]-1*H*-1,2,3-triazolo[4,5-*b*]pyridinium 3-oxid hexafluorophosphate,
HPLC	High – performance liquid chromatography
hr / hrs	hour / hours
HRMS	High resolution mass spectrometry
IFN	Interferon
Ig	Immunoglobulin
IMS	Industrial methylated spirits
Kb	Kilobase
K_M	Michealis constant
L	Lysine
LAMP	Loop-mediated isothermal application
LFD	Lateral flow device
L^{pro}	Leader protease

MM	Michealis Menten
MS	Mass spectrometry
MW	Molecular weight
NCR	Non-coding region
NMR	Nuclear Magnetic Resonance
NSP	Non structural protein
ORF	Open reading frame
PBS	Phosphate-buffered saline
PCR	Polymerase chain reaction
Q	Glutamine
R-110	Rhodamine 110
RFU	Relative fluorescence units
RNA	Ribonucleic acid
RT-PCR	Reverse-transcription polymerase chain reaction
SAT	South African Territories
SDS	Sodium dodecyl sulphate
SDS-PAGE	Sodium dodecyl sulfate–polyacrylamide gel electrophoresis
SP	Structural protein
SPPS	Solid phase peptide synthesis
TCA	Trichloroacetic acid
TEMED	Tetramethylethylenediamine
TEV	Tobacco etch virus
TFA	Trifluoroacetic acid

THF	Tetrahydrofuran
TLC	Thin Layer Chromatography
T_M	Thermal melt
TOF	Time of flight
Trt	Trityl protecting group
UK	United Kingdom
UV	Ultraviolet
v/v	Volume for volume
Vmax	Maximum velocity
VN	Virus neutralisation
VP	Viral protein
VPg	Viral protein linked to the genome
w/v	Weight for volume

TABLE OF CONTENT

LIST OF TABLES

LIST OF FIGURES

LIST OF SCHEMES

CHAPTER 1: INTRODUCTION

1. INTRODUCTION

This introductory chapter covers important points highlighting the research over the last few decades, in the area of foot and mouth disease (FMD) and the reasons why FMD is a major economic problem and the imperative need of the rapid detection of this specific viral pathogen. Based on this choosing a target enzyme is considered followed by selecting a suitable substrate sequence and the fluorophore needed to design and synthesise a suitable fluorogenic substrate.[1]

1.1. TARGET DISEASE

1.1.1. Foot and mouth disease

FMD is highly infectious and contagious; it is responsible for global economic devastation and is classed as a trans-boundary disease. The causative agent is a pathogen made fast-evolving *via* high mutation rates, specifically the foot and mouth disease virus (FMDV).[2]

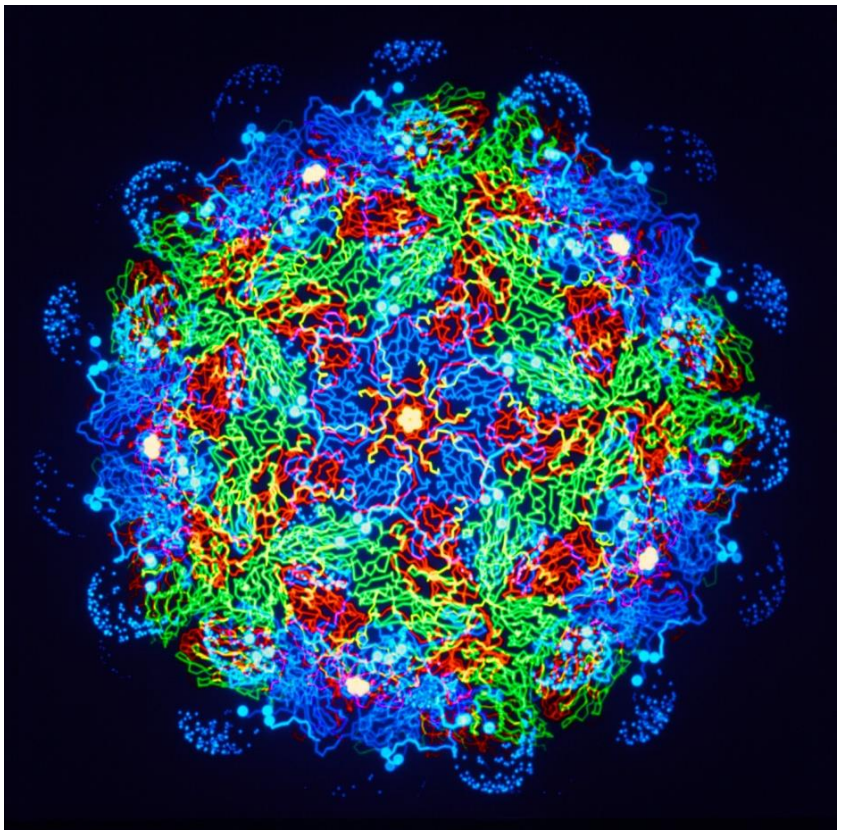

Figure 1 – A visualisation of the 3D X-ray crystallographic structure of FMDV at 2.9Å resolution.[3]

FMDV has a single stranded, positive sense, RNA genome (8,400 nucleotides in length). It is classed as an *Apthovirus* and belongs to the *Picornaviridae* family. The genome is found within viral particles in protein shells made up of 60 copies of 4 different viral proteins (VPs) VP1, VP2, VP3, VP4. These four are a product of proteolytic processing of the polypeptide encoded by an open reading frame (ORF) of 7,000 nucleotides within the viral RNA. The polypeptide also includes two separate proteases: Leader (L^{pro}) and 3C protease ($3C^{pro}$).

Replication of the virus occurs in the cytoplasm and is prone to errors giving rise to antigenic variance. FMDV exists in seven different serotypes, these are: O, A, C, South African Territories (SAT) 1, 2, 3 and Asia 1. Immunity conferred from an infection or vaccination does

not confer immunity for subsequent infections of another serotype or indeed the same serotype after a long period of time as the virus consensus sequence changes at about 0.5 – 1% of its genome per year.[4] This equates to 1-2 nucleotide changes per week. Therefore in an outbreak there is a possibility the spread of virus between farms may be different. However, in terms of classifying subtypes, a nucleotide difference of 15% in VP1 region is needed to define a new sub-type.[5]

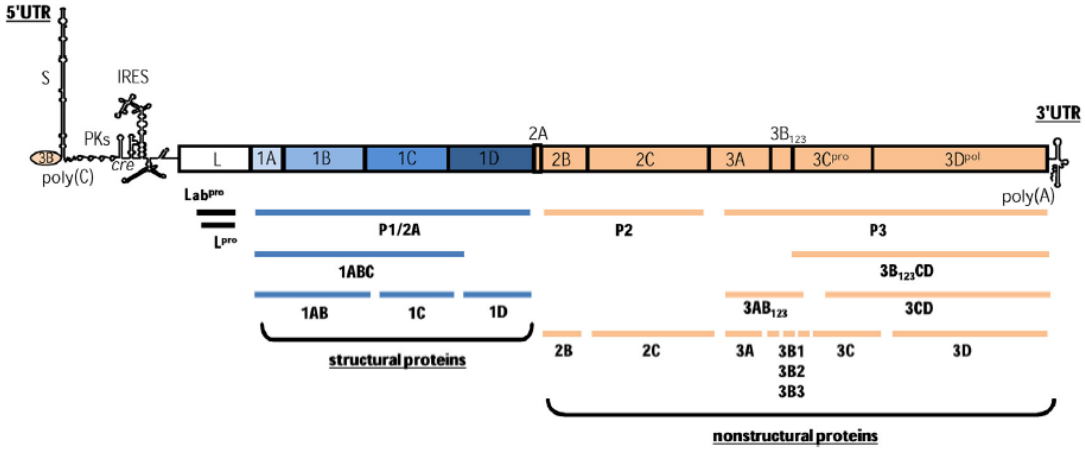

Figure 2 - The FMDV genome, ORF is depicted in the boxed area. Labelled are the structural and non structural proteins.[6]

1.1.2. Clinical Symptoms

The appearance and severity of symptoms can vary between different animal species. FMD affects in cloven-hoofed animals, including cattle, sheep, goats and pigs and a further 70 wildlife species, however, some species show no symptoms during infection.[7] Other factors influencing symptoms include the age of the animal and the strain of the infective pathogen, the host's immunity and the breed of the animal. The zoonotic risk is reported to be negligible.[8]

Typical clinical symptoms seen in cattle are blisters, vesicular lesions in the mouth area and feet hence the name foot and mouth disease. Lameness after blisters burst, fever and reduction in lactation resulting in a major loss in milk productivity. Pigs and sheep develop less obvious blistering on other parts of their bodies, but sudden lameness is the key clinical symptom to raise alarm and in the UK this would involve notifying the Animal and Plant Health Agency vets and failure to do so immediately, is considered a criminal offence.[9] The clinical symptoms seen in pigs are indistinguishable from other vesicular diseases (swine vesicular disease, vesicular exanthema and vesicular stomatitis) therefore people working with pigs presenting symptoms are instructed to treat as FMD until a lab-based diagnosis is sought. As not all FMD susceptible animals present such obvious clinical symptoms, this further complicates the challenge of controlling an outbreak in a population.[10] Disease signs appear within 2/3 days after exposure and can last over a week without further complications.[11]

The case - fatality remains low overall, adult animals have a low mortality rate of <5%, younger animalshave higher mortality rate of >20% from complications of the disease such as myocarditis. With high morbidity there is a significant effect on the economy especially in FMD endemic areas that trade under strict guidelines of terrestrial code of the World Organisation of Animal Health with a further negative impact on the wider economy and a halt in the development of these nations.[12,13]

1.1.3. Current diagnostic techniques employed

FMDV is an extremely contagious viral pathogen and an outbreak caused by this virus depending on its scale and location can cause economic devastation, food insecurity, poverty and restrict food trade. Therefore, strategies to control, manage and possibly prevent the spread of infection *via* early detection are a requirement. The world

organisation of animal health have published a manual of diagnostic tests and vaccines that defines FMDV diagnosis tests and states diagnosis can be achieved *via* virus isolation, detecting nucleic acid, viral antigen, virus specific or viral non structural protein (NSP) antibodies irrespective of vaccination status of the animal. A number of lab-based diagnostic techniques are listed that can be used to detect viral pathogens and give a clinical diagnosis; over the years a range of these molecular biological tests have been modified to specifically detect FMDV; complement fixation test (CFT), virus neutralisation (VN), enzyme linked immunosorbent assay (ELISA) and polymerase chain reaction (PCR).[14]

Over the last decade, there has been a rise in research publications reporting efforts directed in the area of developing, evaluating and validating suitable portable molecular diagnostic platforms (pen-side diagnostics) to address the critical time gap of suspicion of infection and gaining a rapid, accurate clinical diagnosis. The delay in diagnosis is caused by the need of the infected sample being transported to a high containment laboratory with certification to work with FMDVand analysed by skilled personnel using specialist equipment. Other limitations for consideration are; the need of the sample originating from a specific source to comply with the diagnostic technique – epithelial, blood and sputum, and the expenses involved in portable systems and the stability of reagents.[15]

1.1.3.1. Laboratory based biological FMDV diagnostic techniques and how they work.

Complement fixation test (CFT)

The principle of the CFT is based on an antibody – antigen reaction, these are of IgG or IgM classes. The complement attaches to a fixed antibody-antigen complex, a positive result is confirmed through absence of hemolysis. However, if serum without the antibody is being tested, no complement fixation reaction occurs as no complex is formed between the antigen and the antibody, the unused complement causes hemolysis which gives indication of a negative result. CFT is based on a highly specific interaction and therefore used as a diagnostic tool.

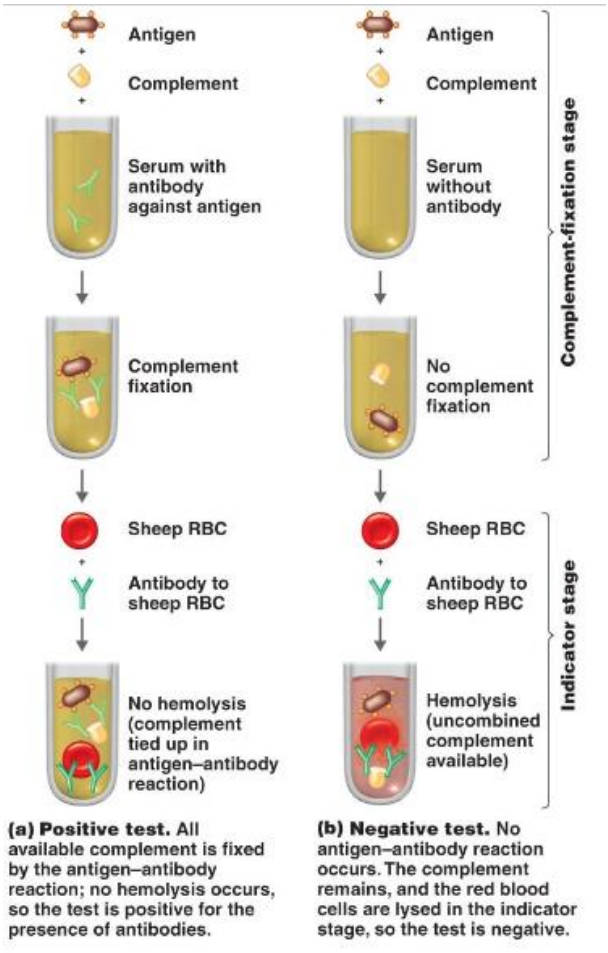

Figure 3 - Complement Fixation Test[16]

Virus neutralisation (VN)

The principle of VN is also based on an antibody and antigen interaction, this technique neutralises the biological effects of the virus through antibodies making it inactive if present in the sample being tested, leaving the virus susceptible cell uninfected, the cells are analysed after 2 – 3 days, investigation is done using a microscope or looking for evidence of viral cytopathic effect.

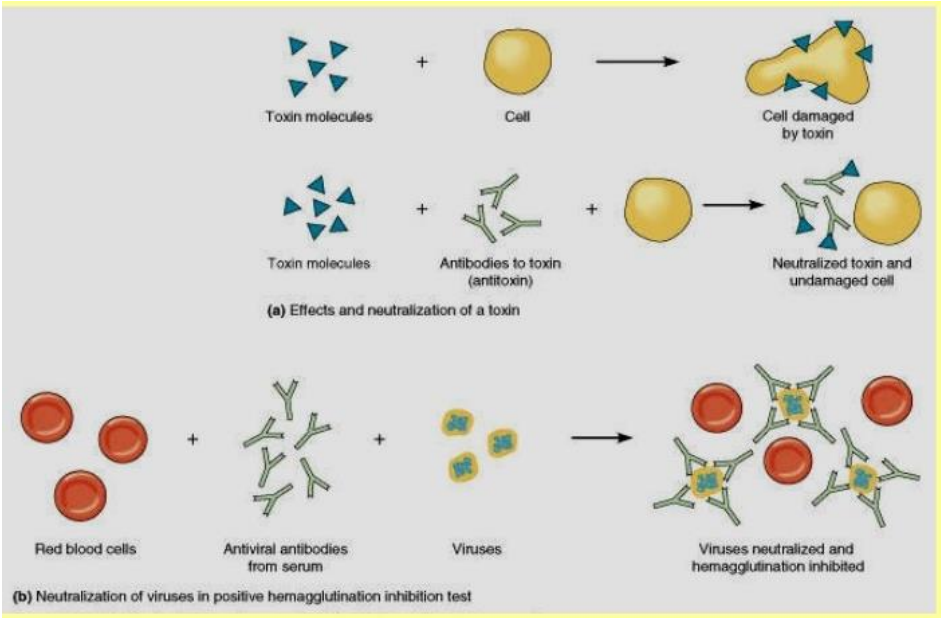

Figure 4 – The Virus Neutralisation Test[17]

Polymerase chain reaction (PCR)

PCR is a DNA amplification process, through steps of heating and cooling to make copies of specific regions of DNA. First the sample is heated to 94°C, causing denaturation into single strands. At a cooler temperature of 68°C primers are annealed onto complementary matches on the target DNA sequence. The Taq polymerase present binds to the primed sequences and extends the second strand, completing the first cycle. In subsequent cycles, denaturing, priming, annealing and extending are all repeated to gain more DNA copies. After 30 cycles, a billion copies of DNA can be produced from the

single starting molecule. PCR technology is always undergoing improvements and now RNA can also be used efficiently. The RNA is first transcribed to DNA using reverse transcriptase, allowing studies to be carried out on RNA viruses and cellular RNA, even in small quantities.

Enzyme linked immunosorbent assay (ELISA)

There are a number of ELISA procedures adapted to detect and quantify antibody or antigens in a sample; Direct ELISA, Indirect ELISA and Sandwich ELISA.

The setup of direct ELISA involves antigen immobilisation onto the wells of a micro titre plate. The antigen is detected by an enzyme-linked antibody that binds to it and is retained. Detection of the retained enzyme is indicative of the presence of the antigen and is observed *via* a colour change, fluorescence measurements or chemiluminscence.

Indirect ELISA, where an antigen is adsorbed and immobilised onto the wells of a micro titre plate, the excess is then rinsed off. The serum suspected of containing antibodies is then added, the enzyme linked antibody is capable of attaching itself to the constant region of the antibody, once attached and in presence of the colourless substrate added, a colour change is observed.

Sandwich ELISA, is used to detect antigen; the procedure involves immobilisation of the antibody in the micro titre plate wells. The test sample is then added with the suspected antigen, time allowed for incubation to enable antibody-antigen reaction to occur. The excess is rinsed out and a second enzyme-conjugate antibody is added, this secondary antibody is expected to bind onto a different epitope of the

antigen and any excess unbound antibody is rinsed off. The colourless substrate solution is added and a colour change is indicative of antigen presence.

CFT was the chosen method for diagnosis in the seventies and is still used in many developing countries where there is a shortage of expensive modern, equipment. This technique requires a large viral concentration to give a positive result. However, result interpretation was also reported to be affected by pro- and anti-complementary activities in the test sample, making the test less reliable due to this reduced specificity. The VN technique in combination with cell culturing techniques was found to be 100 times more specific than CFT, however, cell culture is a time consuming and expensive step to be carried out by skilled staff within suitable bio-containment facilities. The results from VN/CFT were found to be prone to variability and therefore not as widely used. In the late seventies, Crowther *et al*. first reported indirect ELISA as a technique used to screen for antibodies against FMDV. ELISA was modified over the years and applied for viral detection, typing and serotype definition. ELISA was found to be superior to CFT and VN as it gave reliable, accurate, reproducible results in 3-4 hours of reaching a laboratory. However, using ELISA to elucidate the serotype of the virus requires a further four days; this delay is the reason for the further development of PCR as a diagnostic tool for FMDV. Reverse transcription PCR (RT-PCR) has the added advantage of requiring the virus to be rendered inactive by RNA extraction. Arguably, the current gold standard is said to be PCR as the diagnostic tool of infectious agents, the advantages of this technique of greater sensitivity, improved specificity and reduced contamination risk, however, DNA/RNA amplification delays gaining a final result and is costly, therefore a need for cost effective, rapid, accurate diagnostic tests is still apparent.[18]

1.1.3.2. Pen-side diagnostics

To date three main pen-side diagnostic technologies are reported:

i) nucleic acid detection using RT-PCR
ii) antigen detection using different formatted lateral flow devices (LFD)
iii) LFD detection after isothermal amplification using primers of certain regions of the FMDV genome.

PCR techniques are considered first choice by many laboratories,[19]as it can detect viral genome or fragments of the virus in samples that aren't able to grow in tissue culture, whereas ELISA and virus neutralisation techniques require a sample to contain intact antigens or the live virus to test on. PCR is therefore considered a powerful and sensitive technique and potentially a useful detection system to have on the field, hence the development of a portable PCR system for FMDV detectionwas an exciting concept.[20,21,22] However, field testing made apparent the limitations of the system as it requires a precision thermo-cycling step that is carried out using expensive, fragile instrumentation that required a vigorous decontamination protocol of the instrument to be followed after each site use.[23] In order to reduce costs associated with the necessary cycling at different reaction temperatures for the portable PCR system, isothermal amplification strategies were explored in viral diagnostics.[24] In 2000 Notomi*et al*. developed a molecular technique loop mediated isothermal amplification (LAMP) widely used to detect viruses when in combination with reverse transcriptase. Notomi *et al.* proved DNA/ RNA can be amplified rapidly by heating under a constant temperature with a set of four specific primers, also reported is that loop primers can help the amplification process.[25]

Recently, other simpler, cheaper, rapid pen-side diagnostics have been developed in the form of LFDs. Although the lateral flow immunoassay diagnostic platform was first reported in the 1980s,

FMD LFDs are a more recent addition to a diverse range developed and marketed over almost 40 years, a few examples are in table 1.[26]

Application area	**Analyte**	**Label**	**Sample type**	**Detection limit**	**Time to detection**
Clinical analysis	Alpha fetoproteins	Quantum dots	Serum	1 ng /mL	10 min
Pathogens	*Escherichia coli* mRNA	Liposome	Drinking water	5 fmol	15-20min
Metal ions	Mercury	Gold nano-particles	Water	6 nM	5 min
Pharmac-euticals	Sulfonamides	Gold nano-particles	Eggs and Chicken muscles	10 ng/mL	15 min

Table 1- adapted from a literature review of lateral flow assays, showing a few examples of LFDs developed over the years.[27]

There are four main components in an LFD:

i) Sample application pad – where sample is added.
ii) Conjugate pad – holding labelled tags combined with recognition elements.
iii) Nitrocellulose membrane – containing control and test line, this membrane has high affinity for biomolecules.
iv) Adsorbent pad – marks end of the strip, soaks up sample to prevent back or over flow.

FMD LFDs that have been reported over the last decade:

In 2009, Ferris *et al*. reported the development of LFD using a monoclonal antibody (mAb) mAb1F10 as a tracer and conjugated to gold nanoparticles, performance of the LFD was tested against over 1300 samples as vesicular epithelial suspensions. The group also further validated the device by comparing to reference method of

antigen ELISA (Ag-ELISA), with diagnostic sensitivity and specificity for LFD 84% and 99% respectively and for ELISA 85% and 99.9%. The time of detection was between 1 – 10 minutes after sample addition. No false positives were seen with clinically indistinguishable SVD and VS. However, the main limitation of the 1F10 device is it has weaker reactions with serotype SAT-2 resulting in false negatives.[28] In 2010, the group reported the development of a new SAT-2 specific LFD, using Mab2H6, evaluated against over 300 samples as vesicular epithelial suspensions.[29] The validation studies showed the 2H6 device had higher diagnostic sensitivity at 88% than the reference Ag-ELISA at 79% and similarly impressive diagnostic specificity at 99% as compared to 100% by ELISA. The group recommend using the two devices in tandem to screen samples of all known serotypes.

In 2009, Oem *et al*. reported a similar device using mAb 7017, however, LFD didn't react with all serotypes, only four of the seven serotypes were detected, types O, A, Asia 1 and C. The LFD was tested against 704 epithelial samples. The diagnostic sensitivity for the LFD was at 87.3% compared to Ag-ELISA at 87.7%. The diagnostic specificity for the LFD was at 98.8% compared to Ag-ELISA at 100%. The group reported the usefulness of this assay in regions prevalent in the detectable serotypes.[30]

In 2010, Cai *et al*. reported an immuochromatographic strip to detect FMDV performance evaluated on 296 serum samples and validation studies against ELISA, the group reported the strip showed high sensitivity and specificity.[31]

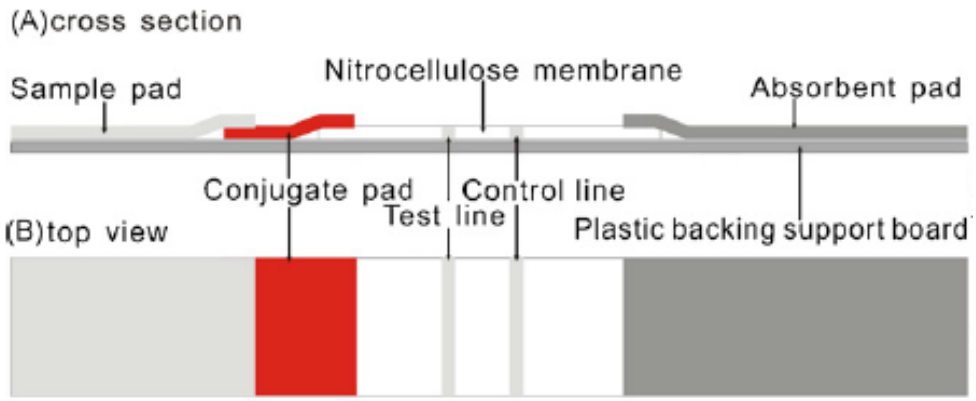

Figure 5- Schematic diagram of an immunochromatographic test strip for the detection of antibodies against foot and mouth disease virus serotype O, using gold labelled antigen, test line is bio-marked with staphylococcal protein A and the control line with swine anti-FMDV antibody IgG. Sample was reported to be diluted 100 fold with saline solution before adding to sample pad, the sample moves towards the absorbent pad *via* capillary action, a positive sample containing target antibodies will bind to the colloidal gold antigen – forming an antigen - antibody complex highlighted by a red band. The time of detection was 5 minutes after sample addition.[32]

The LFDs are rapid, deployable detection platforms, however, antibody / antigen based LFDs offer equivalent or less diagnostic sensitivity to Ag-ELISA of certain serotypes, and can only be applied to the acute phase of FMD where samples collected contain high amounts of viral particles from vesicular or epithelial samples. These application requirements render the device useless in the incubation period and in absence of obvious clinical signs whereas isothermal based assays allow the evaluation of samples from various sample types: epithelial suspensions, serum and oesophageal-pharyngeal fluids.[33]

More recent publications report developments of portable hardware and protocols for conducting LAMP assays on the field. In 2014, Waters *et al*. reported the developments of a modification of an FMDV – specific RT LAMP assay to allow detection of dual labelled LAMP products with an LFD.[34] The group report a 10^4 fold higher analytical

sensitivity than the current antigen – lateral flow device (Ag-LFD) (SVANODIP FMDV-Ag, Svanova) used on sites. Furthermore other advantages are highlighted when comparing to the 'gold standard' portable PCR system, the RT LAMP assay relies on robust isothermal chemistries and therefore doesn't need time consuming, specialist equipment to support prior nucleic acid extraction. Interestingly, after optimisation the RT-LAMP LFD assay was able to detect different serotypes and also able to detect low levels of FMDV in air samples further supporting the group's claim of higher analytical sensitivity. FMDV presence in air sample detection is a very valuable development as this form of indirect transmission is a reported problem in FMD outbreaks making it a trans-boundary disease therefore this assay in a deployable kit would be a valuable tool for early diagnosis and prevention of a mass viral outbreak.

A further complication with pen-side diagnostic kits is the need to maintain the integrity of the reagents such as enzymes being utilised, through temperature controlled storage and transportation needed for stockpiling test kits as a precautionary measure or deployment to suspect cases. All techniques mentioned thus far have been validated by 'wet' reagents, to address this gap methods have been developed to lyophilise reagents making them stable to less optimal/ harsher conditions as seen in many areas affected by FMD. In 2015, Howson *et al*. have reported the validity of the use of lyophilised reagents in field settings of East Africa (FMD endemic location) on RT-LAMP and RT- PCR assays, the group have reported no adverse affect on the performance of the assays.[35]

1.1.3.3. Other strategies to improve rates of diagnosis

Cost effective method to submit FMDV sample; a study has been reported by Kassimi *et al*. on a cost effective protocol for sample submission in conjunction with LFD used for rapid immunodetection,

utilising a positive test strip after rendering the virus inactive by soaking the test strip in 0.2% citric acid, the study was done to reduce the cost of submission thereby increasing the number of samples submitted from suspected animals, especially in endemic areas.[36]

The imminent need for a cheap, rapid, sensitive test for FMDV is apparent for the $3C^{pro}$ enzyme and capable of detecting all serotypes known. However, elucidation of the serotype would have to be lab assisted but this can be done with samples that generate a positive fluorescence response, reducing the number of suspected samples being sent to labs and the costs associated with them. We envisage the use of a marker spray that can produce a fluorescence signal when in presence of the FMDV, with the use of a portable fluorimeter, minimal user intervention and easy to follow protocol that can be followed by non-specialist personnel. Preliminary studies have been carried out on $3C^{pro}$ and further optimisation is needed to apply to actual clinical samples from different sources such as blood, serum, fluids as the presence of other components in the sample may have an effect on the performance of the assay developed. Research efforts have goneinto synthesising a suitable peptide fluorophore conjugate and its biological evaluation in the presence of $3C^{pro}$.

1.1.4. Global distribution and economic impact

Although the mortality rate of FMD remains low, an outbreak affects a large number of animals having a major global impact on livestock productivity, livestock products, milk production and on import/export with other countries thereby adversely affecting the economy of the host country.It is reported that three quarters of the world's population collectively reside in FMD endemic countries; therefore FMD remains a global problem.[37]

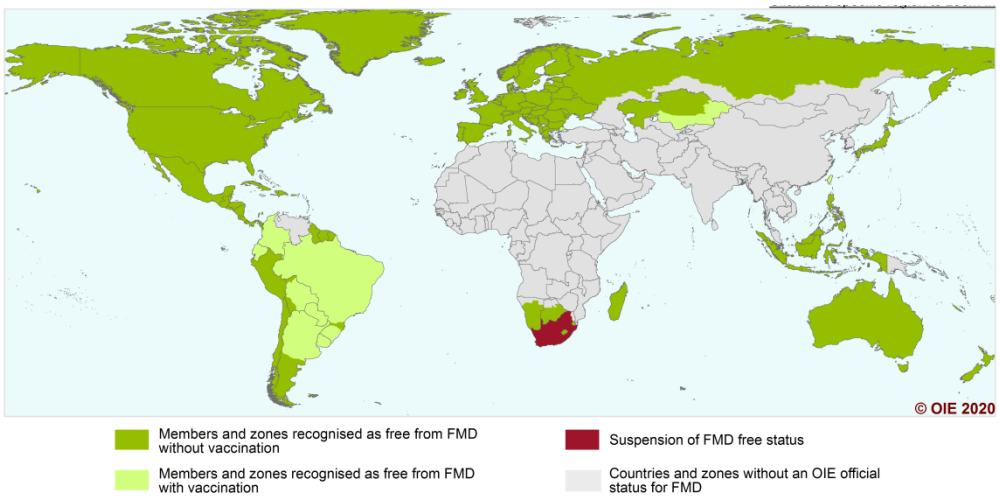

Figure 6 - The map indicates locations with FMD outbreaks and their resolution status, representing data from 2020.[38]

The UK is listed by the OIE as a Member of Countries as FMD free where vaccination is not practised.[39] The UK has suffered two outbreaks in the last 20 years, a major outbreak in 2001 and a minor outbreak in 2007 due to the preparedness of the country after 2001's outbreak. The 2001 widespread outbreak was caused by the Type O, PanAsia strain of FMDV and cases were also reported to be found in Northern Ireland, Ireland, Netherlands and France. The overall cost of this outbreak was reported to be around £8 billion, £3 billion losses to the public sector and £5 billion to the private sector (national audit office). The country faced mass culling of infected/suspected animals in order to prevent the spread of infection; 6.24 million in total were lost. An increase in suicide in farmers was reported around the epidemic. 120,300 farms were affected and depopulated. UK regained its FMD free status in 2002 allowing reopening of export; however, normalised trading was achieved after 18 months of eradication. The agricultural and food chain industries were compensated by the government, but other sectors were also affected, this extension thereby affects the whole British economy this includes the tourism industry that was reported to be hard hit by the outbreak, with direct losses reported from rural and overseas tourism. 90% of positive samples from cattle and pigs were detected *via* ELISA using vesicular

epithelial samples. Less vesicular lesions were observed in sheep and therefore this technique is not as suitable or successful for detecting FMDV in sheep.[40,41,42,43]

The 2007 outbreak was caused by virus strain British Field Strain 1860, serotype O, subtype 1, isolated in 1967 from a surprise leak from the Pirbright site made up of the Institute of Animal Health and Merial Animal Health Limited, both laboratories were working with this strain at the time, 4.4km distance away from the first diagnosed case.[44] The overall cost associated with this outbreak was reported to be £100 million. The FMD spread was more controlled and therefore the spread of infection was localised, the number of animals culled were 2,160 and the number of farms depopulated were 8, with no farmer suicides reported. The duration of the outbreak was 4 months and UK regained its FMD free status after 2 months of eradication allowing reopening of exports.

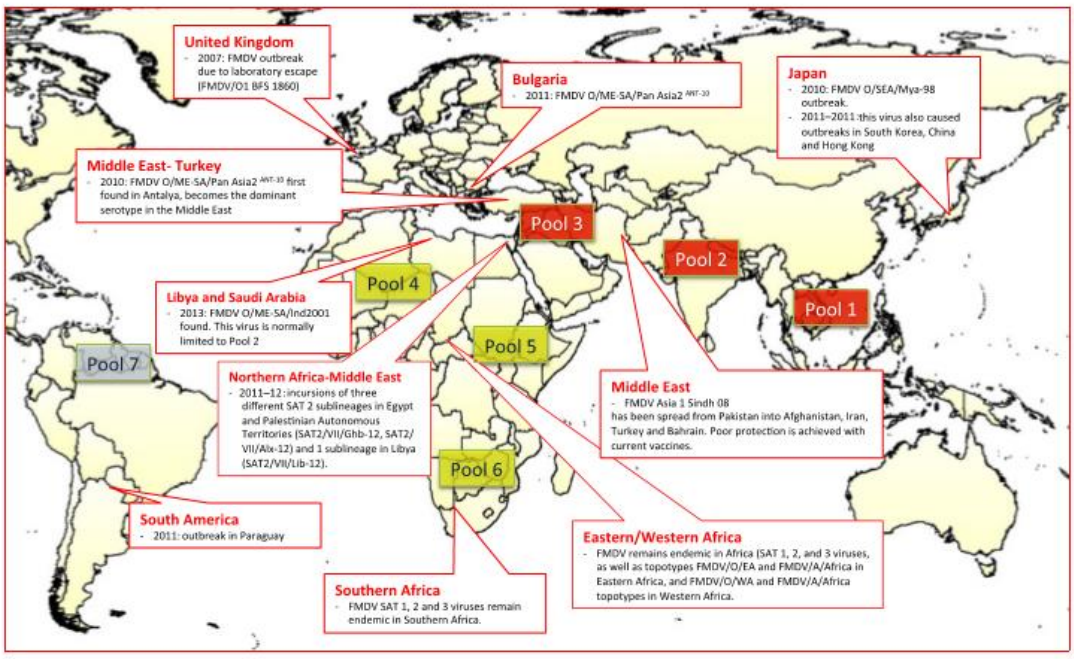

Figure 7- Major FMDV events between 2007-2014 and the pools of serotype in different regions.[45]

The impact of an outbreak varies from country to country and sector to sector, however, the economic losses associated with eradication areinevitably large. In 2013, Rushton *et al*, reported a massive collective loss of over US$20 billion over the last 15 years due to epidemics in countries previously free of disease. The status of a country with regard to FMD is of high importance when considering trading of livestock products. The presence of FMD in a country such as in endemic countries renders its prospects to be low of exporting to FMD free countries. However, maintaining a FMD free status is costly and at times a struggle to maintain in developing countries. Loss of FMD free status results in reduced export revenue, increased supply to domestic markets would reduce meat prices causing a massive loss to the meat industry over a long period of time. Moreover countries sufferingendemics are impacted *via* on-going losses both direct and indirect losses as described in figure 8.

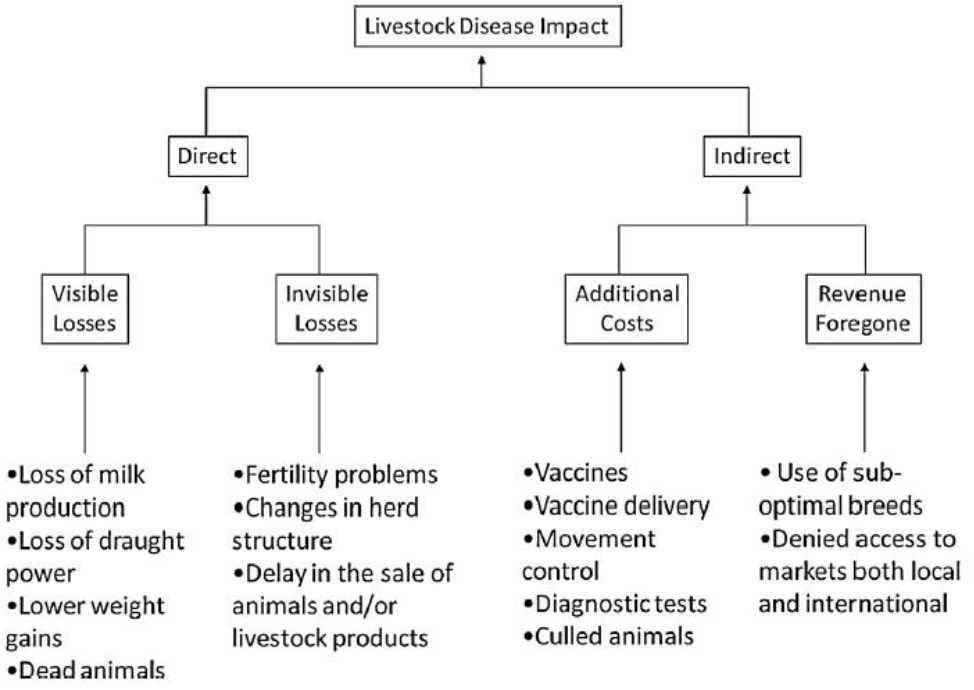

Figure 8 - The direct and indirect losses and problems contributing to the overall impact of FMDV.[46]

1.1.5. Vaccination

Vaccination is a common method of control in infectious diseases and has in the past reported to support eradication invetinary areas. However, conferring immunity against FMDV to prevent or reduce clinical disease is complicated, as the virus undergoes error prone replication giving rise to seven different serotypes, these serotypes have further subtypes. Serotype specific vaccines are available, these vaccines usually only provide resistance for the specified serotype/s. Distribution of the serotypes isn't uniform across endemic regions, however the cluster of serotypes present in each region is known through continuous diagnosis as shown in Table 2 - Distribution of serotypes in some regions suffering endemics. An infection caused by serotype C hasn't been reported since 2004 and is therefore now thought to be extinct.[47,48]

Region	Serotypes
Africa	O, A, C, SAT-1, SAT-2 and SAT-3
Asia	O, A, C, and Asia-1
S. America	O, A, and C

Table 2 - Distribution of serotypes in some regions suffering endemics.

FMD vaccination policies vary from country to country, depending on their policy makers local epidemiological situation and export markets:

- Regions facing FMD endemic situations such as: Africa, Asia and South America all practice preventive vaccination.
  Countries within these areas are reported to be controlling disease *via* mass immunisation using a trivalent vaccine containing inactivated antigens of O, A and Asia-1 serotypes prevalent in India.[49]
- Europe, North America and Australia are free of FMD without vaccination.

> The EU has banned the use of routine vaccinations since 1992, therefore the UK in an epidemic situation (2001) followed a strict stamping out policy causing pre-emptive culling of animals on infected farms and their dangerous contacts. This method of control caused a public outcry resulting in part toa change of policy to use vaccination as a primary method of control spread of infection. The EU regulation now states emergency vaccination (protective vaccination to survive) can be considered in conjunction with culling to control spread of infection, depending on availability and efficacy of vaccine as success in stamping out policy is entirely dependent on early diagnosis.[50]

Use of preventive vaccination is predominantly used in endemic countries, unlike countries usually free of FMD that face sporadic outbreaks who decideagainst the use of preventive vaccination and use emergency vaccination as a last resort because of reasons reported below:

i) In order to develop large amounts of vaccine, the traditional method would involve inactivation of large amounts of the virus and cultivation of the virus poses the major risk of virus escape from a high containment lab as seen in the UK 2007 outbreak.
ii) Unable to prevent sub-clinical persistent infection that is equally as infectious if transmitted as from an animal in acute phase of infection.
iii) Costs associated with routine vaccination – direct vaccination, administration and surveillance of immunity, movement restrictions implied on animals after vaccination. Although in most cases this control strategy would outweigh income generated through trade deals of a country holding a FMD free status, benefitting the overall country’s economy.

iv) An added complexity to emergency vaccine administration is the need for subsequent differentiation of groups of animals that are vaccinated from the ones that are infected - recovering from an infection or suffering an acquired sub-clinical persistent infection. This information cannot be currently achieved using regular diagnostics, however, priority in research is now to develop vaccines alongside specifically designed diagnostics able to differentiate between infected and vaccinated animals (DIVA).

The DIVA strategy allows vaccination producing an antibody response that is different to the antibody response produced by FMDV thereby holding the advantage of serological surveillance for the presence of infection, alongside a diagnostic method optimised to detect carefully selected epitopes and antigenic determinants.[51]

Current vaccines are binary ethyleneimine inactivated whole virus antigen, with newer vaccines developed with markers in the form of deletions of NSPs through biological intervention resulting in genomic mutations of the FMDV. Conventional FMD vaccines provide protection to different extents and come with a few limitations:

i) Working with large amounts of whole antigen can result in viral escape from high containment laboratory.
ii) Vaccines not all compatible with DIVA strategy and therefore not appealing to countries that favour emergency vaccination use over preventive vaccination.
iii) Short term protection period, requires constant booster vaccinations.
iv) Needs constant updating due to evolving FMDV giving rise to subtypes.
v) Specialist storage required for formulated vaccines.
vi) Short shelf life.
vii) Cultivation of some serotypes/ subtypes can be difficult.

viii) Incomplete inactivation – very rare for inactivation to occur today as methods to inactivate are now more understood.

Other types of vaccines have been developed over the years, designed to circumvent problems highlighted above. One type of vaccine developed is with the FMDV rendered harmless to susceptible animals, by producing FMDV with deletions of essential proteins/proteases needed for virulence. An example of this is Leaderless FMDV production, which lacks the L^{pro} enzyme and when tested as a vaccination equivalent protection was described as observed using the wild type antigen. Uddowala *et al*. further developed the Leaderless FMDV by adding mutations in 3D and 3B giving desired DIVA characteristics and when tested as a vaccine - 100% protection was reported. A possible limitation for this type of vaccine for the FMDV is that it may revert back to its virulent form. Moreover, peptide vaccines were developed by synthesising polypeptide chains of the most antigenic region of the viral genome – VP1, more specifically the G-H loop that is the most antigenic site, however, the protection was reported at a low 40%. More recently, synthesis of polypeptides to mimic immunogenic epitopes of VP1, 3A and $3D^{pol}$ gave a more promising protection percentage of 60%. More recently a DNA vaccine was developed containing fragments of the antigen - P1 capsid region and NSPs 2A, 3C and 3D, incurred 75% protection as a vaccine with the added advantage of assembly in lower containment laboratories and with a stable shelf life.[52]

This thesis details the development of a diagnostic technique with potential to have DIVA compliance by targeting an enzyme self-cleaved from the viral genome – $3C^{pro}$. As mentioned above the development of the Leaderless vaccine if modified to delete the $3C^{pro}$ in conjunction with a $3C^{pro}$ marker spray, a positive response would thereby mark the presence of $3C^{pro}$ indicative of infection and the absence would be indicative of vaccination.

1.1.6. Transmission

FMD is a highly contagious disease and understanding transmission pathways is helpful information when containing the spread of infection. Viral particles have been detected in many bodily secretions and excretions of an infected animal before the onset of anyclinical signs; these bodily fluids include blood, saliva, serum, oesophageal and pharyngeal fluids and also in exhaled air. With transition into the acute clinical phase of infectionand formation of lesions, viral particles are also detected in shedding from ruptured lesions as well as all the secretions mentioned before.

Transmission can occur in two ways; direct contact or indirect contact in countries with endemic FMD status. On the other hand epidemics in previously FMD free status can be totally unpredictable and can be caused by air-bourne spread of viral particles as circumstantial evidence indicates from an outbreak seen in 1981 in the Isle of Wight, thought to have originated from Brittany in the North of France. The virus is reported to be able to travel significant distances depending on the wind strength/direction, humidity and climate of area further complicating the spread of infection in an outbreak. FMDV is reported to survive between days to months in surroundings, the virus is also found in animal products such as meat therefore strict guidelines are followed for heating pig swill, as many outbreaks in the past have been linked to FMDV infected products being fed to pigs resulting in an outbreak.[53]

The role of carriers in transmission isn't completely understood. More recently Hayer *et al*.[54] reported the time taken for full viral clearance from Indian cattle to be 13 months, lower than previous reports of carrier state to last between 2-3 years. Another group led by

Bronsvoort have noted younger animals are more likely to be carriers after an outbreak due to sero-conversion.[55]

1.2. THE TARGET VIRUS

1.2.1. Picornavirus

The Picornavirus belongs to the family *Picornaviridae,* which belongs to the order *Picornavirales* that currently consists of 94 species grouped in to 40 genera (as of March 2018).[56] Characteristic features of picornaviruses are; typically small ~18-30nm with single stranded positive sense RNA, RNA molecules range between 7.2 – 8.5 kilobase (kb), they lack a lipid membrane around their genome rendering it resistant to solvents: ether, chloroform and alcohol, but readily inactivated using phenol, formaldehyde or ionising radiation.[57] These viruses are responsible for a range of human and animal diseases that present themselves as sub-clinical infections with varying degrees of intensity from a mild illness to severe illnesses of the heart and liver, a few members of the family *Picornaviridae* are listed in table 3.

Genera that infect animals	**Species and disease**
Apthovirus	FMDV – disease in cloven hoofed animals
Cardiovirus	Theiler's murine encephalomyelitis virus - disease in rodents
Teschovirus	Teschovirus A– disease in pigs
Genera that infect humans	**Species and disease**
Enterovirus	Polio virus – disease of alimentary canal
Rhinovirus	Common cold virus – disease of nasopharyngeal region
Hepatovirus	Human hepatitis virus A – disease of the liver tissue.

Table 3 - Other diseases caused by picornaviruses.[58]

1.2.2. FMDV genome and structure

FMDV is a small non-enveloped virus, each viral particle contains capsids that are protein shells encasing 8.4kb of viral genome that is attached *via* a covalent linkage at the 5' end to the a small viral protein linked to the genome (VPg) and polyadenylated on the other 3' end.[59] Subsequent to viral cell entry, the viral genome undergoes three main steps; (i) rapid translation into a long 2,300 amino acid chain that is processed by twovirally encoded proteases, (ii) cleavage of proteins and (iii) replication of FMDV genome by viral polymerase 3D ^{pol}. The replication of FMDV is thought to be confined to the cytoplasm with an efflux of certain nuclear host factors.

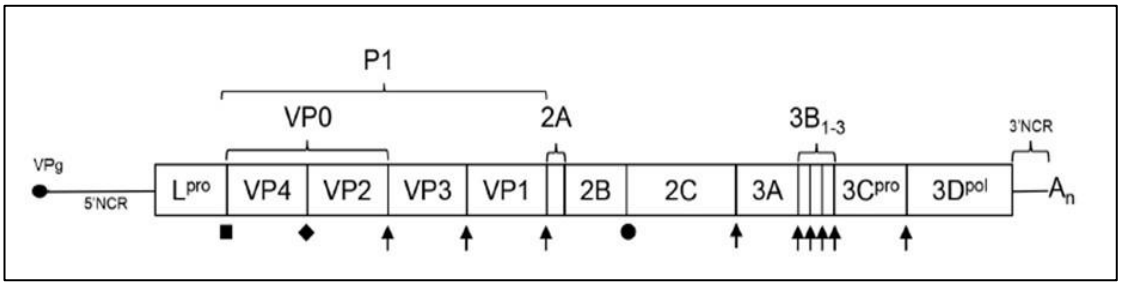

Figure 9 - A diagram representing the FMDV genome, the mature viral proteins are labelled in boxes. Protein processing key: the arrows indicate the cleavages done by $3C^{pro}$, the circle indicates the junction at which a ribosomal skip mechanism occurs and the square indicates the position for auto-catalytic cleavage by L^{pro}, the diamond represents position the capsid proteins undergo maturation cleavage.[60]

The FMDV genome like all picornaviruses is made up of the long single ORF flanked by 5' and 3' non coding regions (NCR). The 5' NCR holds sites – 3 to 4 pseudoknots, cis-acting replication element and IRES type 2 that have important roles in cap-independent translation initiation of viral proteins and genome replication. The 3' NCR end is thought to also hold replication elements needed for efficient replication, deletion of either 5' or 3' sites is reported to cause inhibition to translation in lab based studies.[61] The ORF encodes a

polypeptide cleaved by the virally encoded proteases to give mature viral protein products these include eight non structural proteins 2B, 2C, 3A, 3B, $3D^{pol}$, L^{pro}, 2A, $3C^{pro}$ and four structural proteins VP1-4.

These structural proteins form an icosahedral capsid with pseudo T=3 symmetry to protect the viral RNA genome, it is composed of 60 copies of each VP. The symmetry is described as pseudo as each VP doesn't occupy the same space. The VPs are organised into 12 pentamers to make a whole capsid, each pentamer is made up of five protomers and each protomer is made up of all four structural proteins VP1-4. With VP1-3 making up the outer surface and the VP-4 protein assembled internally. A highly conserved tripeptide of (Arg-Gly-Asp, RGD) motif externally expressed on the surface of each capsid is an important feature for virus neutralisation anda primary contact for initiating viral infection by interacting with integrin receptors on the cell membrane.[62]

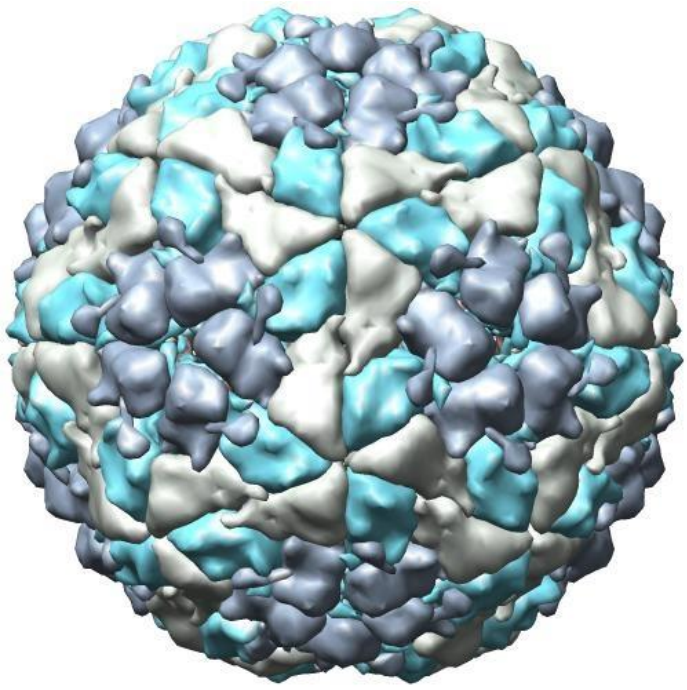

Figure 10 - Biological assembly of FMD viral particle exhibiting icosahedral global symmetry.[63]

The method of viral entry into host cells is *via* receptor-mediated endocytosis. FMDV receptors reported to mediate FMDV infection

include the integrin cell surface receptors - αvβ1, αvβ3, αvβ6 and αvβ8 or using the heparan sulfate receptor *via* interaction with the RGD motif externally assembled in the FMDV capsid. The endosomic area of the host cell is acidic and FMDV capsids are unstable below pH 6.5, causing dissociation into pentamers and release of viral RNA genome. However, the translocation of the RNA genome from the endosome to the cytoplasm remains unclear, as the movement involves the capsid withstanding changes in pH and passing through a lipid bi-layer of the endosomal membrane to reach the cytoplasm before reassembly.[64]

1.2.3. Virally encoded proteases as a target marker

The Le Gresley group have recently developed a rapid detection system as an alternative to the PCR based methodology for *Staphylococcus aureus* (SA) bacteria utilising the probe called LGX - $(BocNH\text{-}Val\text{-}Pro\text{-}Arg)_2$–Rhodamine.[65] The system is originally inspired by the commercially available probe BocNH-Val–Pro–Arg–7–amido–4–methyl coumarin,[66] used for the detection of SA bacteria through an enzymatic approach as illustrated in figure 11.

i)

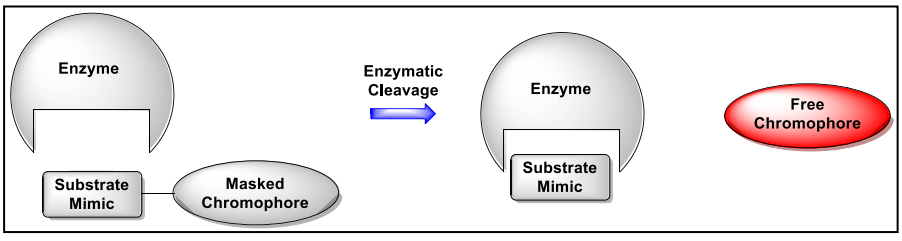

ii)

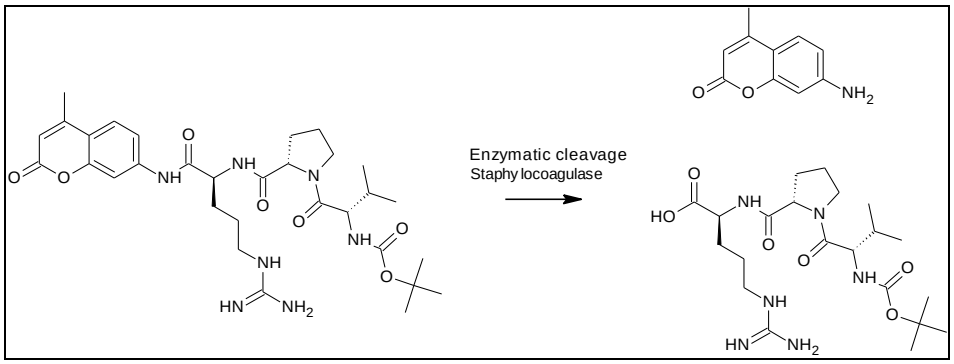

Figure 11 - (i) Pictorial representation of the concept being tested (ii) Structural representation of methyl coumarin dye system.

Taking advantage of the proof of concept gained through the LGX probe on SA bacteria, the method can be further developed to target any microorganism that are known to produce an exo-enzyme with a natural substrate that mimics a synthetic peptide sequence that can be coupled on to a suitable fluorophore like 7-amino-4-methyl-coumarin (AMC) or a suitable chromophore like rhodamine 110 (R-110). FMDV is a suitable target for this tested approach, as this picornavirus replication is reported to be reliant on externally expressed virally encoded proteases. The picornavirus genome is reported to be translated into a polypeptide chain which is processed by cleavage by virally encoded proteases; L^{pro}, $3C^{pro}$ and 2A, all of which have the potential of being possible targets.

1.2.3.1. Leader protease, L^{pro}.

FMDV L^{pro} is a papain-like cysteine protease, its active site residues were identified as Cys-51 and His-148 (fig 12) by inhibition studies and site directed mutagenesis. The protease exists in two iso-forms Lab and Lb as there are two in frame translation initiation codes for the protease, the Lab form has a highly variable extension of 28 amino acids not seen in the Lb form. Both exhibit indistinguishable activities and specificities, they are able to self-cleave from the viral polypeptide chain and induce cleavage of the eukaryotic initiation factor eIF4GI and II resulting in the inhibition of host cells capped protein synthesis. However, this has no effect on the viral protein synthesis which is maintained since it is reliant on an internal ribosome entry site (IRES) within the 5'-NCR.[67]

A mutated version of the FMDV virus - Leaderless virus is reported to be developed and evaluated as a vaccine, the absence of the L^{pro} renders the virus inactive, however, its use as a vaccine is limited because the virus is so weakened that it doesn't replicate enough to cause the host immune system to illicit a protective response. An initial response of the host to a viral infection is the secretion of interferon type I (IFNI), interferons are proteins that bind to host cells and *via* a signal transduction pathway causing the production of anti-viral gene products. The replication of FMDV is inhibited by the presence of IFNI and this IFN activity is detected when infected with the Leaderless FMDV. Interestingly the IFN activity described isn't a problem when using some BHK cell lines as they are reported to have a defect to their responsiveness to IFNs making them compatible with the Leaderless virus for cultivation purposes.[68]

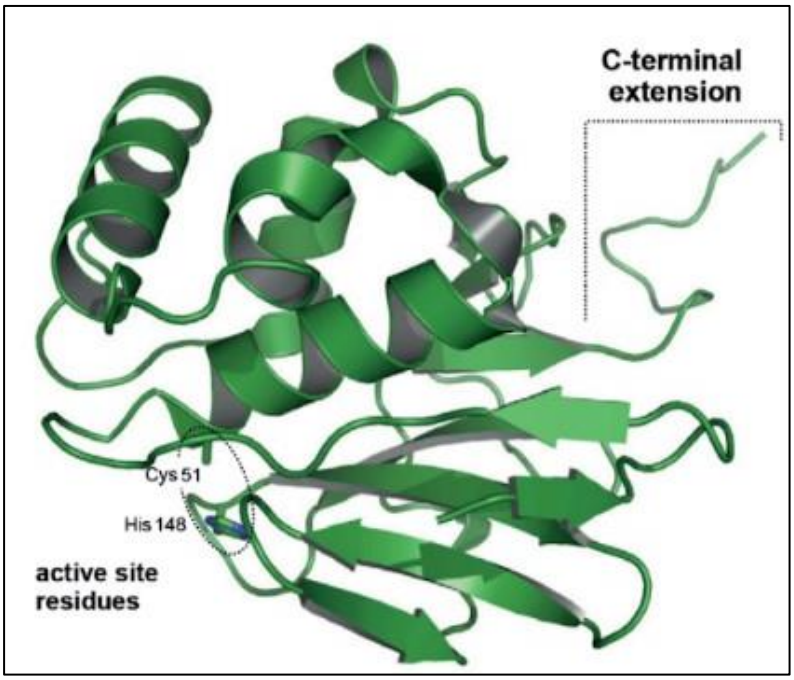

Figure 12 - Structure of L^{pro} and the active site residues are highlighted. [70]

1.2.3.1.1. *Activity of L^{pro}*

L^{pro} is reported to be responsible for only one cleavage on the viral polypeptide chain at its own carboxyl terminus at the L/VP4 junction to release itself, as shown in figure 9. Once released the enzyme is reported to cleave a large number of host-cell proteins as listed in table 4.

Host cell protein	Function of protein
Cyclin B2	Control of cell cycle
Cyclin A	Control of cell cycle
Gemin5	IRES-binding factor
P65/ReIA	Subunit of nuclear factor kappaB
Ubiquitinated proteins	Modulate cellular and immune processes
RANTES expression	Inflammation and immune response
eIF4Gi and ii	Eukaryotic translation initiation factor

Table 4 -Host-cell proteins cleaved by L^{pro} [69,70,71,72,73]

The enzyme is reported to be involved in a large number of reactions; the comparison of the amino acid sequences of three of its known substrates gives an indication of the unique specificity exhibited by L^{pro}:

Protein	Amino acid sequence
Viral polypeptide chain	KVQRKLK*GAGQSS
eIF4Gi	PSFANLG*RTTLST
eIF4Gii	VPLLNVG*SRRSQP

Table 5 - Amino acid sequences of L^{pro} substrates, * marks position in the sequence that is cleaved by L^{pro}.[71]

Studies conducted on the sequences in table 5 by a number of groups revealed that L^{pro} recognises and cleaves peptide bonds before or after basic residues neighbouring glycine. However, basic residues on both sides of the scissile bond have shown an inhibitory effect at a micromolar range which led to the development of nanomolar inhibitor E64, an epoxide that is reported to have a range of uses, one of which is the ability to inhibit Cathepsin B through inducing oxidative stress and apoptosis in filarial parasite.[7475]

1.2.3.2. 2A oligopeptide sequence

The catalytic cleavage of the VP1/2A junction is a consequence of 2A protease activity, in some picornaviruses: the human rhinovirus and the poliovirus. Despite initial theories of similar activity on the FMDV genome, further studies of the FMDV 2A protein by Ryan *et al*. has proved no proteolytic activity and its cleavage at 2A/2B junction is reported to be caused by the mechanism of ribosomal skip. The short 2A oligopeptide sequence is reported to modify the activity of the ribosome by promoting ester hydrolysis of the peptidyl(2A)-tRNAGly causing the release of the polypeptide from the translational complex, however, some of the RNA remains attached to the ribosome allowing the translation of the non-structural proteins but at reduced levels

compared to the structural proteins.[76,77] The absence of any protease activity with this protein renders it useless for this project, as the detection model being applied requires a viral exo-enzyme to be produced acting as a marker for its native virus.

1.2.3.3. 3C protease, $3C^{pro}$.

$3C^{pro}$ is a chymotrypsin-like cysteine protease, it is 213 amino acids long with molecular weight of around 23kDa. The enzymes sequence is highly conserved, ~82-85% identical over all known serotypes without any cellular equivalents in host cells and it is therefore a suitable target for our project. Like the L^{pro} it also self cleaves from the viral polypeptide chain and is vital for further processing of the sequence as it recognises and cleaves 10 of the 13 polypeptide junctions, it also interacts with a wide range of host proteins involved in the host's immunity (table 6), thereby successfully suppressing cellular immune responses. This shows that $3C^{pro}$ plays a critical role in viral pathogenesis.

$3C^{pro}$ cleaves a large number of amino acid pairs during primary and secondary processing, these include; E/G, E/T, Q/L, Q/G, Q/T and Q/M, however, not all such amino acid pairs present in the viral polypeptide chain or in the capsid proteins are cleaved by $3C^{pro}$, the structural positions play an important role in recognition and cleavage.

Host cell protein	Function of protein
eIF4G, eIF4A1	Eukaryotic translation initiation factors
H3	Histone
NEMO	NF-kappa-B an essential modulator for IFN α/β responses
Sam68	Sequence-specific RNA binding protein that regulates alternative splicing

Table 6- Host-cell proteins cleaved by $3C^{pro}$[70,78,79]

1.2.3.3.1. *Active site of 3C^{pro}*

Resolution of the atomic structure of 3C^{pro}FMDV revealed important structural features; the enzyme adopts a chymotrypsin like fold as observed in most serine proteases with a conserved catalytic triad made up of Ser-His- Asp. However, the catalytic triad of the FMDV 3C^{pro} is comprised ofHis-46, Asp-84 and Cys-163, the residue acting as a nucleophile in the active site is cysteine. In recombinant forms of the enzyme, the cysteine residue is substituted with an alanine to produce the inactive form of the enzyme to facilitate expression, purification and crystallisation.

In earlier enzyme structural studies a major difference was spotted in the substrate cleft of the FMDV 3C^{pro}, the β-loop overlaying the substrate binding cleft found in other picornaviruses was disordered and reported to be absent and thought to be the reason to the reduced substrate specificity exhibited by FMDV 3C^{pro} as it is able to recognise and process glutamine and glutamate residues positioned before the scissile bond, not seen in other picornavirus 3C proteases who strongly favour glutamine in this position. However, the β-loop presence was later confirmed in 2005 by Curry *et al*. who produced more soluble recombinant forms of 3C^{pro} single (C95K) and double (C95K/C142S) mutant proteases in order to determine the crystal structure and its proteolytic specificity. The group ran peptide cleavage assays and have reported the need for four residues each side of the scissile bond for efficient recognition and cleavage.

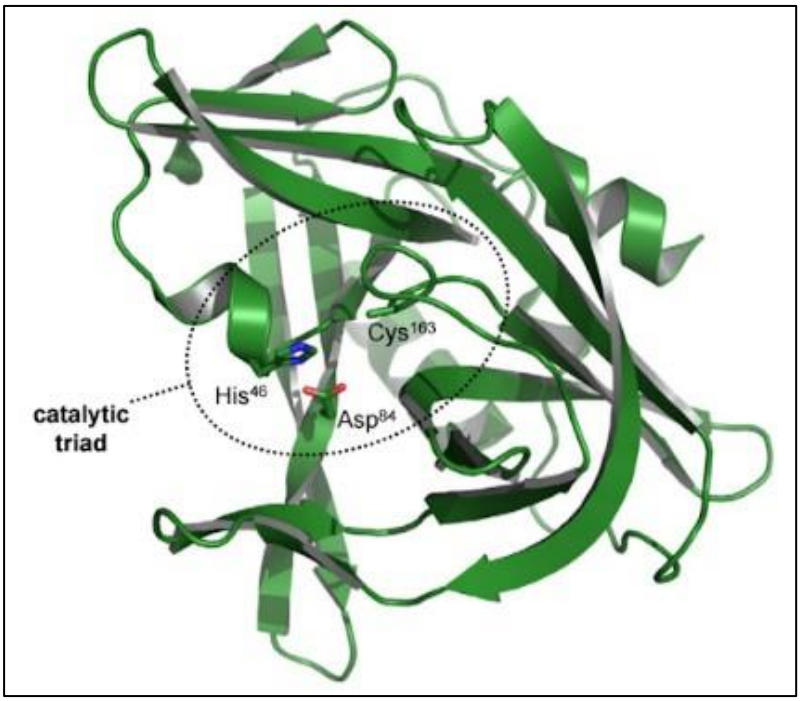

Figure 13- Atomic structure of $3C^{pro}$ and the active site residues are highlighted.[70]

Moreover, structural analysis reported by Curry et al. was based on covalent attached substrates or peptide based inhibitors of the enzyme. However, in 2010, Zunszain *et al*.[80] resolved the X-ray crystal structure of $3C^{pro}$ with bound peptide substrates i) APAKQ*LLNFD = P5-1*P1'-5'effectively mimicking its natural substrate VP1-2A and ii) APAKE*LLNFD, to enable an in-depth structural understanding of polyprotein interaction and enzyme-assisted cleavage. The enzyme was found to be able to mould around its substrate's residues to display the scissile bond to the active site for efficient cleavage, allowing the wide range set of substrates. Detailed interactions of the amino acid residues of VP1-2A and substituted peptide substrates with the binding cleft are listed in table 7 and can be visualised in figure 14.

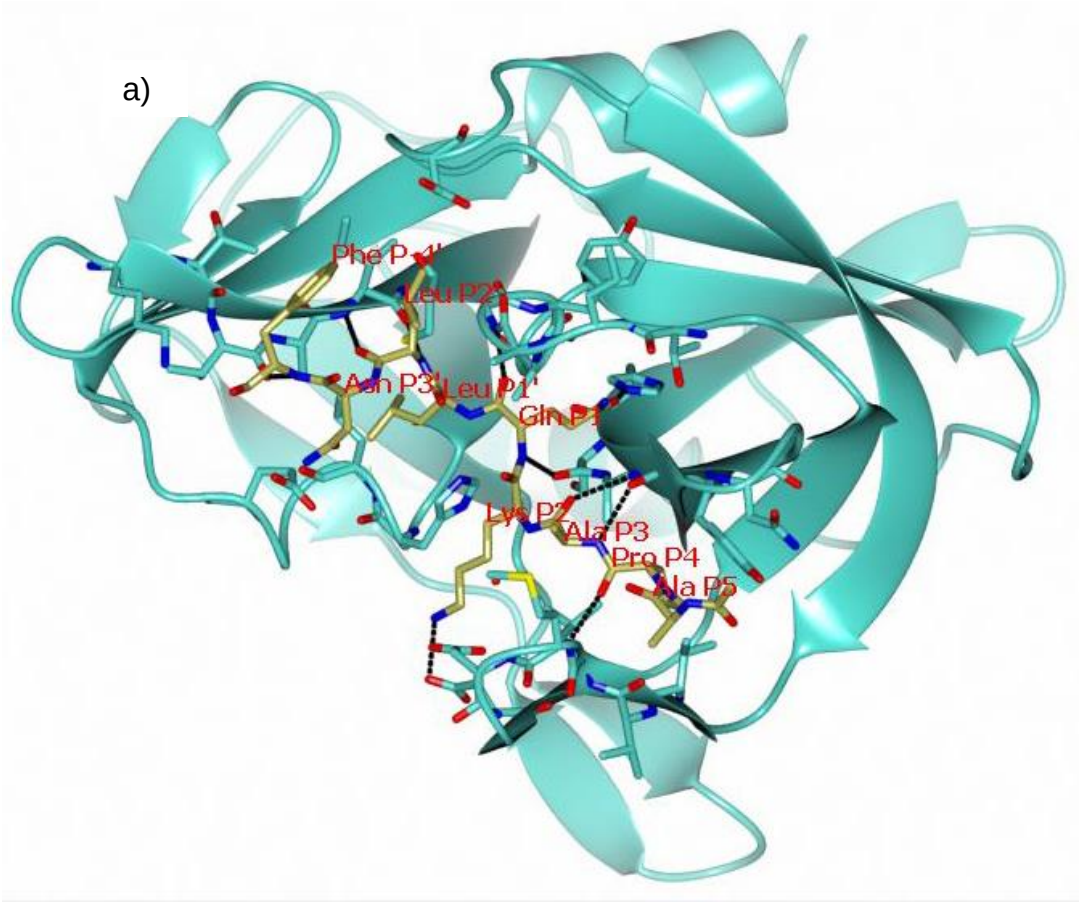
a)
Phe P-4'
Leu P2'
Asn P3'
Leu P1'
Gln P1
Lys P2
Ala P3
Pro P4
Ala P5

b)

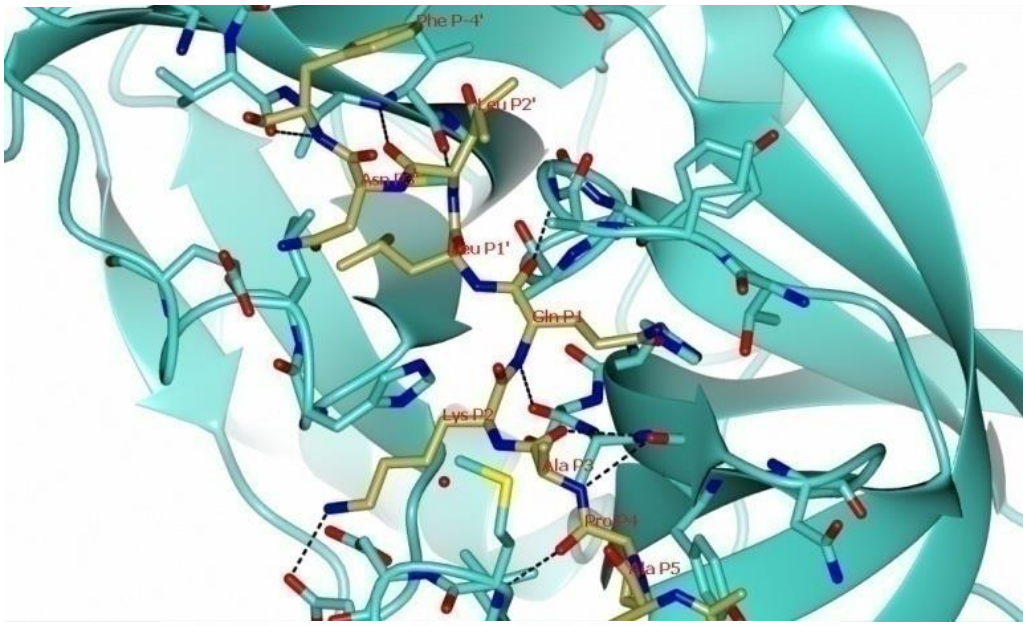
Phe P-4'
Leu P2'
Leu P1'
Gln P1
Lys P2
Ala P3
Pro P4
Ala P5

c)

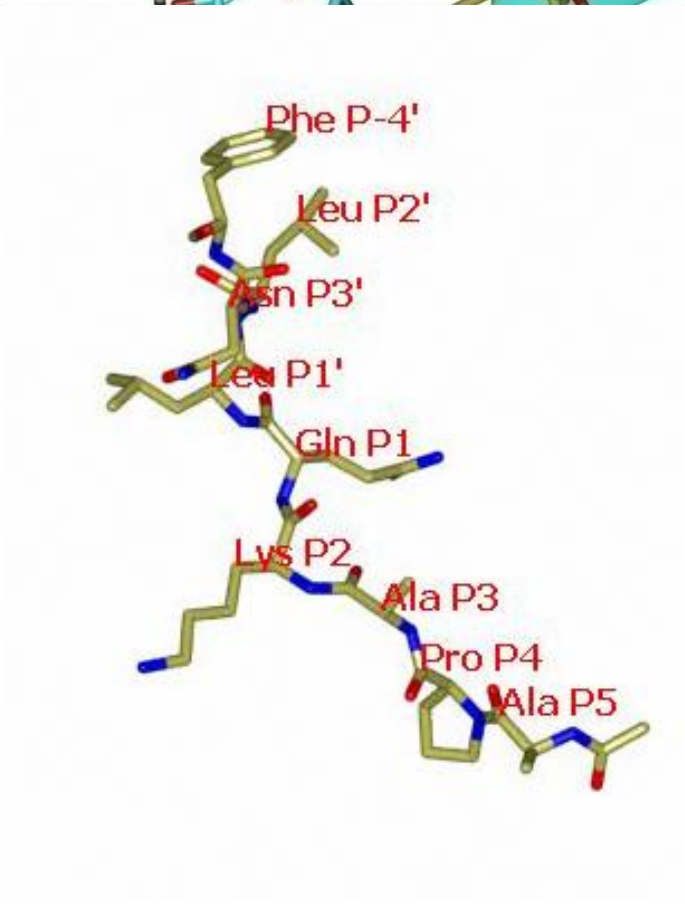
Phe P-4'
Leu P2'
Asn P3'
Leu P1'
Gln P1
Lys P2
Ala P3
Pro P4
Ala P5

d)

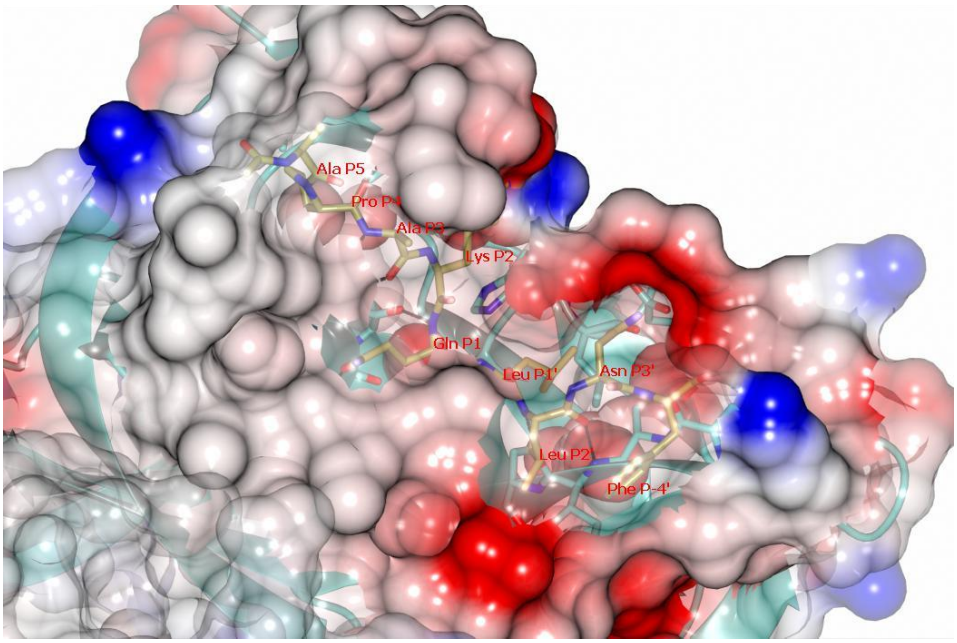

Figure 14 - PDB ID = 2WV4.Overview of $3C^{pro}$ and substrate binding. a) Schematic view of the co-crystal structure of $3C^{pro}$ complexed with the peptide, enzyme represented in ribbon form and the bound peptide is shown in cylinder form, colour coded by atom type (C, gold). The side chains of the enzyme in the neighbourhood of the peptide are shown in turquoise, also colour coded by atom type (C, turquoise; N, blue; O, red). b) Expanded into binding site, black dashed lines represent interactions between the enzyme and ligand. c) Structural representation of peptide substrate P5-P4', Acetyl – Ala – Pro – Ala – Lys – Gln – Leu – Asp – Leu –Phe, shown in cylinder form, colour coded by atom type (C, gold; N, blue; O, red). d) Surface representation of $3C^{pro}$ complexed with peptide substrate c. Electrostatic density represented by colour (red, negatively charged; blue, positively charged; white, neutral).

Position in substrate	**Interactions of peptide chain and enzyme backbone**
P5 N-terminus	Is an alanine residue that is reported to be mainly solvent exposed. The side chain is a methyl group found to be pointing in the direction of the hydrophobic protease Met-143 residue, but too far for any interaction (4.7Å). Therefore substitutions of this amino acid have modest effect on cleavage rate.
P4	Is a proline residue that interacts with what is

	reported to be the beginning of the peptide binding cleft with side chains of Leu-142 (Cys in the wild type), Val-140 and Tyr-190. Part of the residue is solvent exposed, therefore not completely bound to the binding site. Substitution of this Pro with Ala prevented cleavage, however, the authors suggest the size of the pocket interacting with the Pro should be able to accommodate Ala or Val. However, the presence of other residues may affect the binding conformation resulting in improper presentation of the scissile bond to the active site, a possible reason to substrate remaining intact.
P3	Is an alanine residue interacting with Met-143 residue on the tip of the β ribbon, causing the enzyme to alter its conformation on peptide binding to allow closer contact with the substrate. This position has a range of residues making up the natural substrate junctions, provided hydrophobic contact is made with β ribbon, however, the intensity of the interaction can have an effect on other peptide interactions thereby affecting cleavage rate.
P2	Is a lysine residue, whose side chain inserts into binding cleft between the β ribbon and the β barrel of the enzyme.The side group's aliphatic chain interacts with His-46, the other side interacts with apolar side chains of residues Leu-142 and Met-148. The amino tip of Lys side chain interacts with acidic residues of the β ribbon Asp at position 144 and 146, this amino interaction is reported to be necessary for cleavage, absence of the group has prevented cleavage.

	Due to the malleability of the enzyme, the binding by this Lys residue causes a positions to change in residues Leu-142, Asp-144 and Asp-146 giving rise to a pocket labelled S2.
P1	Is a glutamine residue that was observed to cause movements in the backbone of the enzyme'spocket. The side chain forms three hydrogen bonds to the amide bond of the enzymes Thr-158 residue. An identical interaction was reported to be observed with glutamate substitution, however, one of the H bonds is reported to be more distant than seen in glutamine, this is described to be due to the loss of proton on the carboxyl side chain, thereby reducing three strong H-bonding interactions to two and increasing pH of the cytoplasm may also have a negative impact on binding. The substitution of gln to glu causes a two-fold reduction in cleavage.
P1'	Is a leucine residue, whose interaction pocket in the only becomes available in presence of the peptide substrate. An amino acid with a side chain with hydrophobic character is preferred in this position to give efficient cleavage, as substitution of Leu to Gly has a reduction of ten fold in peptide cleavage. The group suggests the residues either end of the scissle bond are important in ensuring it's presented optimally to the active site.
P2'	Is a leucine residue, however, the group have reported that a large number of hydrophobic residues can be tolerated in this position, as its interaction is described to be with a apolar pocket of the enzyme.

P3’	Is a asparagine residue, that is mostly solvent exposed but is able to maintain a H bonding interaction with the protease backbone, this interaction however, isn’t conserved with other natural peptide substrates and therefore thought not be necessary. In the synthesis of a FRET4 peptide substrate, modifications of the Asp side chain are reported with coupling to an EDANS group, this modification is well tolerated by the enzyme, as no change in cleavability is reported.
P4’	Is a phenylalanine residue, also reported to be largely solvent exposed, hydrophobic nature of the side chain is reported to have interactions with an apolar patch of the upper surface of the protease. Amino acids with hydrophobic residues such as Arg, Pro and Ala are all well tolerated with minimal effect on peptide cleavage.
P5’ C-terminus	Is a alanine residue, its position is reported to be unknown since it made no stabilising contact with the enzyme. Furthermore substitutions of this amino acid had no effect on peptide cleavage.

Table 7 - FMDV $3C^{pro}$ interaction with natural substrates and mutated versions of natural substrate to tests its specificity.[78]

1.2.4. Enzyme marker

The chosen enzyme marker for this project is the highly conserved FMDV $3C^{pro}$ as more research has been published on its peptide interactions, this information allows us to design and synthesise a peptide conjugate that can effectively mimic one of its multiple substrate interactions as described the enzyme is responsible for a large number of cleavages between amino acid pairs during primary

and secondary processing, these include; E/G, E/T, Q/L, Q/G, Q/T and Q/M, however, not all such protein pairs present in the viral polypeptide chain or in the capsid proteins are cleaved by $3C^{pro}$, the structural positions may play an important role in recognition and cleavage and the need for an extended polypeptide chain in a detection probe will be investigated.

Although, the malleability of the FMDV $3C^{pro}$ discussed in table 7 is thought to be the reason for its tolerance for a wide range of natural substrates and therefore a suitable target for our project, as the amino acids after the scissile bond towards the C-terminus are reported to require groups displaying hydrophobic properties and therefore an aromatic based chromophore may be able to mimic these interactions in the binding cleft and have little or no adverse effect on peptide cleavage. Whereas L^{pro} displays more substrate specificity and therefore not considered at this point but its potential as an FMDV marker is still to be explored and maybe considered in future work, unlike the 2A oligo-peptide sequence that is reported to have no protease activity.

1.3. THE TARGET FLUOROPHORE

1.3.1. Principles of fluorescence

Fluorescence is a type of molecular luminescence, the phenomenon results from a fluorophore molecule absorbing photons at a specific wavelength (energy provided by an external source, typically a lamp or laser) resulting in electronic transitions, the movement of electrons can be followed in a Jablonski diagram shown in figure 15, initial absorption causes transition of an electron to a higher electronic state, the lifetime in this excited state is typically between 1-10 nanoseconds

and the decay back to the ground state is coupled with the emission of fluorescence.[81]

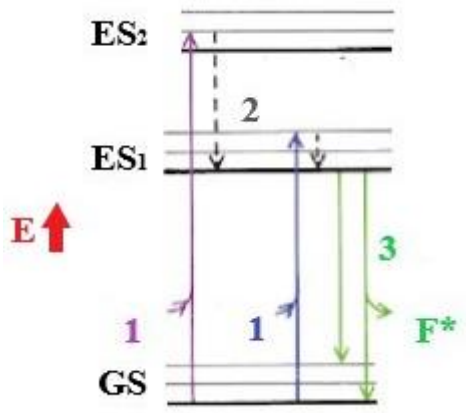

Figure 15 - A Jablonski diagram showing a simple overview of an electronic transition between energy states resulting in fluorescence.[82] Key: E – Energy, ES_1 – Excited state level 1, ES_2 – Excited state level 2, GS – Ground state and F* - Fluorescence.

1 – Absorption of photons causes excitation of electrons

2 – Internal conversion, energy can be lost *via* a number of routes in order to depopulate the excited state, these routes include; collisional quenching, Fluorescence Resonance Energy Transfer (FRET) and intersystem crossing (in case of phosphorescence not shown on diagram). The quantum yield is determined by comparing the number of fluorescence photons emitted to the number of photons absorbed.

3 – Fluorescence emission, due to loss of energy in step 2, the wavelength of the photons emitted is of lower energy and hence longer wavelength when compared to the excitation photons. The difference between the excitation and emission energies or wavelengths is described as the Stokes' shift.

1.3.2. Fluorescence modulation

Most fluorophores have specific fluorescent characteristics which can be followed using a fluorimeter. The use of the fluorimeter is reported to be ten-fold more sensitive than a spectrophotometer and therefore the preferred detection instrument in this project.[83]

Small molecule fluorophore scaffolds display unique properties in fluorogenic substrates, these properties can be manipulated using different chemical strategies to control fluorescence intensity in small molecules and are designed to require activation by enzymatic activity, light or environmental changes as shown in figure 16; the most common method (i) is to covalently attach a group that renders the molecule non-fluorescent and fluorescence is restored once the group is cleaved by enzyme catalysis or photolysis. The example in figure 16 shows that fluorescein is held in its non-fluorescent state after acetylation of the phenolic oxygens and conversion to fluorscein diacetate. Hydrolysis of the ester groups, catalysed by esterase, results in fluorescence generation. In figure 16 (ii) depicts the FRET based method which involves two dye molecules, one acting as an acceptor and the other a donor. An example of a homo-fret substrate assay is shown using boron dipyrromethene as the dye acceptor and donor, fluorescence is generated as a result of phospholipase activity.[84] Non enzyme based methods; (iii) this method involves modification of the core structure of the fluorophore to render it non-fluorescent to undergo some rearrangement to produce a whole functioning fluorophore, the example shows *trans* cinnamic acid derivative which undergoes photochemical conversion, specifically a isomerisation to the *cis* form which rapidly forms a lactone, producing a fluorescent coumarin.[85] (iv) The change of polarity has been reported to have an effect on fluorescence on certain dyes an example of this is Nile Red, a phenoxazine dye, which in an aqueous solution remains non-fluorescent however in a non-polar environment

it is strongly fluorescent and is used to stain hydrophobic regions in living cells.[86] (v) The changes in electronic structure of a dye can affect its ability to generate fluorescence. An example of a probe utilising this method is Fluo-4 used to measure calcium concentrations inside living cells. The lone pair of electrons on the aniline moieties on the chelation motif - (1,2-bis(*o*-amino phenoxy)ethane-N,N,N′,N′-tetraacetic acid) are capabale of quenching fluorescence *via* photo-induced electron transfer. The Ca^{2+} chelation changes the energies of the lone pair of electrons, resulting in less efficient photo-induced electron transfer and therefore this energy is lost through fluorescence.[87,88]

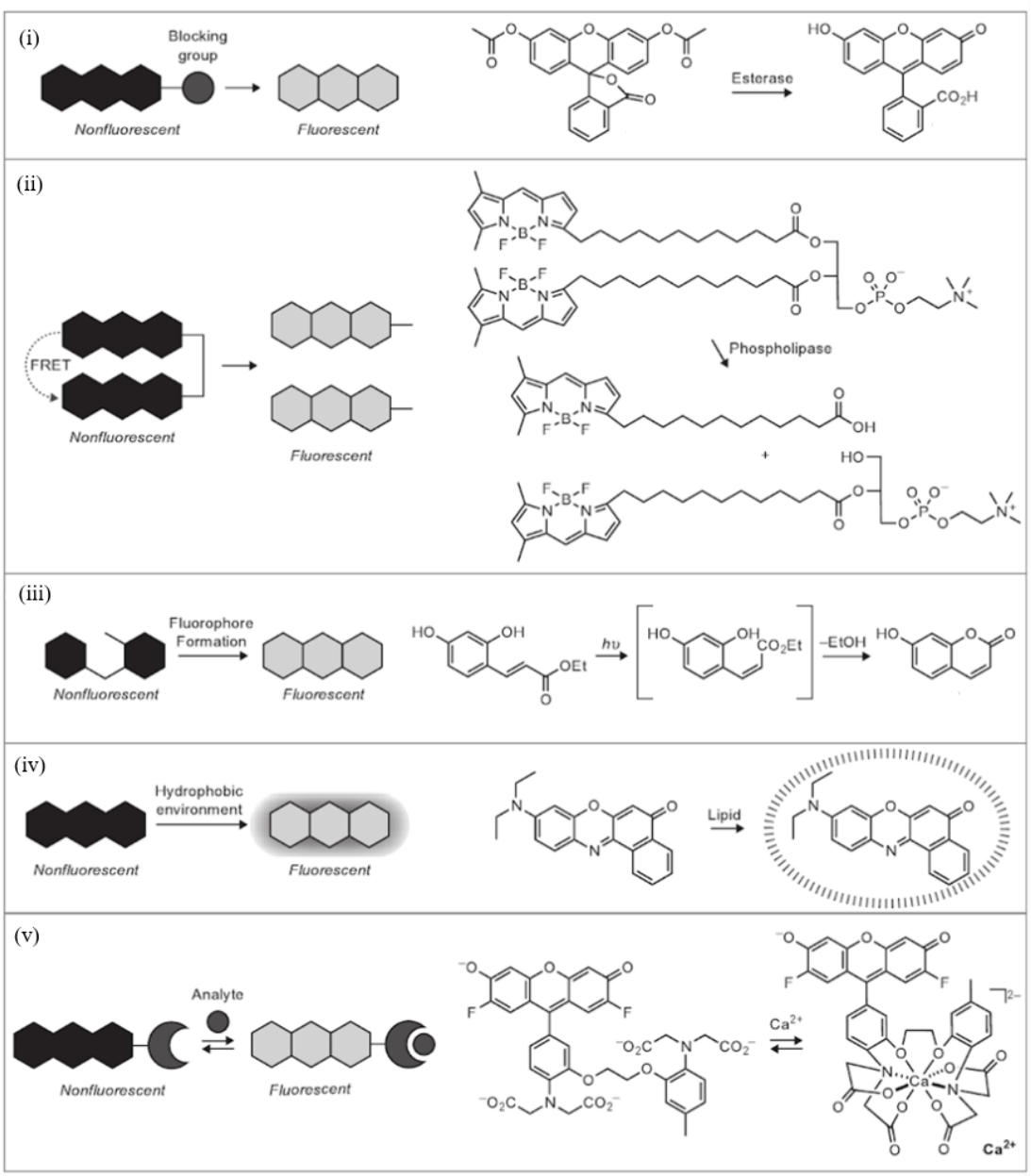

Figure 16 - Different chemical strategies employed in fluorescence modulation.[83]

1.3.3. Small molecule fluorophore scaffolds

Rapid detection and identification of microorganisms is essential in many areas of applied and research based microbiology, these include – food quality control, health care for humans / animals and monitoring in the environment. Many researchers have targeted

different microorganisms developing powerful tools in the form of enzymatic assays to replace traditional lab-based culture methods. The first synthetic substrates reported date back to the early 20th century and their structures are based on simple aromatic chromophores – nitroaniline and nitrophenol, these are less readily used today as they have a similar yellowish colour to microbial media.[89] A range of synthetic substrates are commercially available today and are now regularly used, their chromogenic / fluorogenic moiety is often based on derivatives of coumarin, nitro - aromatics, fluorescein, nitrobenzofurazane or rhodamine dyes.[90]

The classic dyes coumarin, fluorescein and rhodamine are utilised as popular frameworks for simple fluorogenic molecules. These fluorophores can be easily manipulated to a latent form *via* synthetic modifications and designed so fluorescence is generated using enzyme activity. Rhodamine and fluorescein in their original forms exist in an equilibrium between an open and closed form, the open form is highly fluorescent, whilst the closed form is non-fluorescent (figure 18) – this is an attractive property when designing fluorogenic substrates, following fluorescence manipulation method (i) described in figure 16. In 2016, a newer derivative of fluorescein was reported, named Virginia Orange (figure 17); this new fluorophore is reported to be an exceptional scaffold for both single and dual substrate additions. Unlike its parent framework fluorescein, a single substrate addition is reported to be sufficient to suppress fluorescence in Virginia Orange. The fluorophore can also accommodate two independent moieties which can help improve specificity when doing target studies, as removal of both groups would be necessary to generate fluorescence.[91]

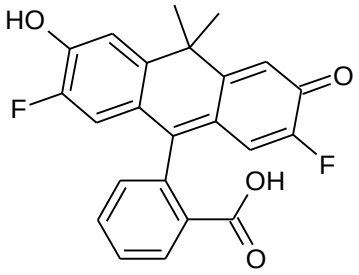

Virginia Orange

Figure 17 – Structural representation of newer derivative of fluorescein - Virginia Orange.

(i)

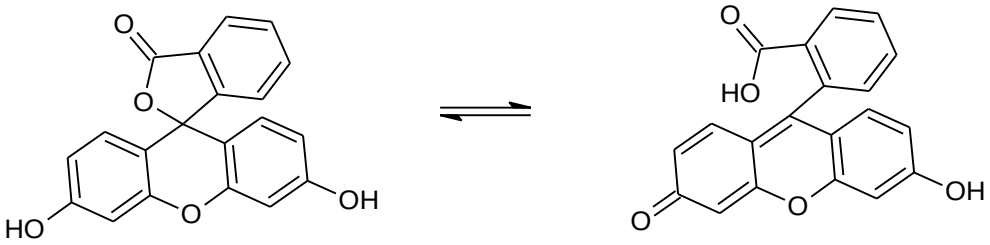

'closed'
Less - fluorescent form

'open'
Fluorescein in fluorescent form

(ii)

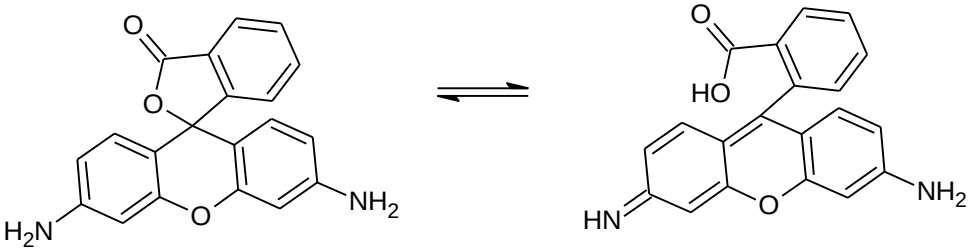

'closed'
Less - fluorescent form

'open'
R-110 in fluorescent form

Figure 18 – Structural representation of equilibrium for R-110 and fluorescein in an aqueous solution.

For our project we required a fluorophore that is non toxic, cheap, commercially available and that has a free amino terminus for a stronger amide attachment to the carboxyl terminus of the substrate sequence instead of an easily hydrolysable ester linkage thereby improving the overall selectivity and shelf life of the probe. In order to meet these requirements, we were limited to consider the following fluorophores for this project: Coumarin derivatives and R-110 – structures in figure 19 and their spectral details and existing fluorogenic substrates are described in table 8.

Fluorogenic leaving groups	**λ_{Ex} (nm)**	**λ_{Em}(nm)**	**Example of fluorometric enzyme assay components**
7-amino-4-methylcoumarin (AMC)	365	455	Substrate-Cbz-Gly-Pro-Arg-AMC Enzyme - Granzyme A[92,93]
7-amino-4-trifluoromethylcoumarin (AFC)	400	505	Substrate-Cbz-Asp-Val-Ala-Asp-AFC Enzyme – Caspase[94]
7-amino-4-carbamoylmethylcoumarin (ACC)	350	450	Substrate-Ac-Arg-Lys-Ser-Leu-Val-Nle-ACC Enzyme - HIV-1 protease[95]
Rhodamine 110 (R-110)	485	535	Substrate-$(Boc\text{-}Val\text{-}Pro\text{-}Arg)_2$-Rhod, Enzyme – Staphylocoagulase[96]

Table 8 – Commonly used fluorophores for synthetic substrate assays. λ_{Em} - Emission wavelength and λ_{Ex} -Excitation wavelength.

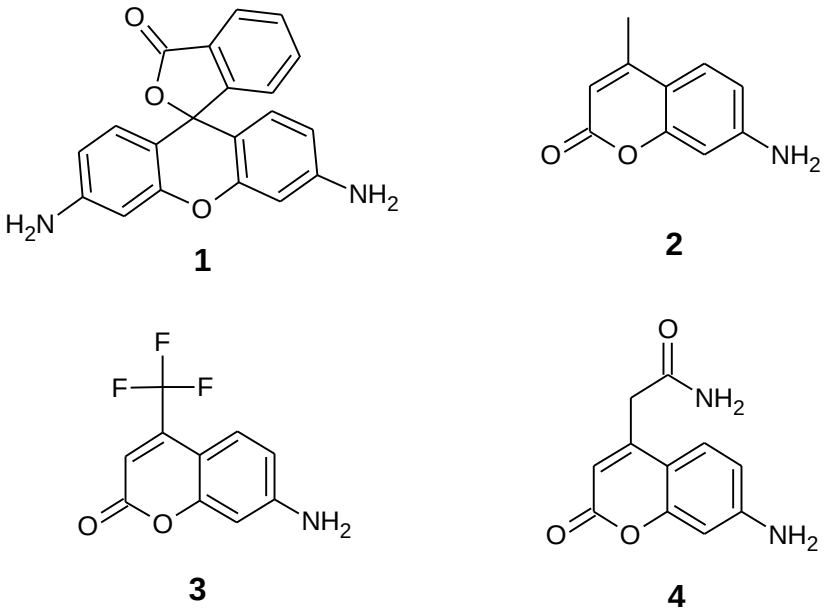

Figure 19 – Fluorophore structures – R-110; ε =8x 10^4 M^{-1} cm^{-1} at 498nm, φ = 0.91 (**1**),[97] AMC,(**2**), AFC (**3**) and ACC (**4**).

R-110 is preferred over coumarin derivatives because it has a higher extinction coefficient and fluorescence quantum yield, exhibiting a higher probability of energy loss from the excited state *via* fluorescence and not a non-radiative mechanism; this is a desirable property as it is capable of improving the overall sensitivity of the detection assay, thereby allowing lower concentrations of enzyme and substrate to be applied efficiently. Another advantage for using R-110 as a fluorogenic substrate is that it effectively circumvents inner filter effects - a common problem faced in fluorescent assays, as the fluorophore is positioned in the red region of dyes with a longer wavelength and most organic molecules tend to absorb at shorter wavelengths.[98]

Substrates made using R-110 are commonly synthesised as a symmetrical molecule with both amino moieties holding the same substrate mimics - usually peptide fragments, this coupling process is described by Bywaters *et al*. as difficult, reflected in very low yields and reported to be less amenable to scale up processes and the

reason to why Rhodamine fluorogenic substrates are less widely used for microbial detection.[99] The structure of R-110 implies a bi-substrate attachment, necessary for suppressing fluorescence efficiently, most commonly in a symmetric fashion; therefore asymmetric substitution of the amino groups would require a number of extra steps resulting in an even lower over yield.[100] Although, the fluorescent mono-substituted substrate is sought after in some cases, as in 2001, Cai *et al*. report the synthesis of mono-substitution of the amino group with an enhancer moiety to improve cell penetration, N-Ac-DEVD-N0-octyloxycarbonyl-R-110 and reported the substituted rhodamine derivative to be efficiently cleaved by the human recombinant caspase-3 and apoptotic HL-60 cells thereby presenting potential use in studies of apoptosis inducers and inhibitors. More commonly now this red-shift dye is used for enzyme-substrate assays and high throughput screening approaches for establishing compound profiles.[101,102]

The acylation / amidation of the free amino groups in the original R-110 structure locks the dye into a lactone form, in this state the dye exhibits no colour and negligible fluorescence (figure 20). The zwitterionic nature of the dye in an aqueous solution giving rise to fluorescence, this unique property observed is only reported in rhodamine, fluorescein and its analogues.

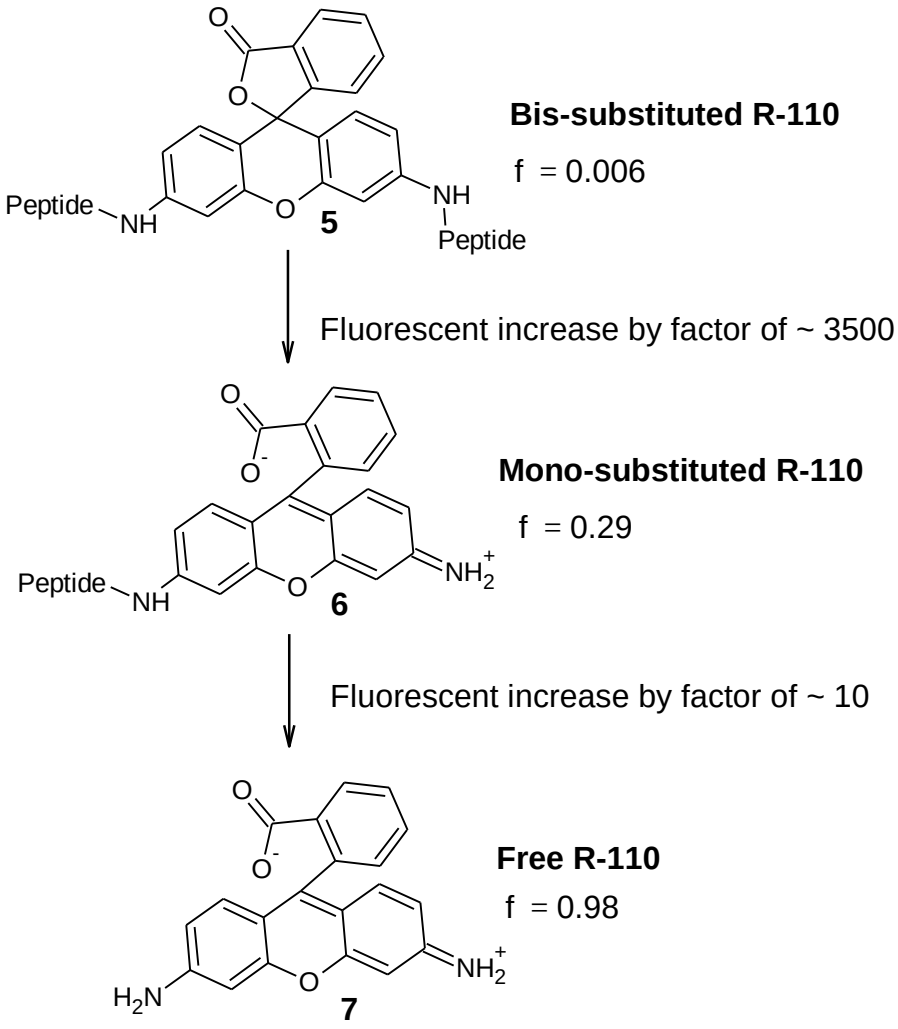

Figure 20 – Peptidase activity on R-110 analogues and their fluorescence profiles.[94 , 95]

1.3.4. FRET assays

Another commonly used strategy for protease based assays is FRET, this sensitive technique utilises two light sensitive molecules with a distance dependant interaction; one fluorescent quenching and the other fluorescence emitting. The fluorophore / quencher pair is selected so the absorption spectrum of the quencher matches emission spectrum of the fluorophore an example of a pair commonly

used is EDANS/DABCYL. The rate of energy transfer is determined using equation 1.

$$k_{\text{FRET}} = \frac{1}{TD}\left(\frac{R_o}{r}\right)^6$$

Equation 1– used to calculate rate of FRET and determine transfer efficiency.

TD - decay time of the fluorophore without a quencher
R_o - distance at which FRET is 50% efficient
r - distance between fluorophore and quencher
Förster distances have to be sufficiently close and these range between 20 - 90Å.

This FRET based enzyme assay has been used over the years to facilitate inhibition studies for many 3C proteases from different viral pathogens; enterovirus 71,[103] rhinovirus 14[104] and the Norwalk virus.[105] In 2007, Jaulent *et al.*[106] utilised the enzyme specificity insights reported by Curry *et al.* in 2005[107] as a framework to develop inhibitors of the $3C^{pro}$ and a continuous based FRET assay for FMDVs $3C^{pro}$. The assay was used in conjunction with the range of $3C^{pro}$ inhibitors synthesised to measure the activity of the enzyme being targeted. However, prior to this point there is a lack of convenient enzyme based assays for $3C^{pro}$. The direction of developing drug-based inhibitors by the research group was reported to be due to the political and technical problems associated with FMDV vaccine control, and $3C^{pro}$ was described to be their target as it is the principal enzyme in polypeptide chain processing to generate the viral proteome and therefore an attractive anti-viral target. The group synthesised a range of FRET substrates to test kinetics, they compared the rate of substrate hydrolysis in presence of the selected protease and found that FRET 4 gave the highest turnover rates, its structure comprised of a DABCYL group on the N-moiety attached to the peptide chain – APAKQ*LLD$_1$FD$_2$LLK, with the EDANS group attached to the side chain of the aspartic acid residue (labelled D_1-closest to the scissile bond).

1.3.5. Synthetic plan for FMDV probe and selection of fluorophore.

Taking into consideration the work published on the structure activity relationship of the $3C^{pro}$ with a peptide substrate mimic (shown in part 1.2.3.3, table 7) and the properties of suitable fluorophores for the development of the fluorogenic substrates for biochemical testing. We initially decided to plan the synthesis of a substrate mimic which comprises of a tripeptide sequence Boc-NH-Ala-Lys-Gln-OH attached to the N-terminuses of R-110, using the liquid phase peptide synthesis (LPPS) analogous to the reported LGX (figure 21) synthesis reported by Sinclair *et al.*[104] following the convergent synthetic plan. The aromatic nature of our fluorophore was predicted to mimic the natural hydrophobic interactions observed between the enzymatic cleft and the natural substrates peptide sequence, with this we were hoping to test the limits of the target enzymes reported enhanced malleability. Commonly fluorogenic substrates are developed to have a tripeptide sequence XYZ-F*,[108] this is therefore our initial approach to this project.

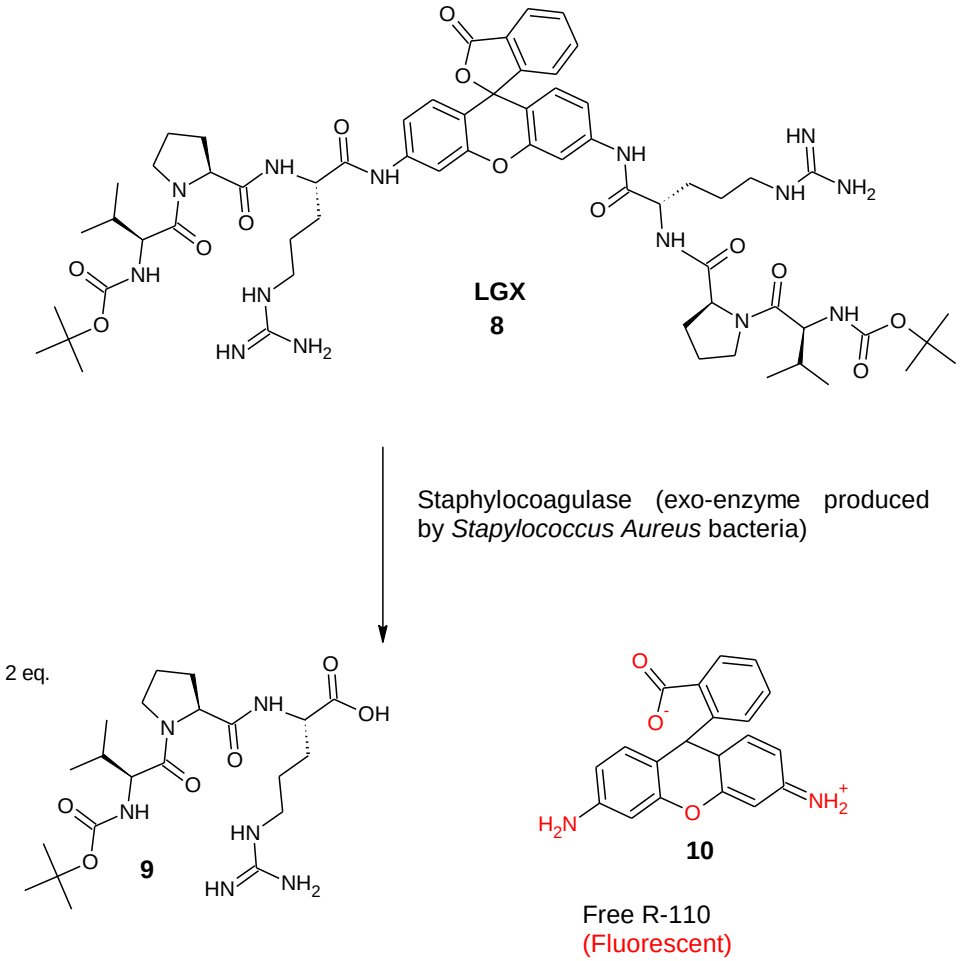

Figure 21- Structural representation of the LGX model[109]

R-110 is reported to be a superior fluorophore than its coumarin derivatives, as it has a higher quantum yield, this property provides higher sensitivity in terms of detection and most recently has been successfully incorporated in bacterial detection, we therefore hoped to transfer this success to FMDV detection by incorporating in our initial attempts to synthesise a fluorogenic substrate.

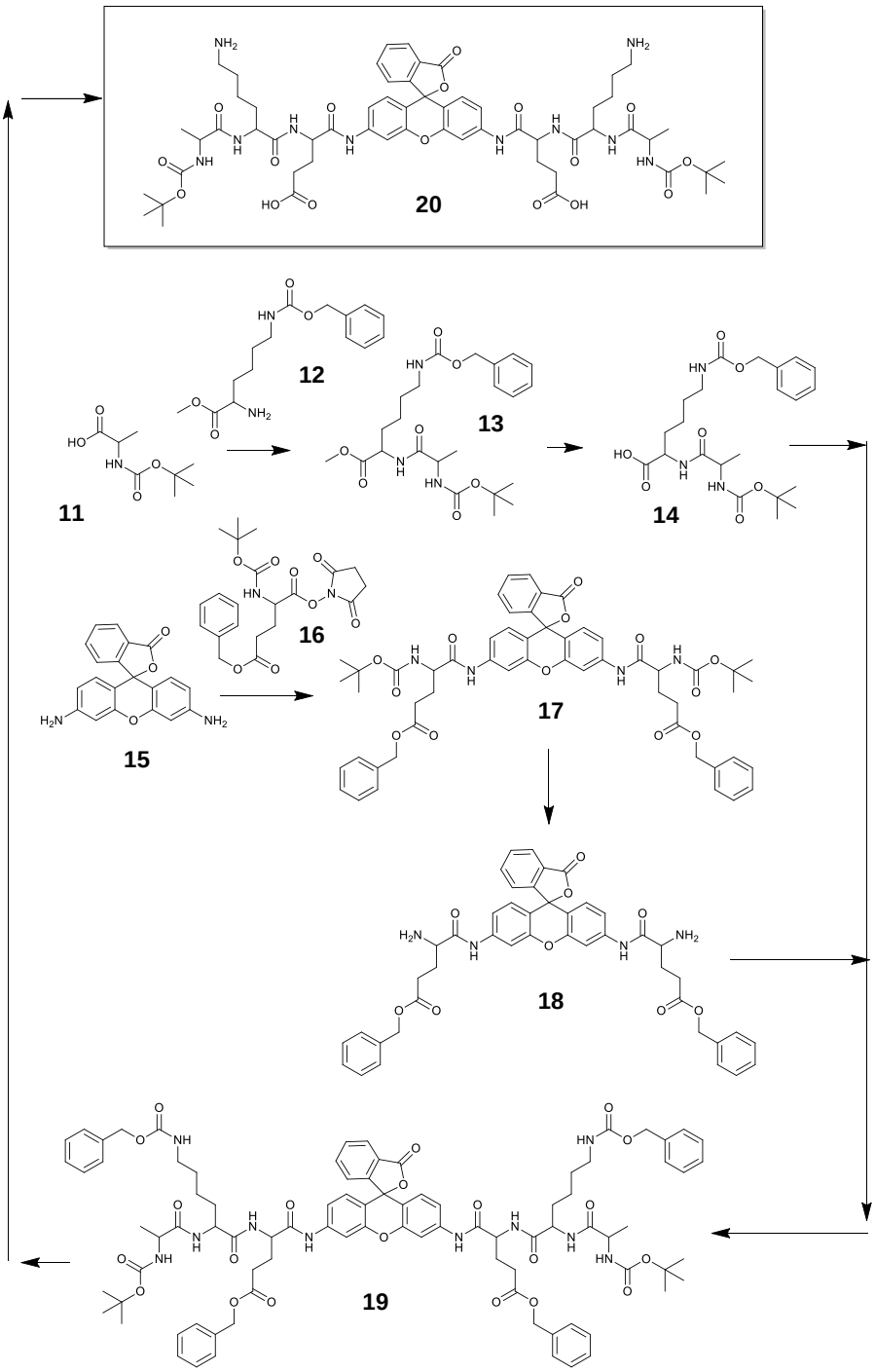

Figure 22 - Initial synthetic plan in order to produce the FMDV probe, optimum coupling conditions to be determined experimentally.

CHAPTER 2: Results and Discussion

2. RESULTS AND DISCUSSION

2.1. SYNTHESIS OF FLUOROGENIC SUBSTRATE

This chapter covers the different synthetic routes attempted in order to make ourfluorogenic substrate /detection probe in order to progress on to biological testing with the selected target enzyme $3C^{pro}$.

2.1.1. Synthetic attempts for total synthesis of the target fluorogenic probe (Ala-Lys-Glu/Gln)$_2$-NH-fluorophore.

2.1.1.1. Peptide fragment synthesis following a convergent synthetic route.

Peptide synthesis is challenging but can be achieved using different techniques; generally small chain peptides are successfully isolated using liquid phase peptide synthesis, however, with increasing chain length the process becomes more difficult due to the presence and nature of side chains that can cause a number of synthetic difficulties due to problems arising solubility and purification. The main drawbacks associated with liquid phase peptide synthesis methodology isthat it is a time consuming procedure and a low yield of the desired polypeptide is often only successfully isolated after the series of purification steps involved. Therefore the presence of these side chains requires a careful combination of orthogonal protecting groups, coupling reagents and racemisation suppressants to be used in developing the synthetic plan.[110]

In 1963, Merrifield first introduced the methodology of solid phase peptide synthesis (SPPS)[111], a method developed to overcome the problems associated with the traditional solution based method. The concept involved the peptide sequence elongation on a solid support, where each reaction step is followed with filtration of unreacted reagents in the reaction mixture alongside any unwanted side products, leaving the desired product attached

to the resin, that is cleaved off the resin as the final step of the synthesis. SPPS has been widely used since 1963 to make peptide sequences as peptide based therapeutics are growing in demand. However, this method isn't compliant with the fluorophores considered in this project as tethering a reactive functional group on to the resin would involve attachment of the same moiety that would be targeted for peptide elongation. And thereby rendering that moiety unusable until it is removed from the resin.

Two general strategies are followed when synthesising sequenced molecules, these approaches are the convergent strategy or a linear strategy. The convergent strategy is reported to be the chosen approach when dealing with complex peptides in solution and involves synthesising separate fragments and coupling them together; on the other hand the linear strategy involves a step by step addition and is preferred in SPPS. Therefore the convergent strategy was the initial approach used to synthesise our target fluorogenic substrate following the liquid phase approach, this combination was favoured due to the reported ease of purification steps when considering smaller fragments and most importantly an improved overall yield of the final product. This approach required looking at our target compound as two fragments and devising a synthetic plan to couple them together.

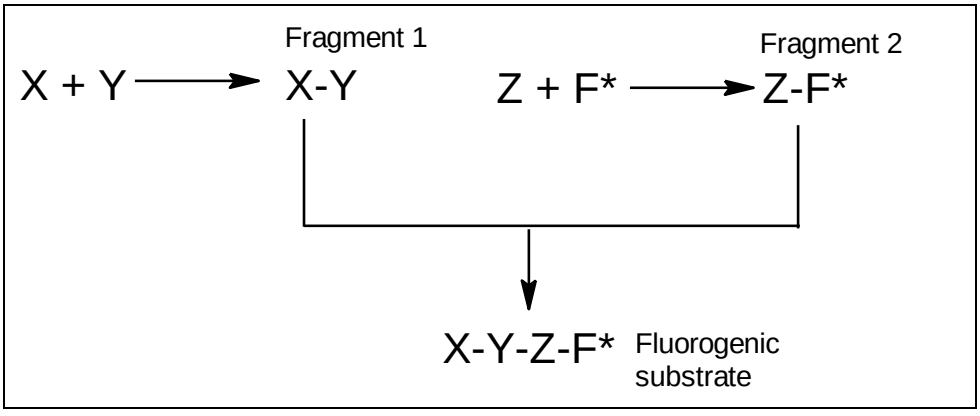

Scheme 1 - A schematic representation of a convergent synthetic plan for our target fluorogenic substrate, F* = fluorophore, X Y Z – generic letters representing amino acids.

2.1.1.2. Fragment 1 synthesis

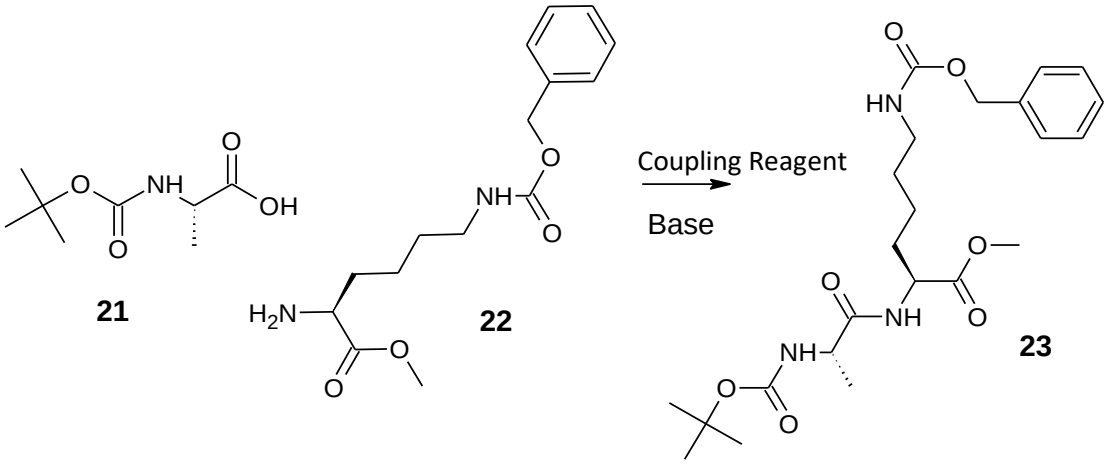

Figure 23 - Coupling of BocAlaOH to Lys(Z)OMe to synthesise the protected version of Fragment 1.

The dipeptide synthesis was optimised using a number of coupling reagents listed in table 9 and the best yielding combination was found to be HATU/DIEA used for the scale up process, to stock pile the dipeptide for future synthesis.

Coupling Reagent	Percentage yield
EDC	0% - no reaction progression observed with a series of experiments run at different temperatures ranging from room temperature to microwave conditions. Other variances incorporated in experiments include: number of equivalents of the coupling reagent and in other experiments the equivalents of base.
COMU	13.8%
HATU	25.6%
EEDQ	15.3%

Table 9 – Optimisation of fragment 1 and the associated percentage yields.

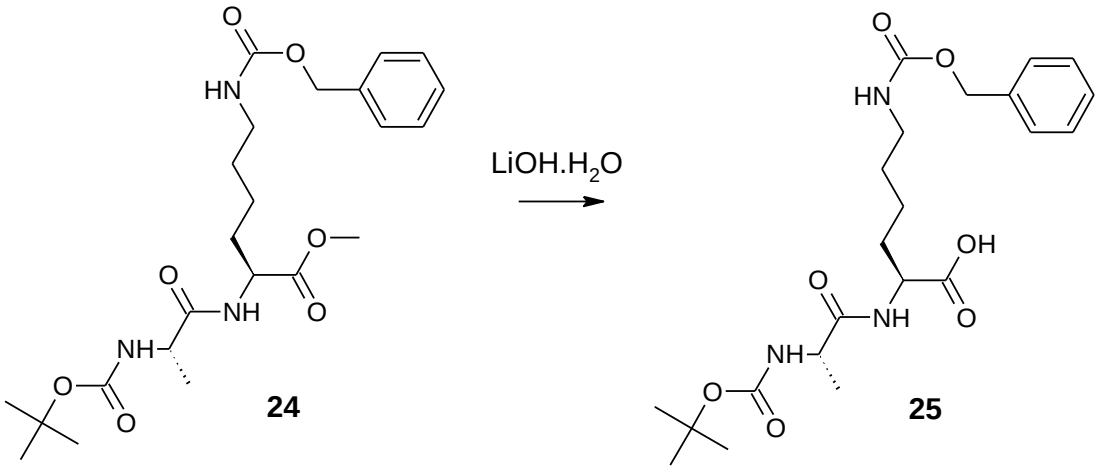

Figure 24 - Deprotection of methyl ester of BocNHAlaLysOMe, **24**, to give BocNHAlaLysOH, **25**.

The deprotection of the methyl ester was achieved under basic conditions in a biphasic solvent system of 1:1, THF:H_2O mix, this solvent mix is chosen as THF is able to dissolve water to 25% v/v this allows contact of the aqueous base predominantly present in the aqueous phase with the organic compounds dissolved in the organic phase. This biphasic solvent system thereby allows nucleophillic attack of the hydroxyl group, thereby removing the methoxy group in the form of methanol. The by-product methanol dissolves in the aqueous phase and is removed.

2.1.1.3. Fragment 2 synthesis

Unfortunately, synthesis of fragment 2 wasn't as straightforward as fragment 1, the coupling described in figure 25 encountered problems, discussed in 2.1.1.4. Initially, we chose to use glutamic acid in place of glutamine as the amino acid adjacent to the fluorophore, due to the side chain protected versions of glutamine commercially available not fitting the synthetic strategy of deprotection when devising a synthetic plan and therefore further steps would be needed to reach the target compound. This substitution was deemed suitable as it would have minimal effect on the biochemical testing

and allow us to move forward to biochemical testing sooner with a sufficient amount of product.[112]

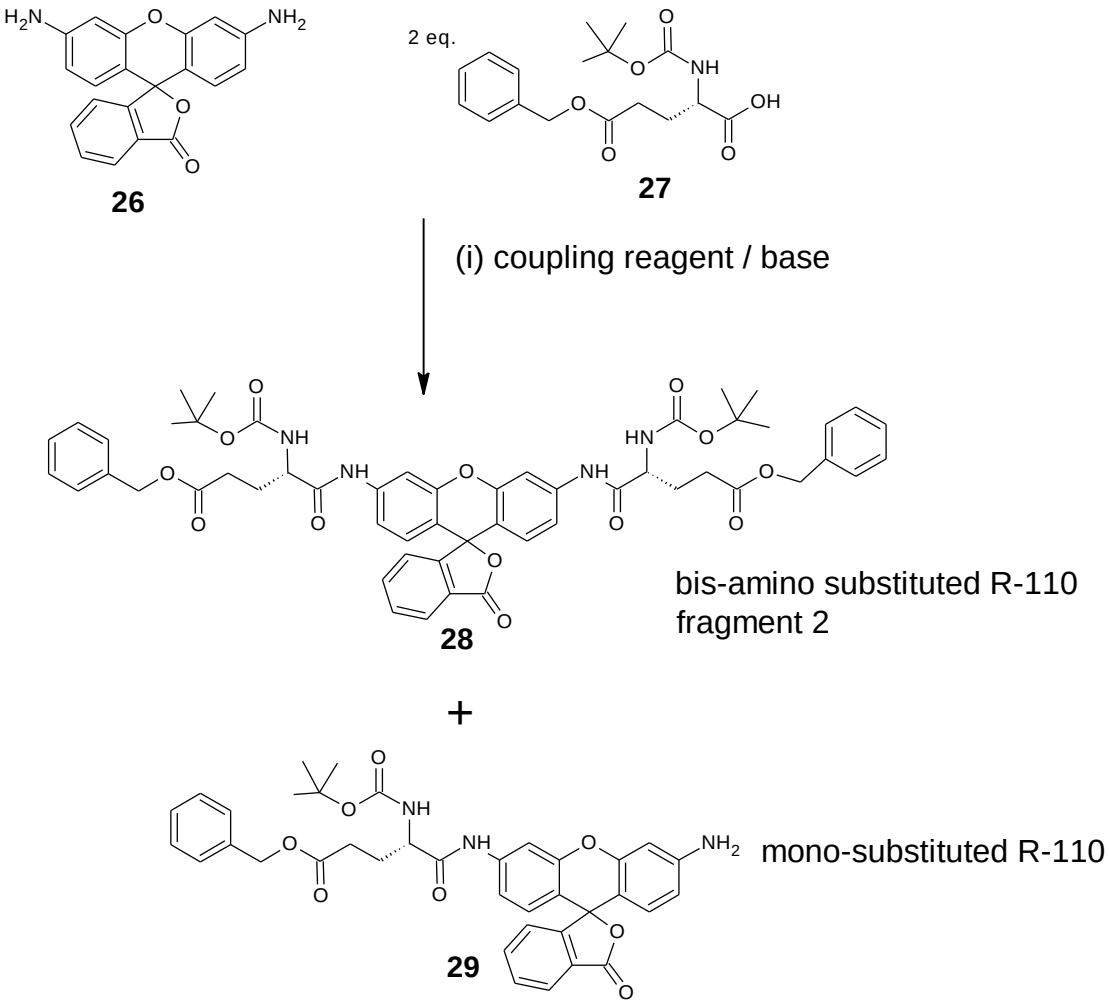

26 **27** **28** **29**

Figure 25 - Coupling reaction of fluorophoreR-110 with amino acid: Glutamic acid.

2.1.1.4. Different synthetic approaches to synthesise fragment 2

2.1.1.4.1. *Peptide coupling* reagents

Coupling Reagent	Outcome
EDCi	0% - yield, no reaction progression observed
COMU	Unresolved via manual purification methods– but evidence of coupling via TLC analysis.
HATU	Unresolved via manual purification methods – but evidence of coupling via TLC analysis.

Table 10 – Different coupling reagents used to improve overall yield of target compound.

Coupling of fragment 2 in terms of ease of handling, and purification proved to be capricious in nature, resulting in very low overall yields,this was believed to be due to the reactive amino groups on the R-110 being poorly nucleophillicdue to intrinsic resonance effects resulting in a mixture of analogues – unsubstituted free rhodamine, a mono amino substituted R-110 and bis amino substituted R-110. A possible reason to why very few rhodamine-peptide based fluorogenic substrates are available commercially and in publications, despite R-110 having such favourable properties for acting latent in a fluorogenic substrate until cleaved in minute amounts.[113]

Optimisation of the essential coupling of an amino acid to fluorophore to synthesise fragment 2 involved testing a range of coupling reagents, listed in table 10 and we found the coupling reagents COMU and HATU to give evidence of successful coupling via TLC. To improve target coupling and purification, the following changes were applied to the reaction conditions and isolation:

i) using an excess amount of amino acid was experimented with, in the hope to promote reaction completion, however, this wasn't the case, the excess amino acidcaused problems with TLC analysis – a crucial tool for investigation, as it significantly increased the amount of streaking on the TLC plate usually a sign of overloading a silica plate and this was the case even after successive dilutions of the TLC sample, this problem translated over to the silica based column causing a mixture of components to elute per fraction. After careful examination of a series of increased glutamine/ glutamic acid reactions it was determined that a slight increase in the number of equivalents to 1.2 equivalents per amino moiety being substituted was sufficient, provided the excess was removed before spectroscopic analysis and purification steps. This was achieved by incorporating extra water washes during the solvent extraction work up procedure. However, the addition of extra water washes could increase number of water molecules in contact with products promoting hydrolysis.

ii) In another effort to improve overall yields of the coupling reaction, higher equivalents of base was tested - ranging between 2 – 10 eq. for $NEt_3$and DIEA; unfortunately the higher concentration had very little effect. Therefore as a more drastic change the stronger base sodium hydride was experimented with and again this showed no significant improvement in yields.

Furthermore, purification of the reaction mixture with varying substitutions *via* column chromatography was challenging with the added disadvantage of the target compound decomposing when in contact with the commonly used stationary phase; silica. This decomposition was initially observed as a change from a colourless spot on a silica plate turning a yellow colour over a few minutes and was further investigated using 2D TLC.

2D TLC involved running a TLC plate in its usual way on a square silica plate with a spot of the sample being investigated in the corner of the plate. After the

sample was run, a vertical line of compounds were visible, the plate wasrotated 90 degrees and ran again. The second solvent elution spots the compounds and the positioning above or below the diagonal line were indicative of decomposition as seen with rhodamine based crude mixtures.

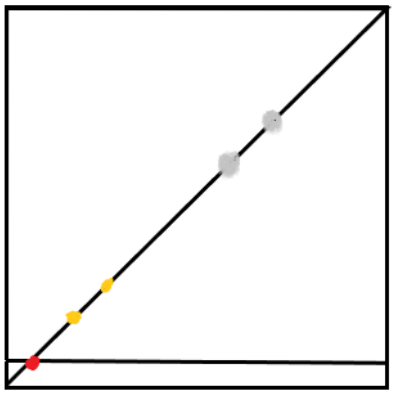

Figure 26 – A pictorial representation of a reaction mixture that has components that are stable on silica, spots are positioned on diagonal line.

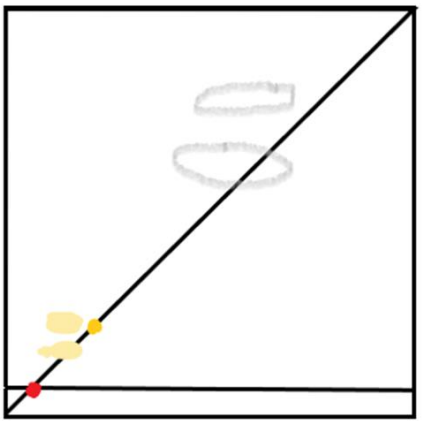

Figure 27 – A pictorial representation of 2D TLC plate of coupling reaction of an BocGlu(OBz)OH and R-110.

Initially, the stationary phase was chosen to be the most commonly used material in most labs for column chromatography, namely silica. Silica has great separation properties, but on reviewing purification issues and evidence of decomposition of our reaction mixture caused by the lone acidic silanol

groups it was thought to be advantageous to try other stationary phases; alumina and reverse phase silica. Alumina is considered to be milder than normal phase silica, with a lower loading capacity and separation resolution than silica compared weight by weight. Alumina surface is less polar than silica, therefore the eluting solvent was adjusted to be less polar too – 2% MeOH:DCM mix from 5% MeOH:DCM mix. However, these TLC plates showed similar streaking/ trailing of spots as observed on silica plates, this was considered to be down to hydrolysis of the compound when in contact with the silica surface. The reverse phase silica is non polar therefore also eliminating any catalytic activity that could be responsible for the decomposition observed, it requires a polar mobile phase therefore 1:1 ACN:H_2O mix was used, results showed more intact spots however purification in a saturated aqueous environment also resulted in lower yields.

Another variance tested in order to improve purification and the overall yield was different ratios of the eluting solvent mixes and their application on to column chromatography. Initially, an isocratic gradient of 1:1 petroleum ether: ethyl acetate wasused for resolution, from previous experiments it is known that decomposition occurs when exposed to silica for during a purification run, it was therefore thought that by increasing the polarity of the solvent mix slowly during the run it may help push the samples out of the column quicker thereby minimising its contact time with silica and hence reduce chance of decomposition, the two solvent mixes that were tested are:

i) Petroleum ether and ethyl acetate

ii) Methanol and DCM

For the first solvent pair the column was initially run at a 1:1 ratio of both solvents, the compound separation was visualised using a UV lamp as the column began to run and as the bands began to resolve the amount of ethyl acetate was increased from 50%-100%. The second set of solvents were selected for testing as methanol is commonly used to flush organics of a column, therefore the amount of methanol was increased in percent increments

from 2% - 5%, the polarity was increased once the separation was visualised using the UV lamp. However, it was found that increasing polarity caused more overlapping in fractions resulting in the need of repeating the column and thereby defeating the purpose of reducing exposure time with the stationary phase, even with increased number of fractions being isolated.

After multiple purification attempts using a range of different variances the isolation of the pure disubstitued rhodamine was difficult, although successful coupling was apparent at a small scale (25 mg – starting material R-110) by TLC analysis, however, the reaction conditions when applied on a larger scale failed to produce the disubstituted rhodamine and successful isolation of the desired disubstituted rhodamine from the small scale reaction was impossible without the use of preparative HPLC.

As using coupling reagents to gain the disubstituted rhodamine was found to be inefficient, in order to gain a good yield of the pure disubstituted rhodamine compound, another approach researched was using the retro-synthetic strategy. However, despite many applications associated with the fluorophore R-110, the synthesis of the main framework of R-110 is described by Grimm et al. as being difficult and archaic and therefore this approach wasn't thought to be suitable for the rhodamine based compound.[114] The group also reportedcoupling to the elusive rhodamine molecule often resulted in less efficient acylation, amidation of the amino moities due to it's nitrogens being low in nucleophilicity, as we also established through testing different coupling reagents described in this section and so other synthetic approaches for fragment two were then sought and are described herein.[115]

2.1.1.4.2. Buchwald-Hartwig coupling of nitrogen nucleophiles with ditriflate fluoresceins.

From an extensive literature search on synthesis of R-110 analogues, another route based on Buchwald-Hartwig coupling was found and considered noteworthy. This approach was of particular interest because it reported an efficient strategy for preparing rhodamine derivatives from fluorescein ditriflates from palladium – catalysed C-N cross-coupling with a range of of nitrogen nucleophiles including free amines and amides, although bonding to our target amino acid isn't specifically described, this method was trialled to synthesise fragment 2 because it involved the cheaper, more readily available fluorophore fluorescein (£71.30/g), whereas R-110 (£255/g), prices stated were correct in May 2018. Also attention was drawn to this method because the problematic amino moieties weren't already apart of the xanthene framework, illustrated in figure 28.[116]

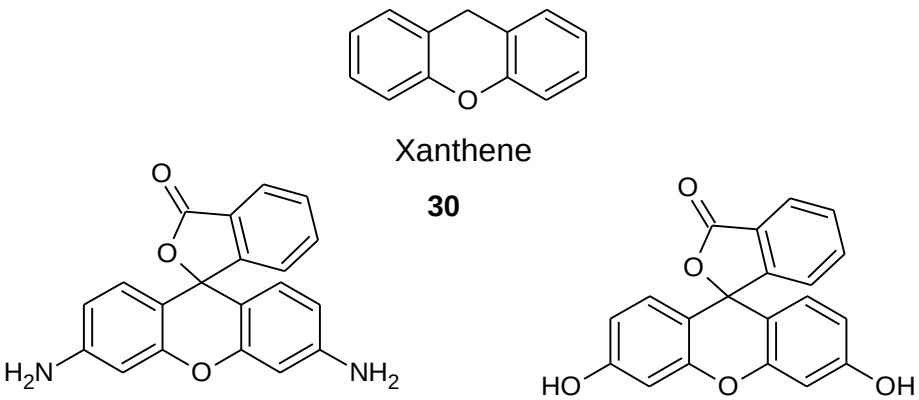

Figure 28 – Structure relationship between xanthene dyes.

Triflate	Percentage yield
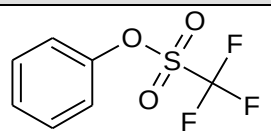 **33**	61%
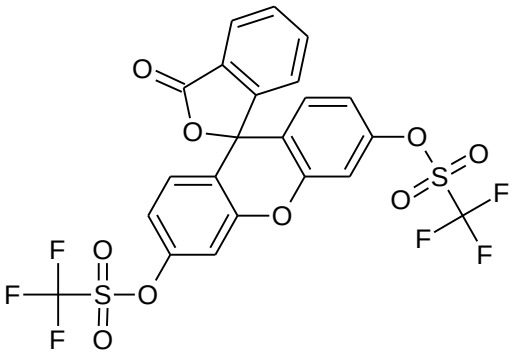 **34**	47%

Table 11 - Triflation was achieved for a simple phenol and fluorescein following method described by Grimm and Lavis.[117] Conditions for **33**: hydroxybenzene, DIEA, trifluoromethansulfonic acid; initial suspension prepared at 0°C thenheated to room temperature over 1.5h. Conditions for **34**: pyridine, trifluormethanesulfonic acid; inital suspension prepared at 0°C then heated to room temperature for 5h.

The sulfonation step was followed by the Buchwald-Hartwig coupling, catalytic cycle shown in scheme 2, using the amino acid, H-Gln-NH_2, figure 29.

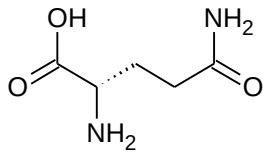

Figure 29 - Structure of H-Gln-NH_2.

Although two amido nitrogens are present, the compound was still used as it gave two routes of possible binding. Two test reactions were run following the reported experimental method, (i) under a N_2 atmosphere at 80°C for 3hrs and (ii) under microwave reactor conditions for the equivalent of the reported 100°C for 18 hrs. However, both test reactions produced the parent compound fluorescein through triflate hydrolysis,we found detriflationto bea problem, also highlighted by the authors Grimm and Lavis, who have described the unwanted competitive side reaction through hydrolysis can be minimised by using a higher loading: 10% of Pd and 15% ligand per triflate in the reactant compound.[107]

Still, even with the increased loadings the same detriflation was observed via spectroscopic analysis in our synthesis. Although, this method possibly requires trialling different reaction conditions to promote the desired synthetic outcome. However, due to lack of reported evidence of it working with our target amino acids in literature, in the interest of time and limited resources associated with the microwave reactor, alongside the previous failed coupling attempts using R-110 and it's framework, the decision was made to research andfollow a procedure where glutamine was reported to be attached to a fluorophore or to look at further simplifying the synthesis of fragment 2, this was thought to be the best choice to complete total synthesis instead of making small changes to the variances associated with this method, in order to move on to biochemical testing and therefore this method was not further considered.

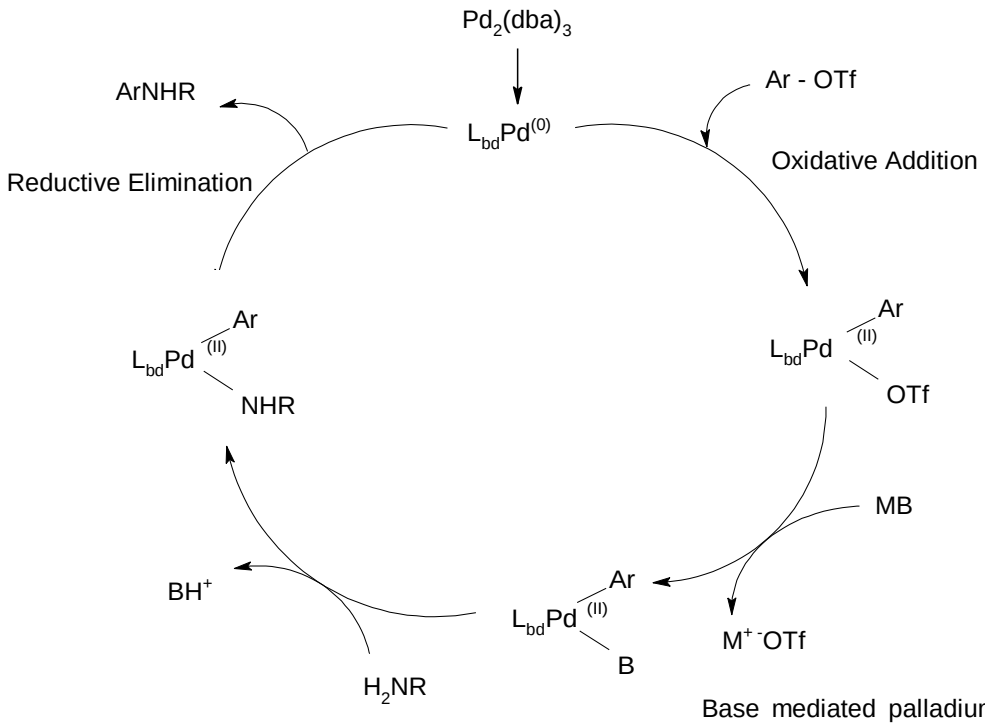

Base mediated palladium - amide bond formation.

Scheme 2 - The catalytic cycle for Buchwald-Hartwig C-N cross coupling, where L_{bd} is the bidentate ligand, xantphos; MB is the metallic base, CS_2CO_3; Ar is the aryl framework of the fluorescein/rhodamine structures; and OTf is the triflate group.

2.1.1.4.3. *Substituting complex xanthene dye for a simpler coumarin dye.*

As a result of the ongoing problems associated with the essential coupling reaction of the fluorophore–amino acid, the decision was made to substitute the complex xanthene dye (R-110) for a simpler flurorophore, one with a simpler frame and a single amino moiety to grow the peptide part of the substrate chain from, thereby eliminating problems with purifying an unstable mix of products as previously seen with R-110 crude mixtures, the new fluorophore selected was AMC, figure 30.

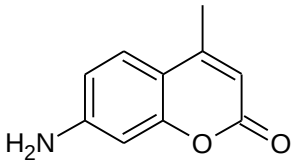

Figure 30– Structure of AMC

2.1.1.4.4. Peptide coupling reagents

A series of peptide coupling reactions were done in order to identify the best coupling reagent of the new fluorophore AMC with the amino acid unprotected glutamine, yields of tested reagents are listed in table 12. It was found that the coupling was achieved at low overall yields, similar to the rhodamine molecule described in section 2.1.1.4.1. The advantages of the AMC over the R-110 was the number of products visualised *via* TLC analysis were less, as expected, due to the reduced number of amino moieties present in the AMC fluorophore. However, the crude mixture was a brown like slurry that was very difficult to redissolve for purification steps even with the use of sonication this was thought to be a consequence of the compound being hygroscopic. Eventually *via* preparative TLC fragment 2 was isolated and the final coupling of both

fragments was achieved using HATU, a novel probe the fluorogenic substrate BocAlaLys(Z)GlnAMC was synthesised and isolated.This compound was stored at –5°C in a freezer, however, the compound's integrity was tested on arrival of the biological enzyme a month later, before proceeding on to the biological testing phase of the project, using TLC the presence of the free AMC (R_f = 0.4, 5% MeOH:DCM) was evident and the need for further purification was an option but at the cost of losing more yield. Another problem associated with this particular method was that it was found not to be amenable to the scale up process to stockpile fragment 2, therefore multiple purification steps were deemed unsuitable for this unstable fragment and therefore other synthetic routes were explored, discussed in 2.1.1.4.5.

Coupling Conditions	**Percentage yield**
EDCi	0% - no reaction progression observed with a series of experiments run at different temperatures ranging from room temperature to microwave conditions. Other variances incorporated in experiments include: number of equivalents of the coupling reagent and in other experiments the equivalents of base.
COMU	0.57%
HATU	1.25%

Table 12 - Different coupling reagents used to improve overall yield of target compound.

2.1.1.4.5. Azide synthesis and selenocarboxylate amidation

With the view of changing the poorly nucleophillic aromatic amino moieties present in the fluorophore part of the fluorogenic substrate to a different nitrogen source, a literature search was conducted on other nitrogen sources that can be used in non-nucleophillicamidationmechanisms, this reviewal led the project in the direction of azides, as azido moieties are described neither to be nucleophillic or basic and their conversion to amide bonds is possible by a number of strategies; Staudinger ligation, Williams thio acid / azide amidation and the more recently published selenocarboxylate / azide amidation.[108]

L. Hu, *et al*. published significant research efforts on promising methods of efficient amidation of aromatic amines using selenocarboxylate / azide amidation. The group deduced that selenocarboxylates are more reactive than thio acidson comparing selenocarboxylate / azide amidation to thio acid/ azide amidation, by specifically comparing reaction progression in the presence of a sterically hindered azide, where the thioacid was reported to show no reaction progression whereas the selenoacetic acid reacted to form acetamide, 75%, shown in figure 31. Therefore the selenocarboxylate / azide amidation route was thought to be potentially more capable of facilitating an amidation reaction hence selected to improve the yield of our target fluorogenic substrate.[118]

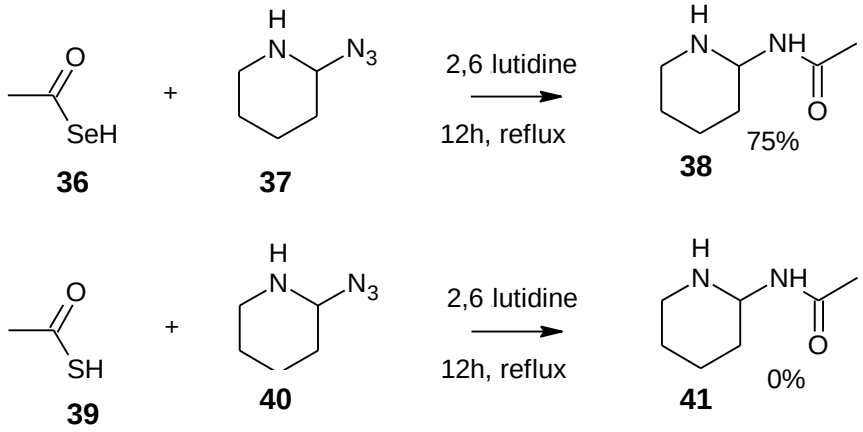

Figure 31 – Comparing azide reactions in presence of thio acid and selenoacetic acid.[115]

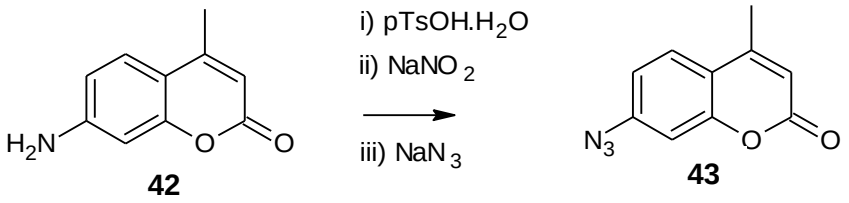

42 **43**

Scheme 3 – Synthesis of azido methyl coumarin (AzMC) *via* an *in situ* diazotisation to generate arene diazonium tosylates followed by azidation.[119]

Azide –chemical structure	**Yield**
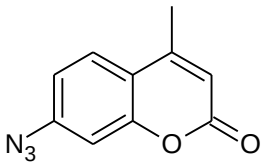 **44**	80-89%
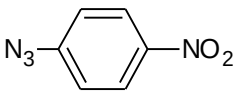 **45**	92%

Table 13 - Azides successfully isolated using experimental conditions highlighted in scheme 3.

The first step involved in the selenocarboxylate / azide amidation route is the conversion of the amino moiety to an azido moiety as described in scheme 3. The synthesis of AzMC was achieved efficiently with excellent yields at 89 - 92% by selecting a click reaction route published by Parello *et al*.[116] This was a one pot synthesis carried out in water which involved the preparation of the intermediate aryl diazoniumtosylate [Ar-$N_2^+TsO^-$] followed by a instant click reaction with the addition of sodium azide producing nitrogen gas and an insoluble aryl azide isolated *via* vacuum filtration. This reaction step was successful and confirmed by comparing experimental data to reference NMR and melting point data. Also the substitution of an amino moiety (electron donating group) with an azido moiety (electron withdrawing group) causes a distinct change in the proton NMR spectrum and used specifically as the point of investigation was the positioning of the aromatic proton signals in a proton NMR spectrum, as the signals move downfield with the same splitting pattern as the rest of the aromatic structure remains unchanged.

The scaling up of the AzMC was easily achieved and carried out to 0.25g, this class of molecule required careful storage, as azides are known to be energy rich molecules that can be both heat and shock sensitive and are reported to be capable of explosively decomposing with little input of external energy.Thesafe amount of AzMC ($C_{10}H_7N_3O_2$) to scale up to was evaluated before proceeding,using the guidelines; i) C to N ratio that states the number of N atoms in the azide shouldn't be more than the C atoms and ii) the 'rule of six' which states that every energetic group such as an azide (diazo / nitro) should be diluted by 6 carbon atoms being present in the compound. Using these guidelines it was determined that AzMC fit the more - safe category and upto 20g could be stored of its pure form, as a single azide group was being added and characterised.[120,121]

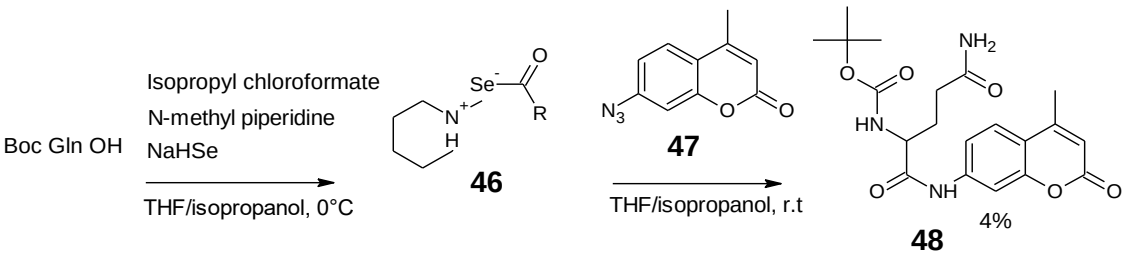

Scheme 4 – A three step, one – pot selenocarboxylate / azide amidation to synthesise Nᵅ – protected aminoacyl amino methylcoumarin.[122]

After isolation of AzMC was achieved, the first step of the one pot selencarboxylate / azideamidation described in scheme 4, involved preparing an isopropanol sodium hydrogen selenide (NaHSe) solution *via* a borohydride reduction. This was achieved by following the procedure published by L. Hu *et al*., the group reported isolation of BocGlnAMC, 84%, where the amount of $NaBH_4$ was at 1.2 eq. to every equivalent of Se dissolved into solution until a colourless solution was produced. This procedure was followed and allowed us to isolate BocGlnAMC, at only 4% overall yield.

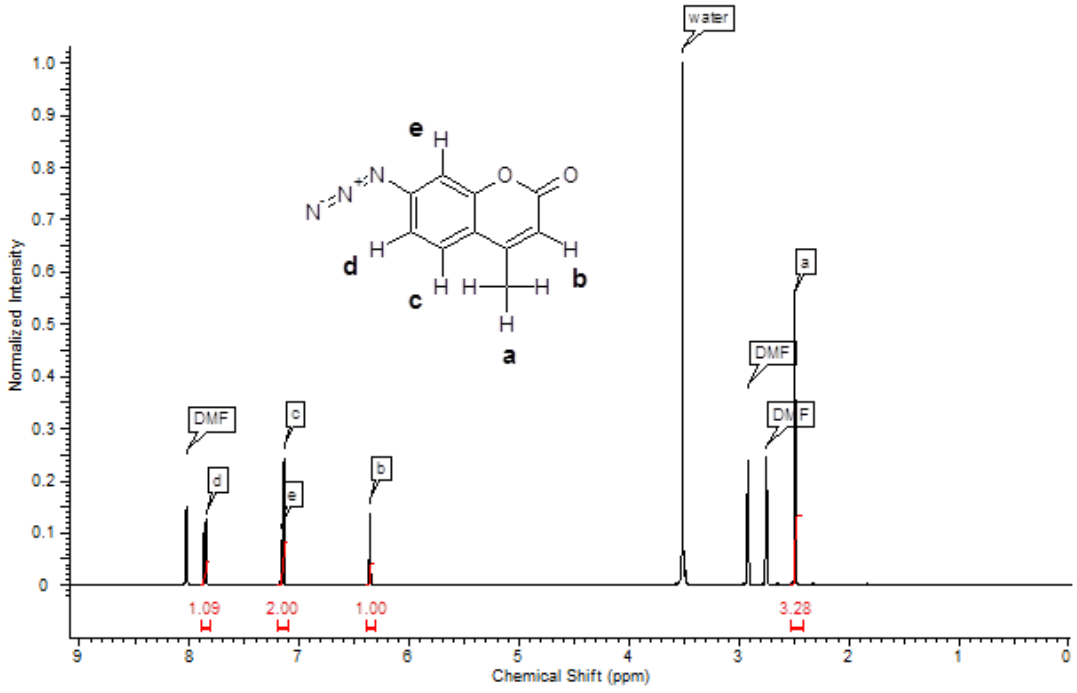

Figure 32 – ^1H NMR spectrum for AzMC in DMF, aromatic protons characterised using ^1H-^1H COSY 2D NMR spectrum (shown in figure 33).

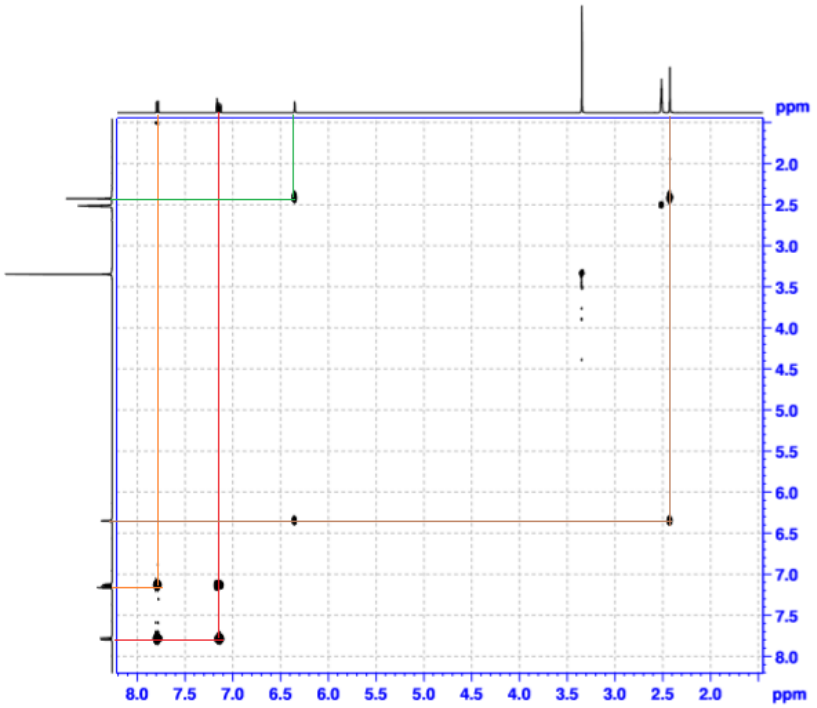

Figure 33 - ^{1}H-^{1}H COSY 2D NMR spectrum in DMSO for AzMC, showing interactions used to characterise aromatic protons labelled c and d in figure 32.

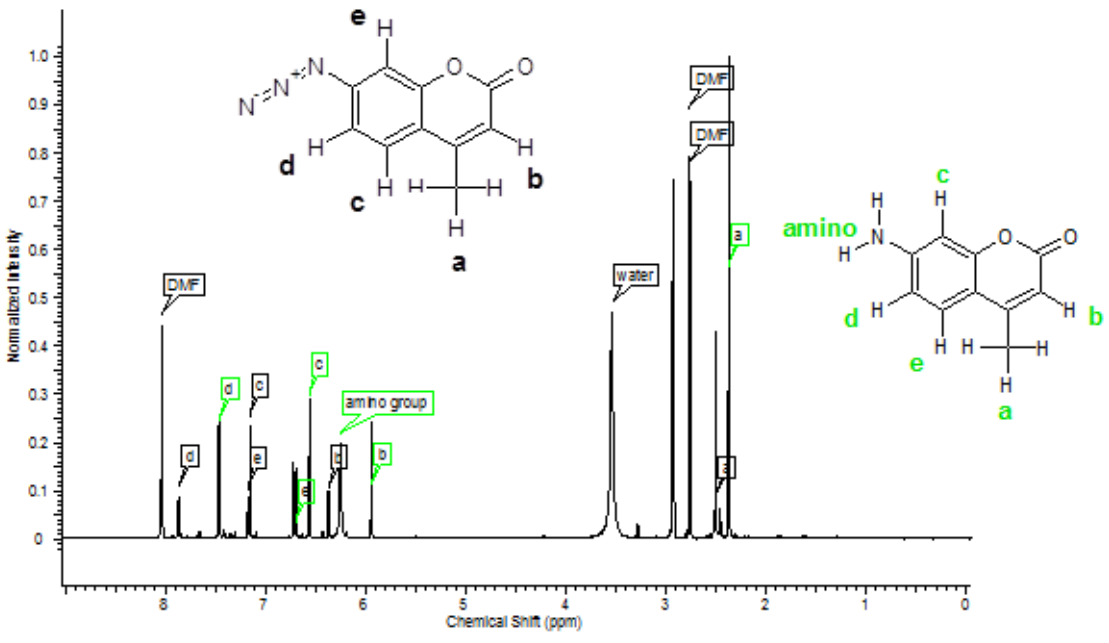

Figure 34– AzMC and 1 eq. $NaBH_4$ in DMF, reaction time 5 minutes at room temperature, experiment conducted in the NMR tube. The reduction of the azido moiety to the amino moiety is evident.

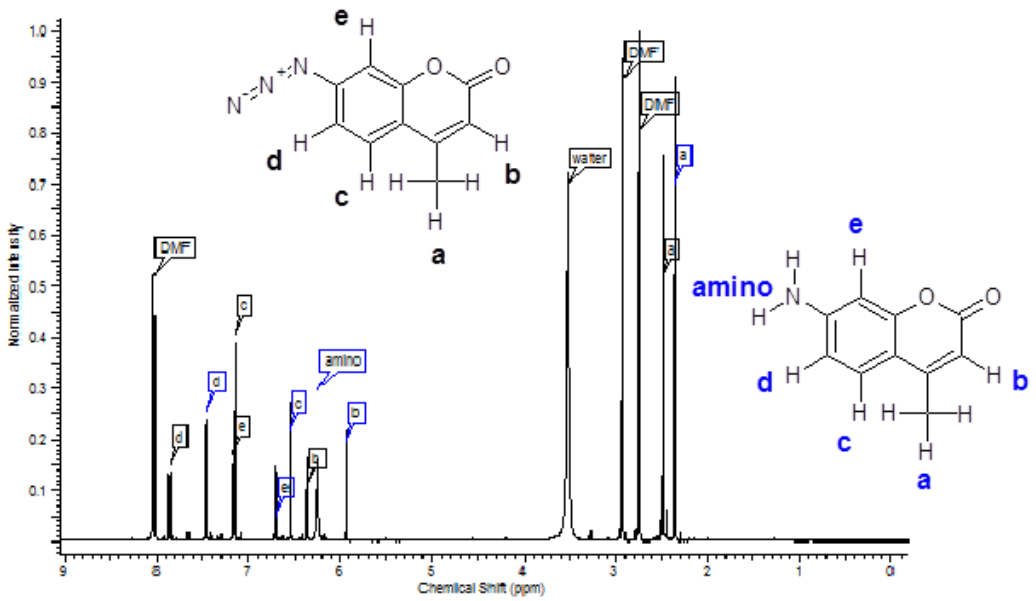

Figure 35 – AzMC and NaHSe solution, no reaction was observed after 5 minutes on comparison to figure 34, reaction time was therefore increased to 30 mins at room temperature, NMR run after workup, as original reaction mixture was saturated with isopropanol therefore reaction mixture was washed through celite and concentrated under reduced pressure and dissolved in DMF to obtain a comparable NMR spectrum to previous runs.The reduction of the azido moiety to the amino moiety is also evident.

In order to improve the overall yield of BocGlnAMC, the experiment was critically analysed and the reduced yield was initially thought to be due to trace amounts of oxygen getting into the reaction mixture atmosphere causing oxidation to diacylselenides, as carbonyl based selenium derivatives are described in literature as being relatively unstable that can undergo replacement of the Se atom with an O, N or S atom and convert to a more stable C-O bond.[123] Therefore, to minimise any loss of unstable selenocarboxylate *via* oxygen presence, the experimental set up for following reactions were conducted under an oxygen free, nitrogen abundant atmosphere passing through three separate dreschel flasks containing i) Feiser's solution, ii) concentrated sulphuric acid, then iii) sodium hydroxide pellets then a $CaCl_2$ packed tube prior to reaching the reaction vessel.[124]However, this intervention didn't produce the results we expected, the first reaction carried out caused no reaction to take place. Further experimentation was carried out using this set up and resulted oddly in100%

conversion to the original starting material AMC, confirmed by TLC and NMR analysis.

The low percentage yield and the full conversion from an azido to an amino moiety was furtherinvestigated and the rapid reduction of the azido moiety to an amino moiety was evident *via* NMR studies in presence of $NaBH_4$, as shown in figure 34 and therefore efforts to minimise unreacted $NaBH_4$ were undertaken, by reducing the slight excess to equimolar ratios. However, this modification had no significant effect in improving yield of the desired compound, therefore on further review another point for consideration was that NaHSe itself is also a mild reducing agent, therefore a test reaction was conducted with an azide being exposed to the NaHSe solution at room temperature. Interestingly we found *via* NMR (figure 35) and TLC evidence of reduction of azido moiety to amino moiety too.[125]

Moreover, it is known that H_2S can cause reduction of azides and of oxidised nitrogen species, this conversion is used in fluorescent probes and is accepted as a method to detect H_2S. H_2S has been recently recognised as the third endogenous molecule involved in signalling pathways, following NO and CO. Their presence is reported to be abundant in most tissues with diverse biological uses. H_2S specifically is known to be produced mainly by enzymatic pathways involving these enzymes; cystathionine β synthase, cystathionine γ – lyase and 3-mercapatopyruvate sulphur transferase. Studies have also shown that H_2S levels can be linked to a number of diseases including Alzheimer's disease, liver damage and diabetes. More recently studies have shown that H_2S levels can have neuroprotective benefits and maintenance of these levels can have therapeutic effects. Therefore researchers have highlighted the need to develop detection systems for H_2S, as described earlier it is linked to numerous physiological and pathological pathways in living organisms, however many of their molecular events are still unknown. Traditionally methods of H_2S detection included colorimetry, electrochemical assay, gas chromatography and sulphide precipitation. More recently fluorescent probes based on azido–R-110 have been developed, shown in figure 36.[126]

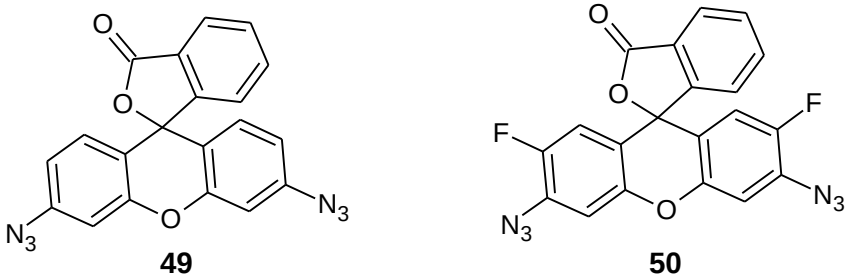

Figure 36 – Chemical representation of azido- rhodamine analogues.

Interestingly, this interaction of H_2S with azido moieties supports the possibility of H_2Se a by-product being formed (as shown in scheme 4) that can be potentially be responsible for the loss of the reactive azide functionality, as selenium and sulfur are two elements that are reported to have both similar physical and chemical properties.[127] Therefore the chance of H_2Se acting in a similar reductive manner to H_2S in presence of an azido moiety is a plausible concept. This specific property for H_2Se hasn't been addressed in literature before in this context, however, it is known that hydrogen selenide is a toxic volatile gas and in its lowest oxidation state (-Ⅱ) is capable of acting as a reducing agent and is readily oxidised by oxygen to it's more thermodynamically stable oxidation state Se(0) and water, hence in an oxygen free environment the H_2Se is still present thereby promoting reduction of the azido moiety to amido moiety as was the result of experiment described with Feiser's solution attached. Moreover, the reported pKa value for H_2Se is reported to be 3.89, therefore dissociation into free positive protons that can create an acidic environment would be considered not ideal for promoting amidation.[128]

In order to minimise loss of the azide functional group due to reduction, an alternative approach for the interconversion of carboxyl to selenocarboxylate was found in the form of using Woollin's reagent a selenium analogue of Lawesson's reagent, however the method of producing selenocarboxylates wasn't compliant with retaining the stereochemistry of the glutamine, due to the procedure involving reflux at a high temperature for long periods of time, this introduces risk of racemisation and therefore not used as retaining stereochemistry is crucial for optimal biological interaction. Also this method

would require complicating an already complex purification by introducing stereoisomers, also further reducing the overall yield of the desired product.[129]

Additionally, in terms of purification of fragment two, the reaction mixture was cleaner with respect to the number of compounds resolved from the reaction mixture in comparison to the R-110 based coupling to an amino acid. However, the crude product mix was difficult to get in to solution for purification, a range of different solvents: MeOH, THF, IMS, ACN, $CHCl_3$, DCM andEtOAc were experimented with in order to test the crude products solubility. Pure THF was chosen, as it gave the most dissolved compound after gentle swirling, oddly, we found that sonication caused more crashing out, NMR verified the material crashing out to have identical peaks as seen in the crude NMR spectra. The resultant solution of crude products was a kind of brown slurry like consistency, the poor solubility displayed by the crude mix presented problems of sample loading on to pre-packed silica cartridges used in automated columns or even a manual column therefore dry loading was attempted but the compound gathered on the bottom of glassware instead of loading on to silica. Instead purification was achieved by using preparative TLC (3% MeOH:DCM), where the slurry was painted onto the baseline using a modified spotter made out of aglass pipette thread through with cotton wool, forming a tip for more precise application of the slurry and also it gave better handling of the reaction mixture and gave resolution not obtained from manual column chromatography.

Furthermore, after the purification was achieved, the compound was stored in a sealed vessel under a nitrogen atmosphere, at -20°C. However, evidence of breakdown was apparent through TLC and ^1H NMR analysis (figure 37) through testing before progressing on to coupling to fragment 1. On comparing the experimental methods of synthesising fragment 2, it was noteworthy that the selenocarboxylate/ amidation method gave the highest overall yield of fragment 2 when comparing to peptide coupling reagents described in section 2.1.1.4.4. Although this method was also found not to be amenable to process chemistry, instead stock piling of fragment 2 was achieved by repeating a series of experiments until 7.4 mg of pure BocGlnAMC was isolated and

progressing on to the final coupling step using the most efficient of the coupling reagents tested, namely HATU.

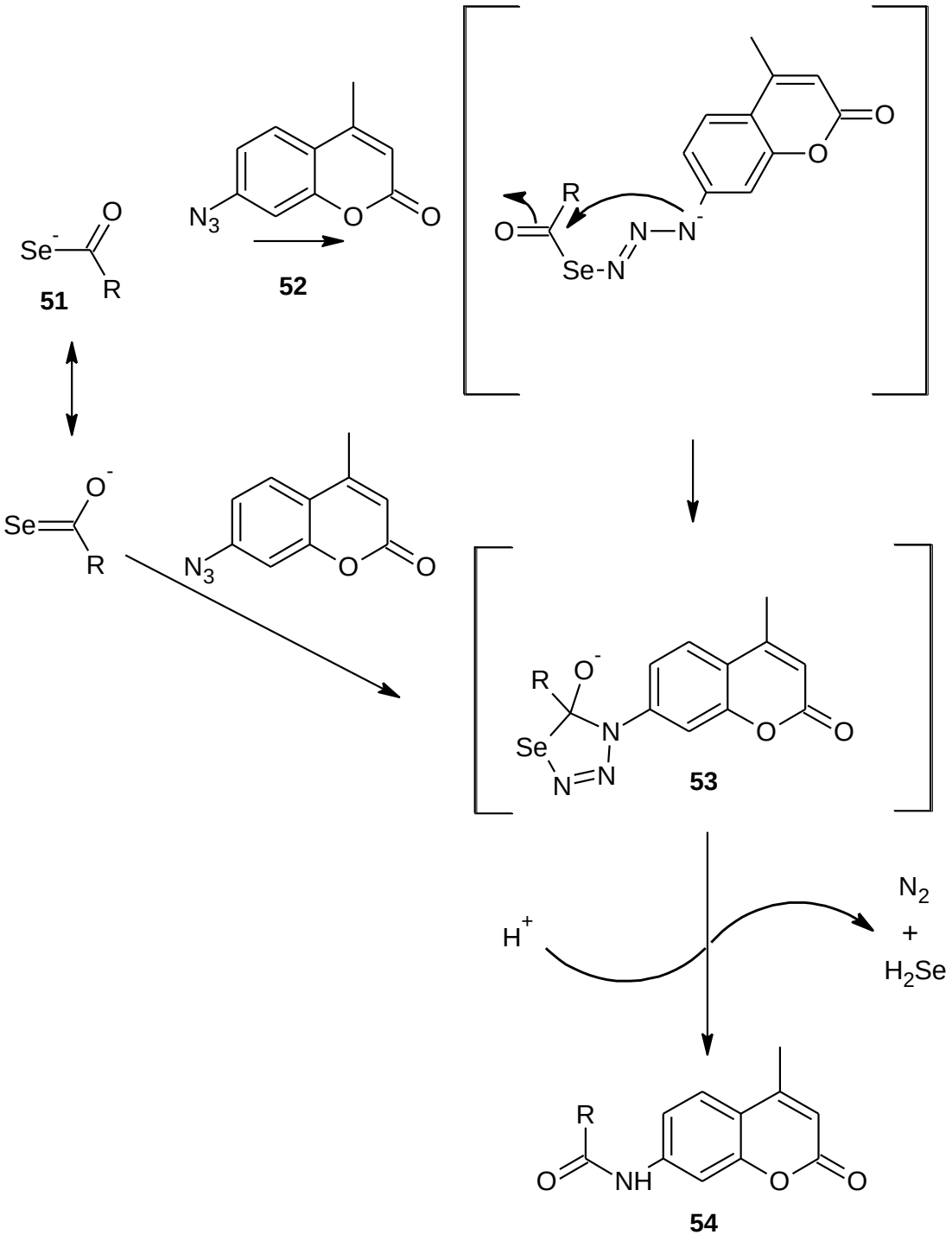

Scheme 5 – The mechanism for reaction of selenocarboxylates with AzMC[130]

Reproducibility of the selenocarboxylate amidation experimental procedure wasn't consistent and was found to be unsuitable in terms of the scale up process. Furthermore, the handling of the compound was problematic when purifying, as the crude mixture presented solubility problems and continuosly crashed out of solution when trying to purify, this solubility problem was an issue in both methods of peptide coupling reagents and selencarboxylate / azide amidation process. In order to stock-pile the fluorogenic substrate for biochemical testing, the structure was critically analysed and modifications were made in protecting groups in order to improve stability shown in figure 38.

a)

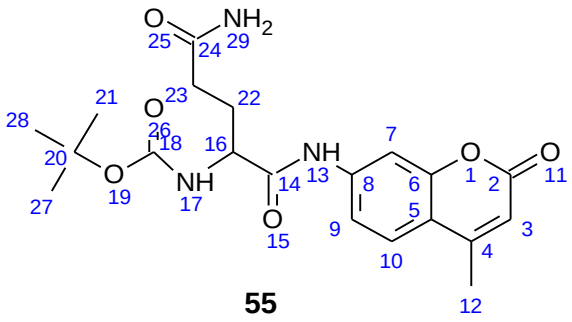

55

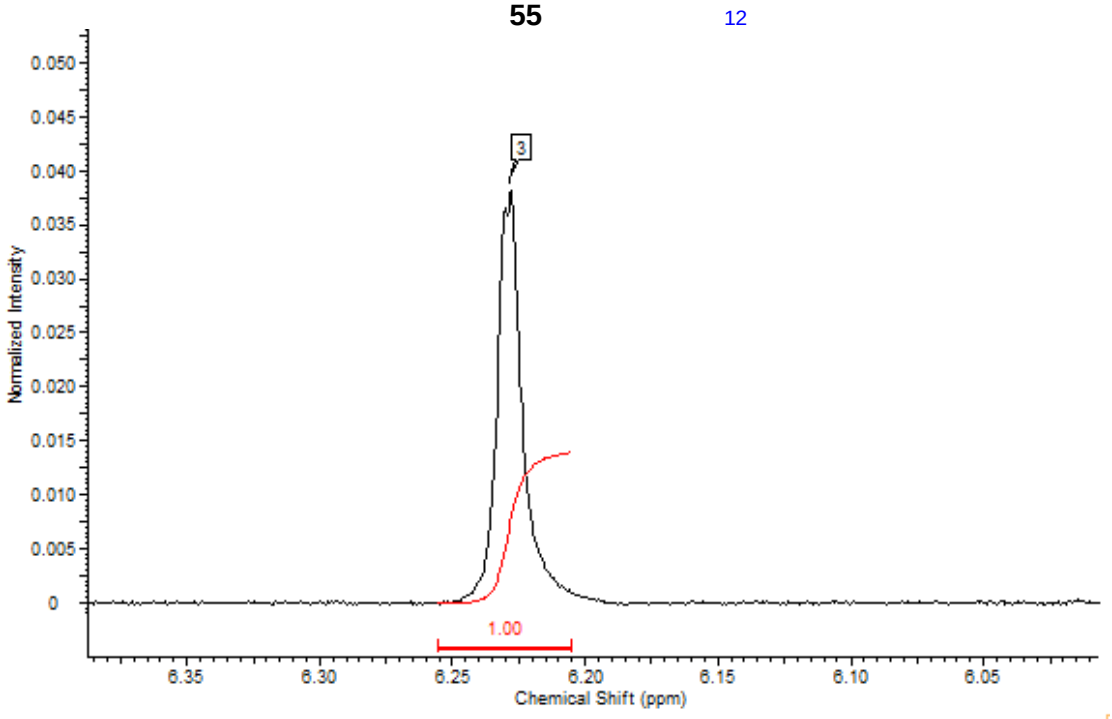

b)

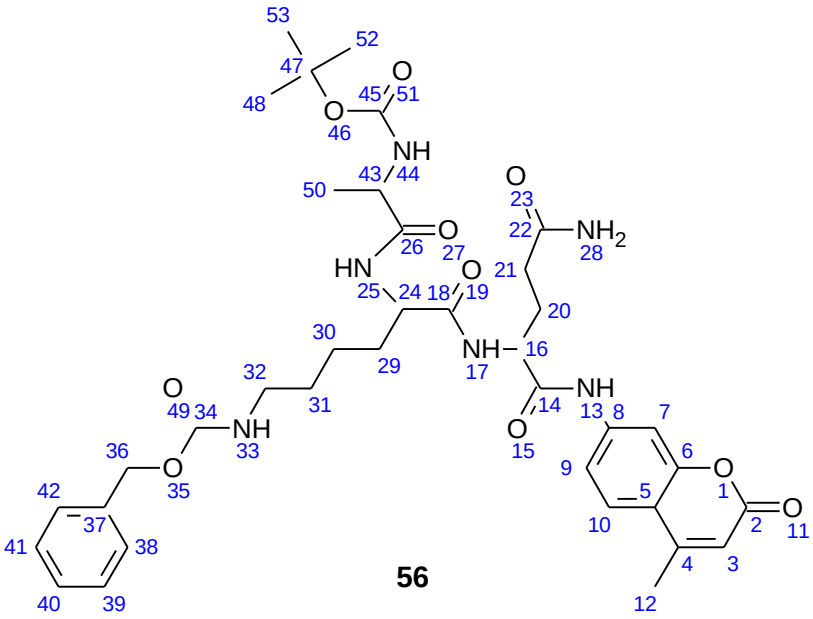

56

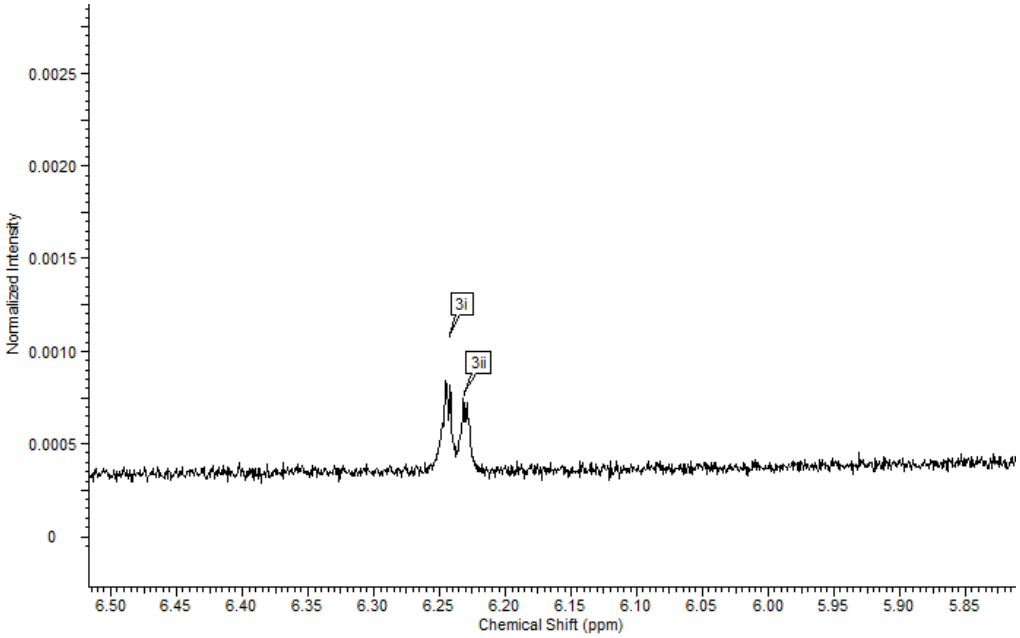

Figure 37– Expanded version of proton NMR spectrum of samples, a) Pure BocGlnAMC, **55** and b) BocAlaLys(Z)GlnAMC, **56** and free AMC, the region magnified in b) confirms the presence of two compounds alongside TLC visualisation(RF values 0.12 and 0.4 respectively, 5% MeOH:DCM) as there are now two signals resonating in area of vinylic proton that is neighbouring two quarternary carbons, labelled as position 3.

2.1.1.4.6. Protection strategy altered to overcome substrates solubility and purification issues.

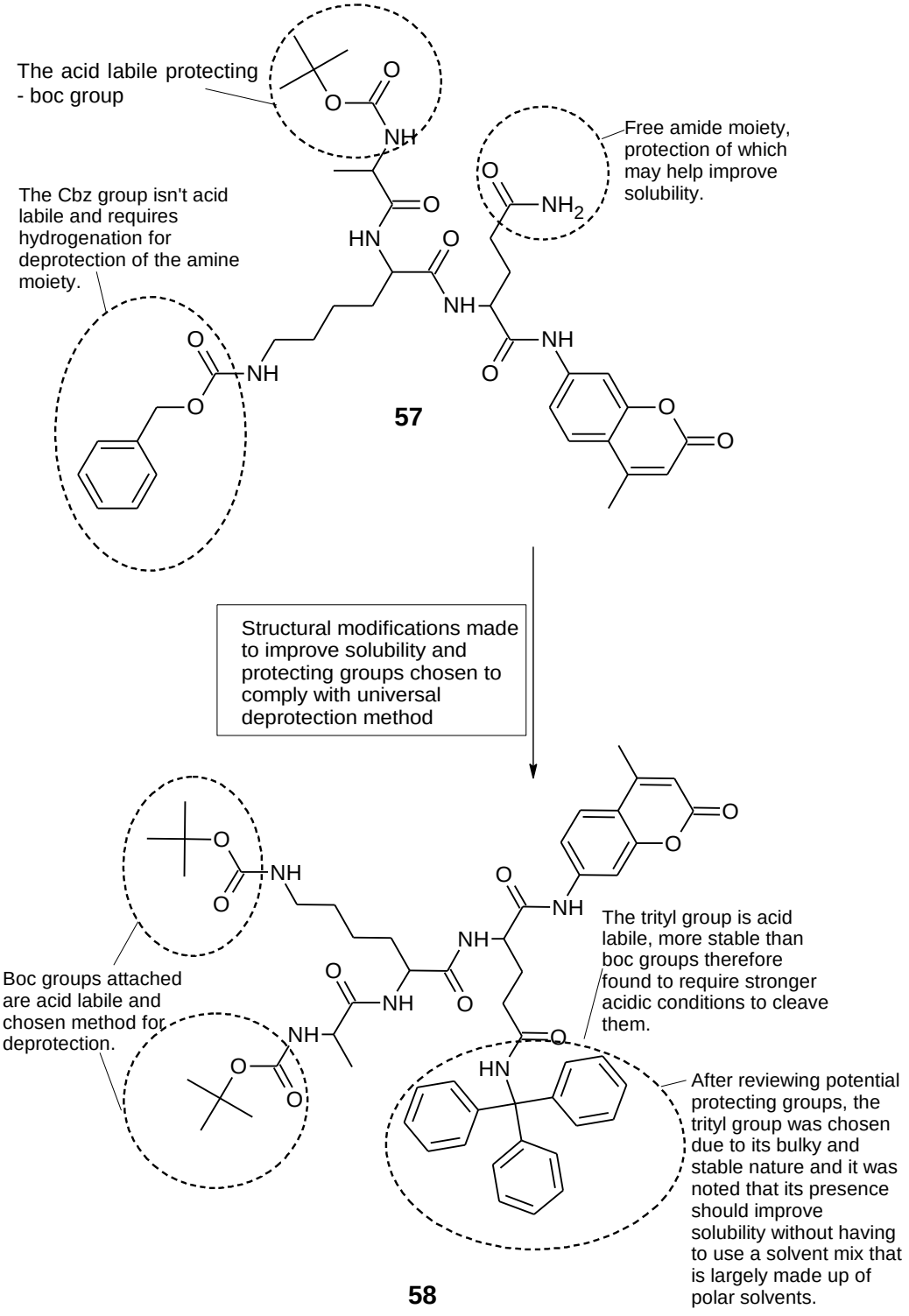

Figure 38 – Protecting group modification highlighted for the target fluorogenic substrate.[131]

A literature search was done to find appropriate reaction conditions to facilitate global deprotection, thereby reducing the number of deprotection steps and preserving the structural integrity and the substrates overall yield. Although, from previous synthetic steps it is known that the target compound is unstable and acid sensitive, to address this instability experiments were undertaken to determine the lowest possible acid concentration needed to deprotect both the trityl protecting group and the boc groups.

Trityl deprotection of ethers are more widely reported than of amides. In 2001, A. Pathak *et al*. specifically reports working with acid sensitive compounds and reports successful detritylation, by using between 1% - 5% TFA and running through a silica gel column to get pure detritylated deoxynucleosides and pentoses.[132] As a starting point this method was used to deprotect the BocGln(trt)OH, however, global deprotection was not achieved. The amount of TFA was slowly increased as it was determined that the amino-trityl group was significantly more stable and required a stronger acid to cleave them.[133] Testing higher acidic concentrations found that 1:2:0.1 chloroform:TFA:water and passing through a silica plug and immediate drying under reduced pressure was efficient in achieving boc removal and detritylation of BocGln(trt)OH to give NH_2GlnOH, this was verified using proton NMR, where the loss of a boc group involved the loss of a singlet peak at 1.45 ppm integrating for 9H and loss of a multiplet at 7.19 – 7.33 ppm integrating for 15 protons as shown in figure 39.

a)

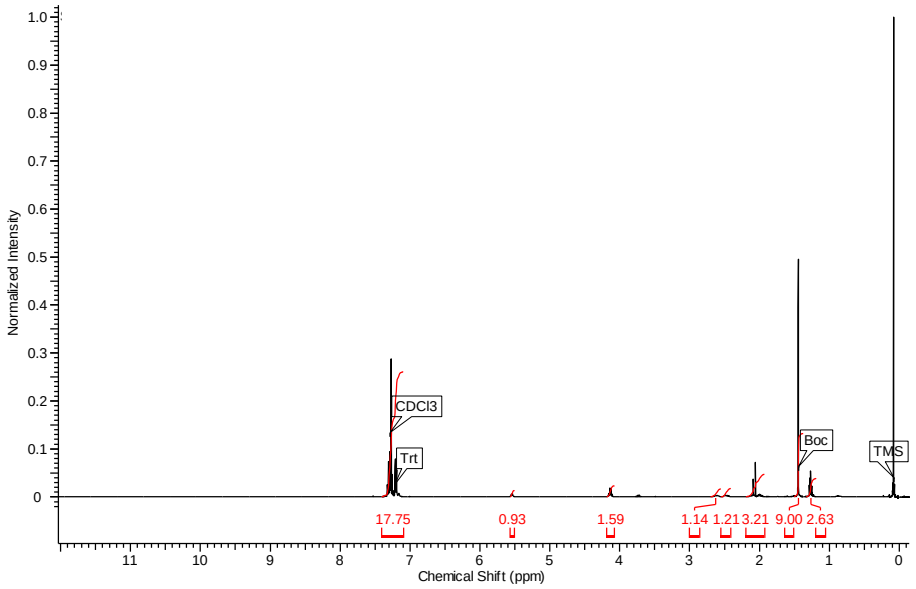
Normalized Intensity
Chemical Shift (ppm)
CDCl3
Trt
Boc
TMS
17.75
0.93
1.59
1.14 1.21 3.21 9.00 2.63

b)

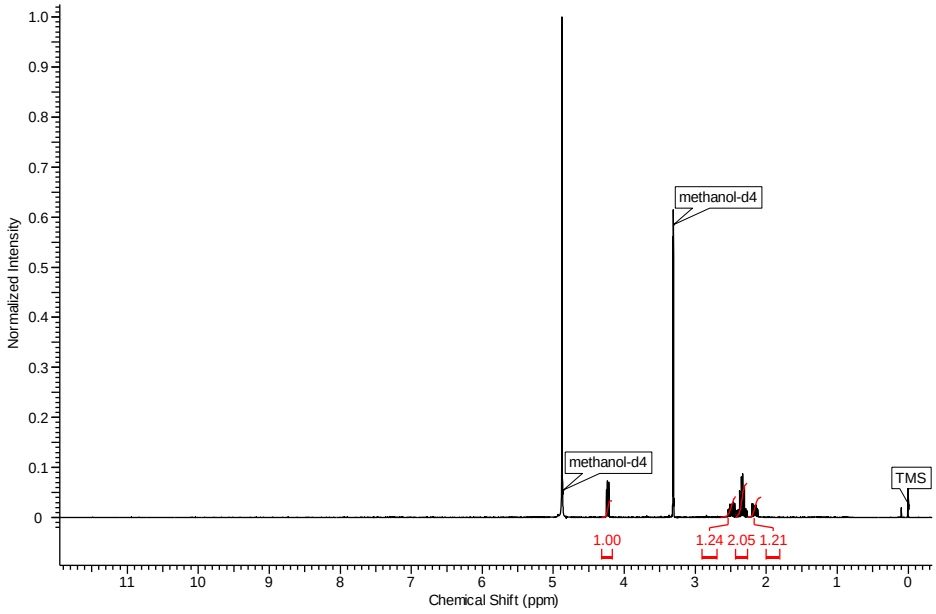
Normalized Intensity
Chemical Shift (ppm)
methanol-d4
methanol-d4
TMS
1.00
1.24 2.05 1.21

c)

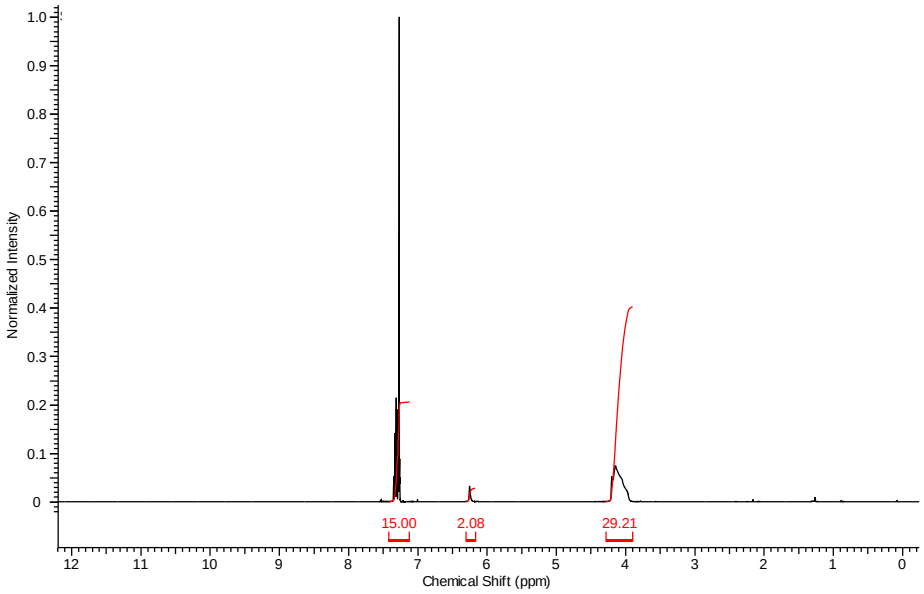

Figure 39 - a) ^{1}H NMR of BocGln(trt)OH in $CDCl_3$, TMS b) ^{1}H NMR showing the removal of both protecting groups of BocGln(trt)OH, full NMR spectra data attached in the appendix c) ^{1}H NMR of trityl group crashed out on to the silica plug wash using water.

To improve the overall yield of the fluorogenic substrate, the synthetic strategy was modified from the original plan of using the convergent strategy described in scheme 1 to the modified plan of using the linear strategy as decribed in scheme 6. To accelerate synthesis the decision was made to source in a custom-made peptide of sequence; BocAL(Boc)Q(Trt)OH, synthesised using an automated peptide synthesiser by Sigma Aldrich and purified using preparative HPLC.

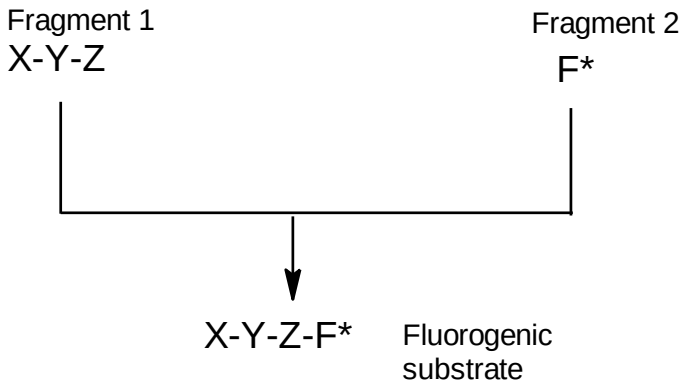

Scheme 6 – Schematic representation of the new linear strategy adopted, where: X, Y and Z are generalised symbols for amino acids.

The tripeptide was coupled to the AMC using peptide coupling conditions optimised and described in table 14.

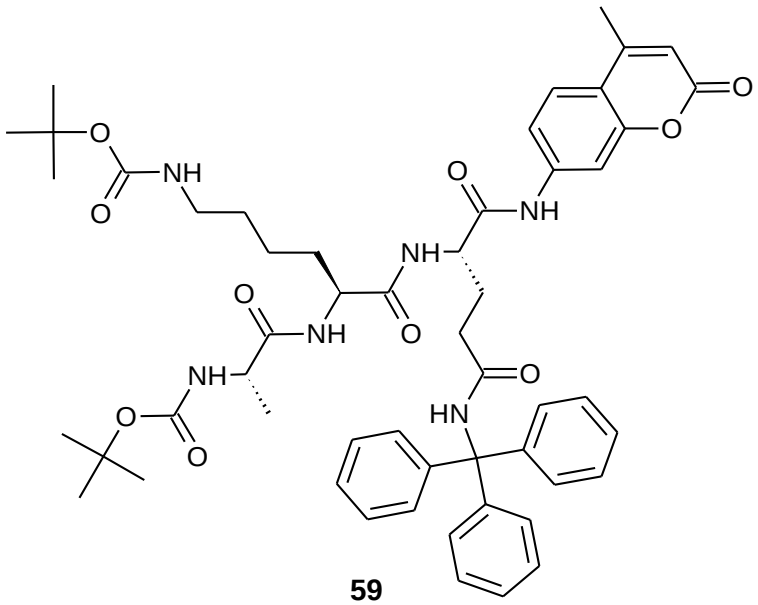

59

Introduction of the trityl group on to the glutamine's side chain increased the stability and solubility of the compound, thereby improving the handling of the compound during the purification process. Problems with loss of yield during purification due to crashing out and decomposition on silica as observed with the substrate BocAL(Z)Q-AMC was overcome by the addition of this bulky protecting group. However, the overall yield was still very low, due to the

reliance of the final coupling on a coupling reagent, a problem faced throughout the project.

Furthermore, as it has been determined through deprotection studies on BocGln(Trt)OH discussed earlier in 2.1.1.4.6 that the BocAL(Boc)Q(trt)AMC also requires acid treatment in order to deprotect the substrate ready for biochemical testing. From previous experiments it is also known that the unprotected tripeptide sequence is unstable therefore the ideal situation for the biochemical testing of this compound would be, to achieve its deprotected status in presence of the target enzyme to minimise any premature decomposition, this was tested and reported as a DSF study in chapter 3.

Fluorogenic substrate successfully isolated	**Overall yield**
Boc AL(Z)QAMC, **60**	0.4%
Boc AL(boc)Q(trt)AMC, **61**	15.7%

Table 14 – Fluorogenic substrates successfully isolated and their overall percentage yields.

CHAPTER 3: BIOCHEMICAL TESTING

3. BIOCHEMICAL TESTING

3.1. CHAPTER AIMS

i) Determine purity of the enzyme sample extracted from clinical sample
ii) Determine optimum conditions for biological assay
iii) Biological testing of the conjugated probe to gain proof of principle
iv) Test selectivity of detection probe in a clinical model and against other enzymes with similar activity.
v) Compare the AMC detection probe shelf life with a commercially available detection probe.

3.2. SDS-PAGE ANALYSIS OF 3C PROTEASE

3.2.1. Materials and method

$3C^{pro}$ was kindly provided by the Pirbright Institute in Surrey (volume of 100 µL at concentration of 13.8 µM). Details of the mutations in the supplied $3C^{pro}$ strain are C95K and C142A, these substitutions are reported to improve solubility and proteolytic activity respectively.[134] The enzyme was stored at-80°C on arrival and thawed to room temperature for biological assays.

To verify the purity of the enzyme sample we received from the Pirbright Institute, the technique SDS-PAGE was used. The gel was run in a MiniProtean Tetra system (BIO-RAD) with a SDS running buffer (National Diagnostics). The acrylamide gels consisted of a resolving gel and a stacking gel of concentrations 12% w/v and 6% w/v respectively. The protein sample was prepared by adding a loading dye in a 1:1 volume ratio (Table 15). The sample mix was denatured by heating at 95° for 5 minutes to ensure protein

conformation had no effect on the protein migration through the gel and the distance travelled can then solely be attributed to the molecular weight. 20 µL of the protein sample/ loading dye mix was added to the well and run alongside the molecular weight marker ECL Full-Range Rainbow molecular weight marker (Amersham) in a neighbouring well. Electrophoresis was run under 180V for 60 minutes (BIO-RAD PowerPak 300). The gel was stained for 30 minutes in a 1% w/v Coomassie Blue solution at room temperature under gentle shaking conditions: 90 RPM. The gel was then rinsed with water and de-stained using 10% v/v ethanol, 10%v/v acetic acid for 17 hours at room temperature under gentle shaking conditions: 90 RPM. The destained gel imaged using a Geldoc XR+ (BIORAD).

Materials	Components	Concentration of each component
Resolving gel	Acrylamide: bis acrylamide (37.5:1)	12% v/v
	SDS	0.125% w/v
	Ammonium persulfate	0.05% w/v
	Tetramethylethylenediamine (TEMED)	0.002% v/v
	Tris-HCl	390 mM
Stacking gel	Acrylamide: bis acrylamide (37.5:1)	6% v/v
	SDS	0.125% w/v
	Ammonium persulfate	0.05% w/v
	TEMED	0.002% v/v
	Tris-HCl	116.6mM
Loading dye	Sucrose	40% w/v
	Bromophenol blue	0.25% w/v
	Dithiothreitol (DTT)	5 mg/mL
SDS running buffer	Tris	0.25M
	Glycine	1.92 M
	SDS	1% w/v
Staining solution	Ethanol	50% v/v
	H_2O	40% v/v
	Acetic acid	10% v/v
	Coomassie brilliant blue	0.1% w/v
Destaining solution	H_2O	80% v/v
	Acetic acid	10% v/v
	Ethanol	10% v/v

Table 15- Materials used for SDS-PAGE.

3.2.2. SDS-PAGE Results

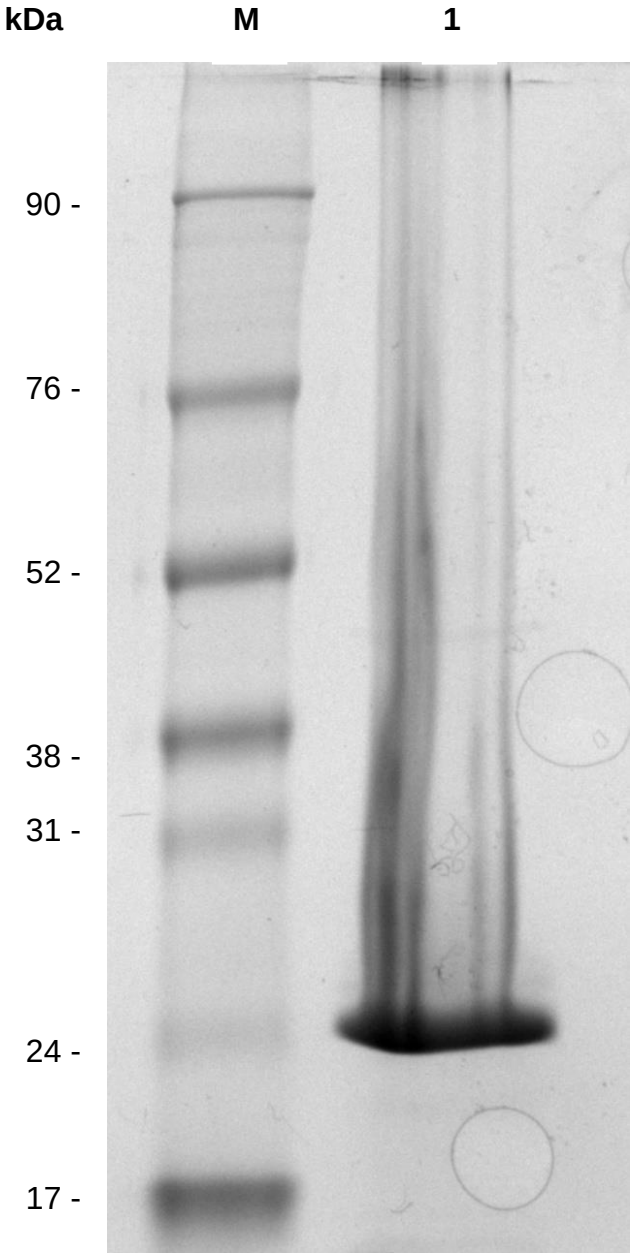

Figure 40 - Image of SDS-PAGE: the molecular markers were run in the left lane, marked as 'M' and the $3C^{pro}$ in the right line, marked as '1'. The streaky nature of lane 1 is due to the enzyme sample being in a high concentration of salt. The $3C^{pro}$ (MW = 23kDa) stained a band adjacent to a faint band of the molecular weight ladder of 24kDa.[135]

3.3. DIFFERENTIAL SCANNING FLUORIMETRY (DSF).

3.3.1. Materials and method for DSF

Following an adapted protocol reported by Niesen et al.[136] pepsin was diluted to 64µg/mL in PBS pH 7.4, 0.5mM EDTA and 5x Sypro Orange (Oxoid). The fluorescence was measured using an Mx3005p qRT-PCR (Stratagene), the temperature was increased from 25˚C to 95˚C at an increment of 1˚C/minute. Spectral properties used for detection of Sypro Orange; excitation wavelength at 300/472 nm and the emission wavelength at 570 nm.Data analysis was completed using software tools obtained from the Structural Genomics Consortium Oxford (ftp;//ftp.sgc.ox.ac.uk/pub/biophysics). The raw DSF data was fitted to the Maxwell-Boltzmann distribution in Graphpad Prism to determine the T_M value.

Enzyme	Extracted from	Use	Supplier
Pepsin	Porcine stomach mucosa	Testing parameters for detection assay with TCA	Sigma Aldrich

Table 16 - Biological material for TCA study.

3.3.2. Investigating parameters needed for the enzymatic assay of detection probe.

In order to define the parameters needed for the unstable detection probe in the enzymatic assay, DSF was employed as a technique to monitor the effects of the percentage TCA on an enzyme; the plan was to establish a balance between maintaining the protein's structure whilst providing a suitable environment needed for the deprotection of the protecting groups attached to the detection probe. These conditions would allow the deprotection of the detection probe to occur in the presence of its target enzyme, therefore eliminating risk of the probe decomposing before having contact with its target enzyme.

Thermal stability of the protein was tested by adding the dye (Sypro Orange) which binds to the hydrophobic parts of the enzyme as it denatures with increasing temperature. The intensity of the fluorescence detected by DSF is directly proportional to how effectively the dye is bound therefore the temperature at which the protein denatures is ascertained by the increase in fluorescence.

3.3.3. DSF Results

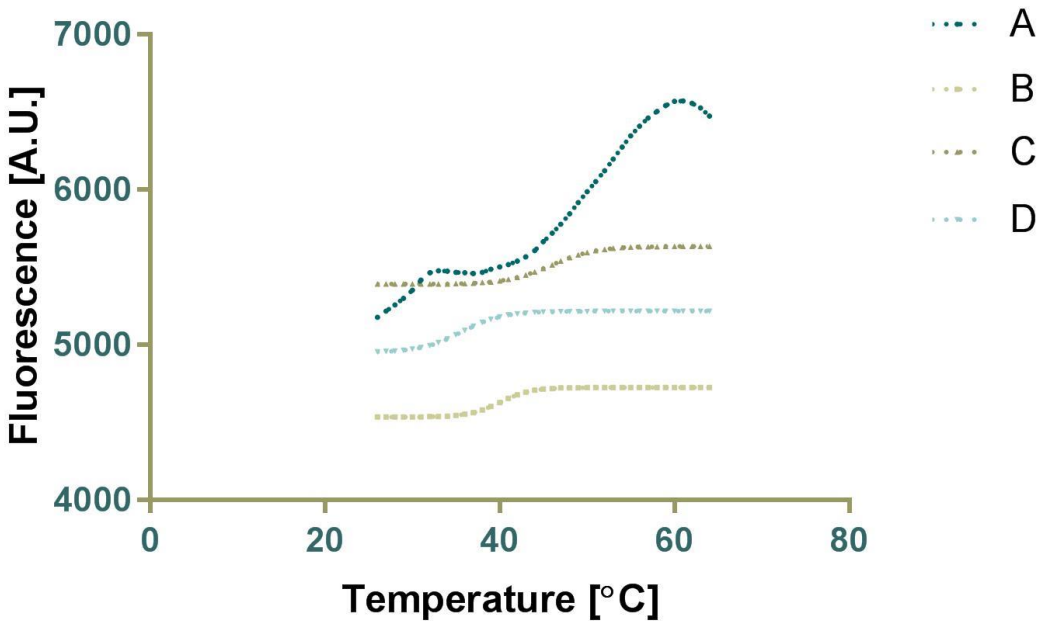

Figure 41 - Measuring the effects of TCA on the thermal melt curve of the common enzyme pepsin.The changing percentages of acid are: A (control), 0% TCA; B, 1% TCA; C, 0.5% TCA; D, 0.25% TCA.

Figure 41 represents the changes in thermal stability of the enzyme pepsin and emission of fluorescence by Sypro Orange. The data shows a significant reduction in stability of the protein in the presence of all tested TCA levels therefore T_M value: 50˚C ±0.5˚C could only be determined from curve A- the acid free sample. These results show the addition of an acid to the detection based assay would not be suitable as the enzyme is significantly destabilised even at the lowest 0.2% TCA tested, decreasing the acid percentage further would not be sufficient for deprotecting the boc and trityl protecting groups attached to the amino acid sequence of our detection probe. Therefore the deprotection step was designed to precede the enzymatic assay.

3.4. DIAGNOSTIC PROBE TESTING

3.4.1. Materials and method for probe testing

The activity of the $3C^{pro}$ in the presence of the conjugated detection probe was monitored using fluorescence. A triplicate series of assays were completed initially to gain optimum conditions for both the substrate and the enzyme, the results obtained were used to gain proof of concept. All enzyme assays were carried out in Nunclon 96-well flat transparent plate at volume 100 µL/well. The details of the assays are listed in appendixtables 1 – 5 the assays were run in triplicate or duplicates (the latter due to limited amount of $3C^{pro}$ enzyme). Fluorescence readings were taken on the Infinite M200 PRO plate reader and the parameters were set to: excitation wavelength of 360 nm and at the emission wavelength of 455 nm in order to analyse the release of the fluorophore AMC.

3.4.2. Proof of concept testing.

3.4.2.1. Fluorescence results

a)

Initial Biological Testing, one–way anova data and Dunnett's Multiple Comparison Graph.

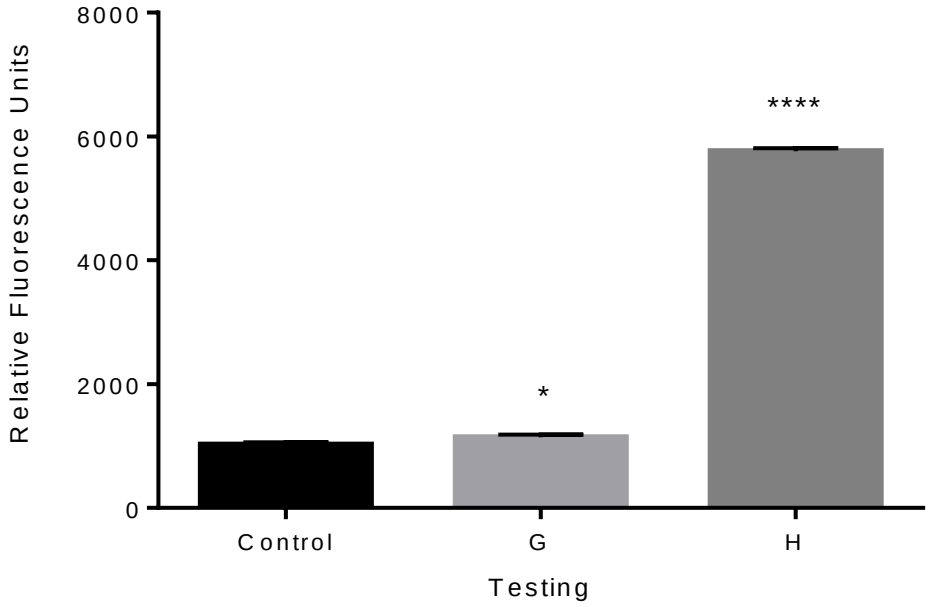

Figure 42 – The graph represents the fluorescence data from biological testing, after 10 minutes of incubation at 37°C, one-way ANOVA data and Dunnett's multiple comparison test results, both these tests were run on Graphpad 6, the Dunnett's multiple comparison datais represented using asterixes (*), where the more significance is marked with more asterixes.1: control, 2: G; [E] = 1.38µM, 3: H; [E] = 13.8µM, [S] was controlled in all wells. The full details of concentrations and volumes used are in the appendix table 1. The error bars represent the standard deviation of replicates (n=3).

On analysing results in figure 42, a significant statistical difference was seen using the one-way ANOVA test between the negative control and the testing wells ($p<0.0001$) indicative of a significant change in fluorescence measurements. Further statistical analysis using the Dunnett's multiple comparison testwas performed to determine significance from the negative

control and each testing well, this is represented in the graph shown in figure 42. So from the Dunnett's multiple analysis we found the higher [E] of 13.8µM and 10 minute incubation caused a more significant change in fluorescence when compared to the ten fold less [E] of 1.38 µM with the negative control wells, therefore the higher concentration and volume of $3C^{pro}$ was used in furher assay tests.

After proof-of-concept testing, further fluorescence generation studies were planned to gain a better understanding of $3C^{pro}$, therefore particular interest was in recording initial kinetic data, in order to define an enzymatic model for the target protease and compare to the established Michealis-Menten (MM) Model in order to define the enzyme's kinetic parameters.

In the interest of gaining a better understanding of our target enzyme, it would have been ideal to use a larger spread of [S], ranging between 0-150 µM. However, from the initial biological testing it was determinedthat 50µM didn't show any fluorescence generation and therefore was not considered further due to limited supply of the target enzyme and the unstable nature of the detection probe once deprotected.

Furthermore, on progression to the enzyme kinetics study it was apparent that the fluorescence measurements at time=0 were slowly increasing over time, for the stored substrate solutions. An increase for the [S] at 100µM from ~1000 RFU (in figure 42) to ~2000 (in figure 43) RFU was seen after 4 hours in buffer solution. This was thought to be due to the detection probe decomposing, releasing the free fluorophore and highlighting a major problem with stability, an issue faced throughout the synthesis and purification part of the project. Eventually, no change in fluorescence measurements was being recorded, indicating no substrate hydrolysis, as a possible result of the inevitable denaturation of the target enzyme or the decomposition of the unstable probe. Unfortunately, sufficient number of assays weren't completed in order to define the kinetics of the FMDV protease enzyme mathematically; however, further

evidence of cleavage in the presence of our target enzyme has been gained through increased fluorescence, as seen in figure 43 at substrate concentrations of 100μM and 150μM, this increase in fluorescence was found to be a significant change in comparison to the negative control using the one-way anova statistical method ($p<0.005$).

Fluorescence results from biological testing.

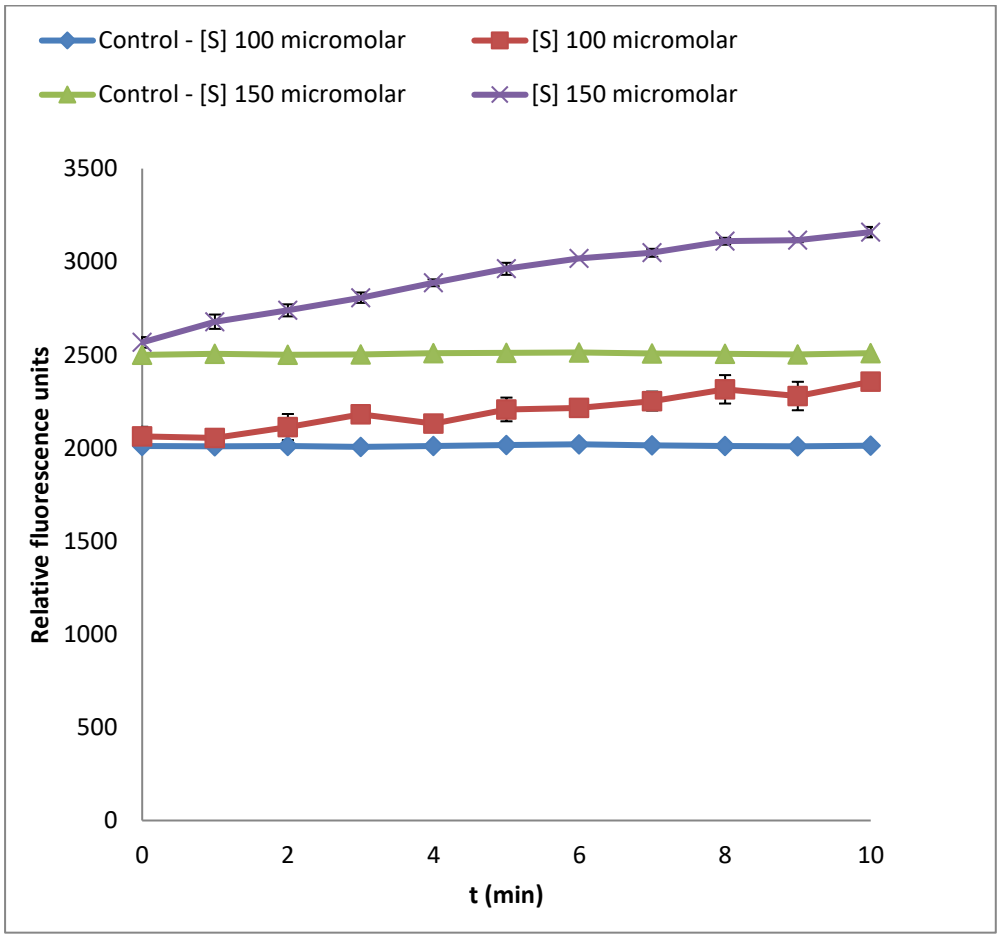

Figure 43 - Performance testing results represented as fluorescence generation in the presence of the target enzyme, $3C^{pro}$, [E] = 13.8µM. The error bars represent the standard deviation of replicates (n= 3).

3.5. SELECTIVITY TESTING OF THE DETECTION PROBE.

3.5.1.1. Biological materials for selectivity testing

Enzyme	Extracted from
Trypsin type 1	Bovine pancreas
Chymotrypsin type 2	Bovine pancreas
Thrombin	Bovine plasma
TEV protease	Recombinant expressed in *Escherichia coli*

Table 17 - Biological materials for selectivity testing**.** All enzymes were stored at -5 to -20°C and thawed to room temperature before running biological assays.

To further test the application of the detection probe, a series of experiments were designed to expose the conjugate to other proteases that may be found in a clinical sample taken from livestock infected with FMDV. The $3C^{pro}$ enzyme is reported to have properties characteristic of cysteine and serine proteases, therefore the following commonly occurring serine type proteases were selected to test against: chymotrypsin, thrombin and trypsin. Also to specifically test the amino acid sequence attached to the fluorophore another enzyme was selected: Tobacco Etch Virus (TEV), as this is a related cysteine protease with a Q/G and Q/S selectivity similar to that mentioned for 3C protease in section1.2.3.3; this shows the importance of this protease when testing selectivity, although the consensus sequence for TEV is Glu-Asn-Leu-Tyr-Phe-Gln.[137]

3.5.1.2. Results from selectivity testing

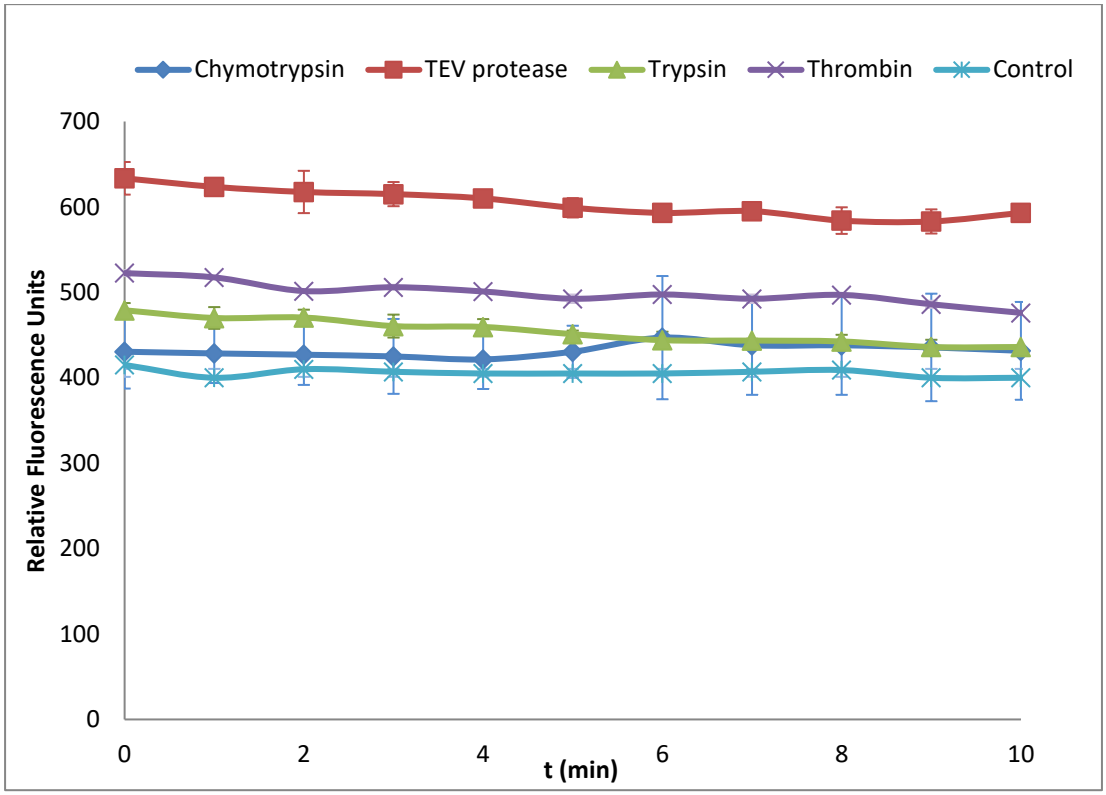

Figure 44 – Selectivity testing results represented as fluorescence generation over time. Enzyme assays made up of the substrate = (ALQ-AMC) 100µM, in presence of the selected enzymes: Chymotrypsin, Trypsin, Thrombin and TEV protease 15µM. The error bars represent the standard deviation of replicates (n=3).

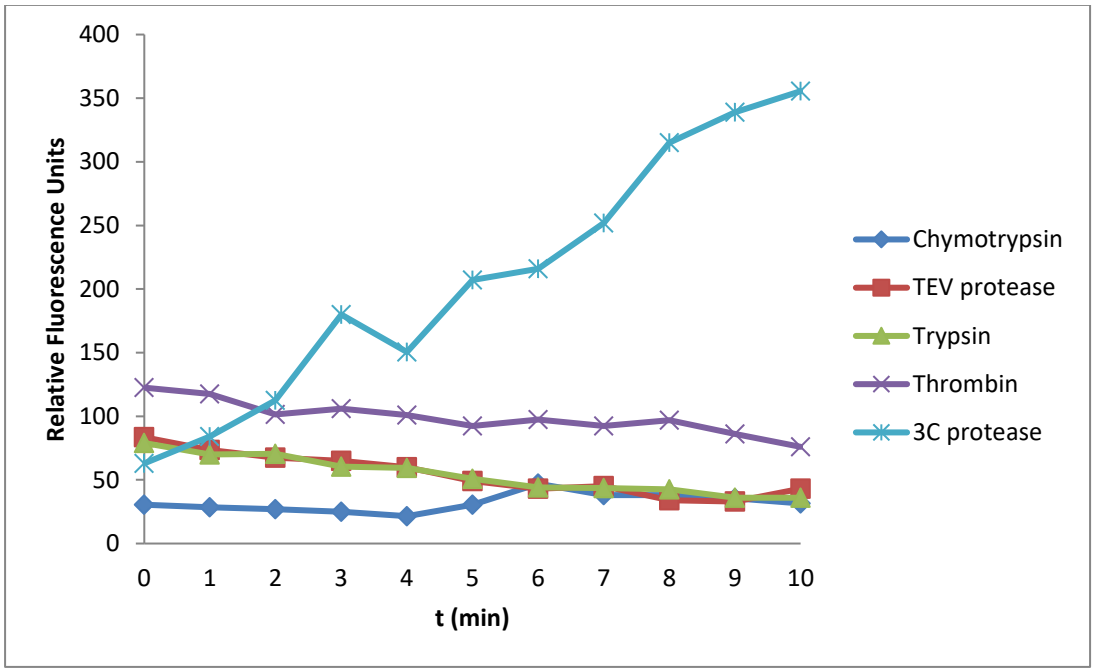

Figure 45 – Graph of normalised data between 0-400 to show comparison of all enzymes tested with substrate (ALQ-AMC) with $3C^{pro}$. Concentrations for enzymes between 13.8µM - 15µM and substrate 100µM.

From figures 43 - 45, it can be deduced that the detection conjugate breakdown has shown selectivity to the $3C^{pro}$ enzyme over commonly occurring enzymes in clinical samples, also the TEV protease, was found to have no significant change in fluorescence measurements recorded in comparison to the negative control using the one-way anova statistical method ($p>0.05$). Furthermore the duration of time fluorescence measurement was chosen to be the same length as the assay experiments run with the target enzyme $3C^{pro}$ reported earlier, as in the presence of the $3C^{pro}$, fluorescence would be generated more rapidly and therefore a delayed increase in fluorescence would be indicative of breakdown of the conjugate *via* other routes.

3.6. STABILITY TESTING OF AMC DETECTION PROBES.

The stability of the AMC probe became a point of investigation, as it has been a major problem throughout this project. Where specifically decomposition has been observed during purification steps and storage handling, therefore it can be deduced that unusually the amide bond is prone to autohydrolysis, the increase in initial fluorescence between readings from 1000 RFU to 2000 RFU over a period of 4 hours was indicative of the detection probe breaking in 5% v/v DMSO:PBS buffered solution mix with a resultant increase in free AMC concentration without enzyme assistance. This substrate decomposition was thought not only due to autohydrolysis but was also thought to be a consequence of trace amounts of TFA in the assay. As the preceeding deprotection step involves the removal of the orthogonal protecting groups (boc and trityl) by exposure to TFA, this is removed under reduced pressure, prior to making up substrate concentrations for biochemical assays. So trace amounts of TFA could be trapped in the sample which when reconstituted in DMSO and the aqueous buffer can cause acidic degradation. Degradation would occur *via* hydrolysis of amide bonds over time of the main backbone of the substrate, in the absence of the acid labile protecting groups. An acidic environment would also have an affect on the structural integrity of the target enzyme, thereby reducing activity, a consequence determined from earlier studies of TCA presence on the more common and readily available enzyme, pepsin. Moreover, the presence of trace amounts of TFA coupled with the increasing temperature to meet the optimum temperature of 37°C of the $3C^{pro}$ enzyme, giving extra thermal energy to the detection probe otherwise stored at -80°C, to prevent decomposition, could also be contributing to the breakdown of the substrate molecule.

Furthermore, a separate study was conducted on a comparable, commercially available, well documented and robust AMC based detection probe, BocValProArgAMC for the target enzyme thrombin. This specific probe was of interest because like our novel probe, AlaLysGlnAMC, is also based on a

tripeptide sequence although with a completely different sequence and biological target. Due to the difference in specificity the probes were only comparable in their sample preparation and shelf-life. To test the shelf life of the established probe, biochemical testing of BocValProArgAMC with thrombin was completed and the Michaelis- Menten parameters were determined and are defined in figure 45.

On comparison of the solubility of the probes BocValProArgAMC and AlaLysGlnAMC, it was noted that the established probe was sourced in as its hydrochloride form and could be dissolved in pure buffer solution, PBS, unlike thenovel probe that required 5% DMSO to stay in solution. Also, it was noted that the activity of the established probe's sample didn't change by much after 1 month of storage in a freezer at – 20°C and the biological enzyme at - 80°C, determined by comparing fluorescence at time 0 of the control wells and the calculated MM parameters (table 19), both of which didn't show a significant enough change through one-way anova statistical test ($p>0.05$). Whereas our novel probe showed evidence of decomposition through comparing initial fluorescence measurements described earlier in section (3.4) only a few hours after assay preparation.

A major difference can also be noted between the two probes in the amounts of volume and concentration required to gain significant fluorescence response, as a higher concentration of both the S and E is needed by our novel probe (appendix table 2) in comparison to commercially available detection probe for Thrombin (appendix table 5).

Set	Km (μM)	Vmax (μM/s)
1	150.11	3.5
2	152.24	3.9

Table 18 - The MM parameters are tabulated for the enzyme assay sets run a month apart for thrombin in presence of Boc-VPA-AMC.

In order to determine the rate of fluorescence emission from the cleaved fluorophore AMC and the Michaelis Menten (MM) parameters of thrombin, kinetics were measured through the fluorescence data, using the spectrophotometer. Graphs were plotted as fluorescence vs time for each concentration and the gradient (rate) was determined using the straight line equation: $y = mx + c$ (Equation 2). The average of the rate of the multiple (triplicate) data sets was then plotted against [S] and fit against the MM model. The kinetic data for thrombin was fit to the Michaelis Menten (MM) model and further analysed to determine the MM parameters graphically.

$$v = \frac{Vmax\ .\ [S]}{Km + [S]}$$

Equation 3, MM equation, where; v, the initial velocity of the reaction; $Vmax,$ is the maximum velocity; [S], Substrate concentration and $Km,$ is the dissociation constant for substrate, also described as the Michaelis-Menten constant.

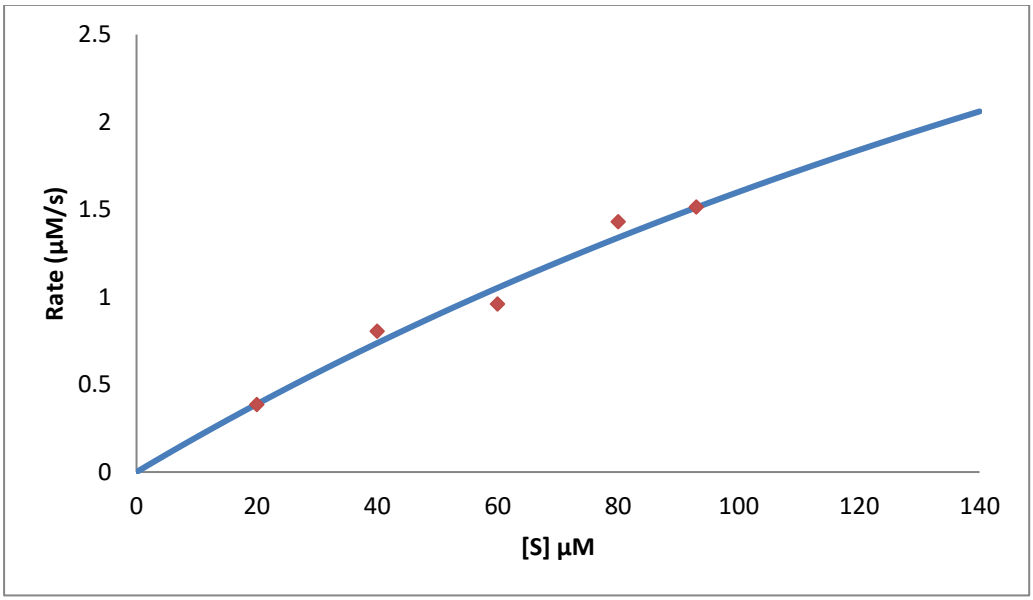

Figure 46 – Comparing experimental data for thrombin in presence of Boc-VPA-AMC to mathematical model.The blue curve represents the mathematical model generated using the MM equation**.** The red data points represent the experimental data. This graph shows a good correlation of the data points with the curves indicating activity of thrombin is of Michealis nature, as is known.The MM parameters ascertained from the graph are K_M = 150.11µM and V_{max} = 3.5µM/s [138]

3.7. CONCLUSION AND FURTHER WORK

The total synthesis of the detection probes: BocAL(Z)Q-AMC and BocAL(Boc)Q(Trt)-AMC were successfully achieved after trialling a range of different synthetic routes. Although, rhodamine is described to be the more superior fluorophore for a latent enzyme-based detection system based on its physical chemical properties, from the results obtained and discussed from the synthetic work done in this project, the overall consensus was reached in agreement with other researchers, that synthesising rhodamine based detection probes is capricious in nature, due to its low nucleophilicity of amino moieties caused by intrinsic effects and difficulties associated with building upon the main framework is the possible reason to the lack of commercially

available rhodamine based detection probes and also the reason to the change of direction in this project to a more simple fluorophore, AMC.[139]

Here I have described briefly the methods that failed to produce isolatable R-110 based detection probes, this includes the conventional peptide coupling reagents; COMU, EDCi and HATU. An alternative method was also attempted, using Pd catalysed C-N cross coupling, where the starting material involved the more readily available fluorescein. However, the success reported by Grimm et al. wasn't mirrored in the case of attaching our target amino acid Q to the fluorophore.[140] Instead, autohydrolysis of the ditriflate was encountered multiple times, a problem circumvented by the authors by increasing Pd loading, however this wasn't the case in our experiments.

Still following the original plan of convergent synthesis; after an extensive literature search, a method was found that specifically described the synthesis of part of our AMC based target compound (fragment 2) via a selenocarboxylate / azide amidation route. Following this method the synthesis of BocQ-AMC was successfully achieved and isolated supported by spectroscopic analysis. However, this method also had its limitations, the overall yield achieved was relatively low ~ 5%, also the method was found not to be amenable to the scale up process and the target compound BocQ-AMC was found to be unstable determined through its decomposition during purification and on storage, verified by TLC and fluorescence measurements.

Also noted, through experimentation of this method was a possible reductive link between the different reactants in the reaction mixture resulting in the reduced overall yield of fragment 2: sodium borohydride a strong reducing agent, therefore used at equimolar ratios; sodium hydrogen selenide a mild reducing agent, supported by NMR analysis and hydrogen selenide a possible side product but also a possible reducing agent of azido moieties, all of which contribute to the reduced overall yield of the target compound.

In order to stock pile a more stable compound for biochemical testing, the following changes were implemented: A trityl group was introduced to the structure, to improve on the solubility, stability and the overall yield. A linear strategy was successfully used to synthesise BocAL(Boc)Q(Trt)-AMC of yield ~15%, supported by spectroscopic analysis. Although a stable compound was formed, deprotection of the compound would reintroduce the instability observed in earlier reactions. Therefore the idea of deprotecting the detection probe in presence of the enzyme was tested and it was determined using DSF analysis that the acidic deprotection of the boc and trityl group in the enzymatic assay would compromise the enzyme's structural integrity, therefore deprotection was carried out as a separate step before the enzymatic assay.

The purity of the enzyme sample received was verified, to ensure no biological impurities were present in the enzymatic assay, the purity was verified using SDS PAGE analysis, a single band of the expected weight of 23kDa was found.

From the biochemical testing the proof of breakdown has been gained of our detection probe as a consequence of our target enzymes activity. The $3C^{pro}$ also displayed selectivity for the detection probe when tested over other commonly found enzymes in FMDV clinical samples: chymotrypsin, thrombin, trypsin and the TEV protease. From the results obtained it can be concluded that our detection probe is recognised by the $3C^{pro}$ and the enzyme is capable of recognising and processing shorter fragments of peptides, previously reported not to be the case.[141]

Despite the stability of the detection probe causing problems throughout the project, we can confidently conclude the cleavage of the free fluorophore was enzyme-assisted and not due to spontaneous decomposition as the measurements recorded from the control wells (enzyme-absent well) remained constant, further verifying the release of the fluorophore in enzyme - containing wells to be enzyme-assisted.

However, the deprotected detection probe was found to have a short shelf-life in comparison to a commercially available AMC probe, this limits its use and increases chances of false positive results, unfortunately rendering the probe commercially useless, in this state. Although the imminent need of a rapid detection probe has been highlighted in this project and the recognition of the smaller peptide fragment by $3C^{pro}$ has been proved, further work on the stability of the detection probe can potentially provide a more commercially viable detection probe.

On reviewing the results gathered from this project of the synthesised and biologically evaluated detection probe, the two major areas for further work in order to implement a commercially viable detection system are; stability and sensitivity. These points have been discussed herein:

- Improving the stability of the detection probe and thereby relatively increasing the shelf-life. The target amino acid sequence of ALQ - although proved to be recognised by $3C^{pro}$, is known to be unstable through our experimental results when attached on to the AMC fluorophore, during synthesis, purification and storage. From research published on $3C^{pro}$; the enzyme is known to accept a range of substrates and is therefore described to have the enzyme property of it being malleable.[142] This property can allow a trial of a number of different tripeptide sequences in order to develop a more stable and thereby more useful substrate-fluorophore conjugate for a deployable detection system.
- After improving on stability of the detection system, it would be useful to get information on the methods sensitivity by performing comparative studies against the reported ‘gold standard’ – portable PCR.
- Improving the sensitivity of the dye system by substituting the simpler, well known coumarin dye – the AMC fluorophore for a

more superior fluorophore. As reported by many authors, the R-110 is described to have superior fluorogenic properties such as higher quantum yield and a higher extinction coefficient than the AMC coumarin dye, therefore having a detection probe with this xanthone based fluorophore would improve the probes sensitivity. However, from synthetic work in this project we have found simple coupling on to the R-110's free poorly nucleophillic amino moieties in a symmetric mode is capricious in nature. Therefore substituting the coumarin dye to a fluorophore requiring attachment of the substrate sequence in a non-symmetric mode would be advantageous. Taking all this into consideration the two possible suitable synthetic strategies for this fluorophore substitution are:

(i) Using a Singapore Green (SG) analogue (figure 47) this compound structurally allows attachment on to a single amino moiety, thereby fulfilling the requirement of non-symmetric functionalisation. The dye is reported to have a higher quantum yield and extinction coefficient like rhodamines in comparison to coumarin dyes as shown in table 19. SG is of particular interest as recently it has been demonstrated by Bywaters et al. as a dye that can be used for protease based detection systems.[143]

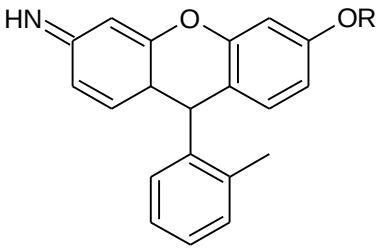

Figure 47 – Structural representation of Singapore Green – R = alkyl

Fluorophore	ε ($M^{-1}cm^{-1}$)	φ
AMC	$1.7x10^4$	0.63
Rhod 110	$6.8x10^4$	0.98
Singapore Green	$4.6x10^4$	0.65

Table 19 – List of fluorophore and their quantum yields and extinction coefficient values.[143, 144]

(ii) Synthesising a novel fluorophore and incorporating the tripeptide functionalisation to a simple framework, a possible synthetic plan is attached of a hybrid of rhodamine b and R-110.[145]

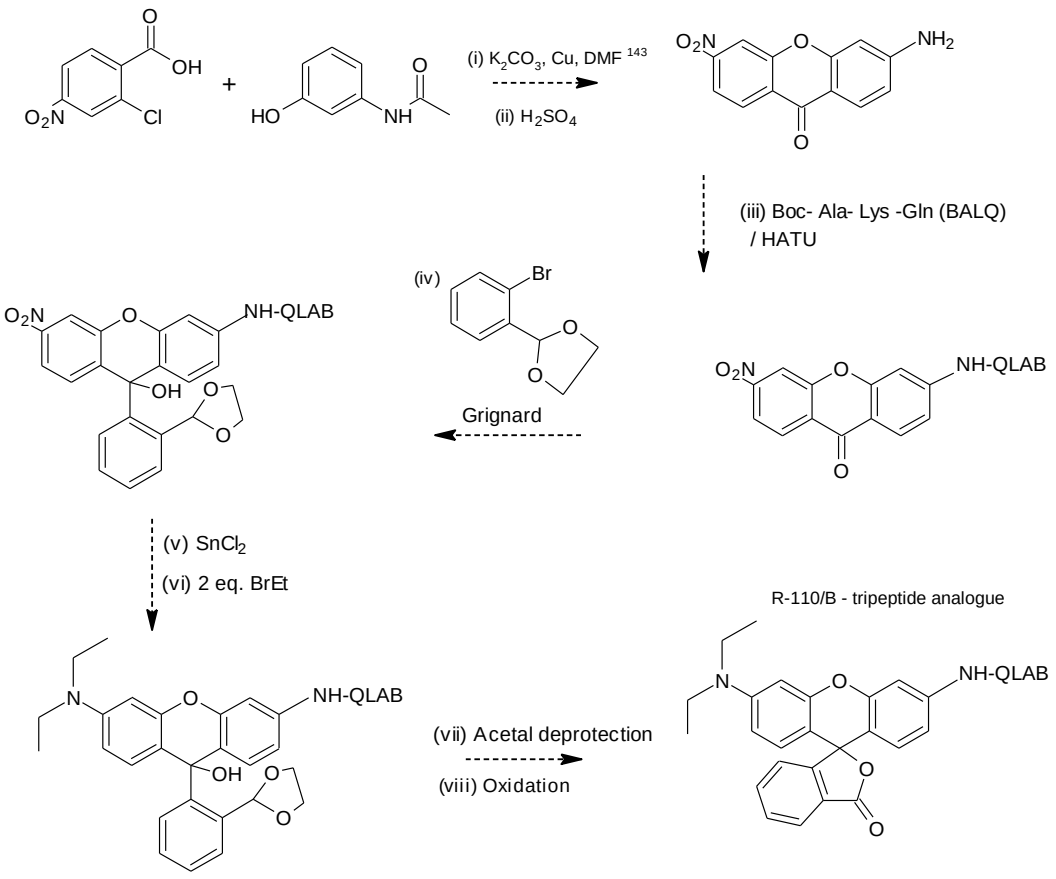

Scheme 7 – Synthetic plan for rhodamine b/ R-110 hybrid conjugated to tripeptide analogue.

CHAPTER 4: EXPERIMENTAL

4.1. GENERAL PROCEDURES AND INSTRUMENTATION.

NMR was recorded using Brüker Avance III 400 two channel FT-NMR spectrometer and the Brüker Avance III 600 three channel FT-NMR spectrometer. ^{1}H NMR spectra were recorded at either 400 or 600 MHz and ^{13}C NMR spectra were recorded at 100 MHz. ^{19}F NMR spectra were recorded at 376 MHz. Chemical shifts were referenced to the solvent used and noted in the experimental. IR (infrared) was recorded using Perkin Elmer Spectrum 100 FT-IR spectrometer. GC/MS was recorded on Agilent Technologies 5973 mass selective detector, 6890 N Network GC system. HRMS and elemental analysis results were obtained *via* Medac Ltd.

TLC analysis was carried out on silica, aluminium oxide, reverse phase silica coated plates and were visualised by a single method or a combination of the following methods: (a) viewing under UV at 254 nm; (b) viewing under UV at 365 nm; (c) exposure to a ninhydrin solution, containing 2g of ninhydrin in 60mL of ethanol; (d) exposure to a vanillin solution, containing 6g of vanillin, 250 mL of ethanol and 1.5 mL of 12M aqueous sulphuric acid.

Preparative TLC was carried out on normal phase silica based plates; the mobile phase solvent mix is described in ratios in the procedure details. Manual columns were run using normal phase silica of particle size 250-500 µm, 35-60 mesh.

4.2. EXPERIMENTAL PROCEDURE

4.2.1. Synthesis of fragment 1

4.2.1.1. Synthesis of BocNHAla-LysOMe (62)

HATU dipeptide coupling, product = **BocAla-Lys(Z)OMe**

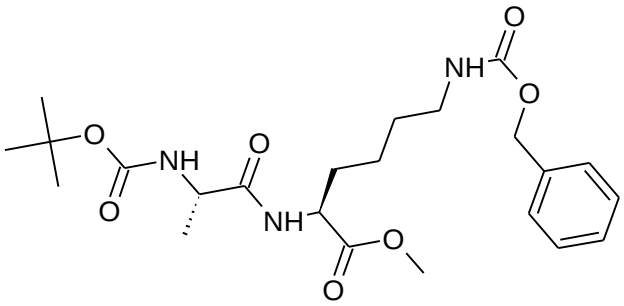

62

Under a nitrogen atmosphere, BocAlaOH (2.5g, 1.5eq, 13.2mmol), Lys(Z)OMe.HCl (2.91g, 1eq, 8.8mmol), HATU (6.69g, 2eq, 17.6mmol) were dissolved in 33 mL of anhydrous DMF. To this solution the base diisopropylethylamine (5.68g, 7.6mL, 5eq.) was added. The resultant yellow solution was left at 50°C overnight. Reaction progression was monitored *via* TLC. The reaction was quenched with 55mL of water and extracted with 3x50mL ethyl acetate and further washed 3x40mL with saturated lithium chloride solution and dried over Na_2SO_4. Reaction mixture was concentrated under reduced pressure and placed on the high vacuum. The crude mixture was purified using the biotage autocolumn on silica with solvent conditions: 2%MeOH:$CHCl_3$to give BocAla-Lys(Z)OMe as a yellow oil (0.55g, 13%).^{1}H NMR (400 MHz, chloroform-*d*) 1.32 (d, 3H), 1.37 (m, 2H), 1.43 (s, 9H), 1.53 (m, 2H), 1.68 (m, 1H), 1.87 (m, 1H), 3.17 (m, 2H), 3.73 (s, 3H), 4.59 (m, 1H), 5.01 (br.s, 2H), 5.10 (br.s, 1H), 6.73 (br.s, 1H, NH), 7.29-7.34 (m, 5H).^{13}C NMR (400 MHz, chloroform-*d*) 172.6, 172.5, 156.5, 136.5, 128.5, 128.2, 128.1, 77 (reference peak), 66.7, 60.4, 52.4, 40.4, 31.8, 29.1, 28.3, 22.0, 21.1, 14.2, 10.0 Mass confirmed by GC/MS, as found 500 $C_{23}H_{30}N_3O_7K$, requires 465 for $C_{23}H_{35}N_3O_7$.

4.2.1.2. Synthesis of BocNHAla-Lys(Z)OH (63)

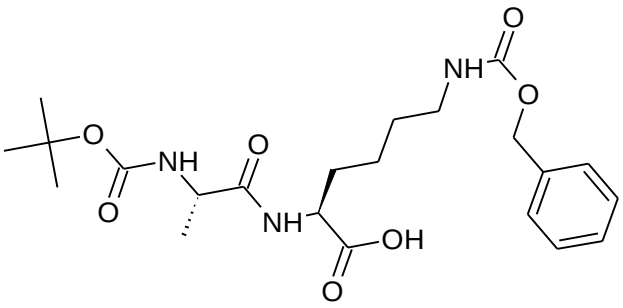

63

Under a nitrogen atmosphere, to a solution of BocAla-Lys(Z)OMe (0.55g, 1.18mmol) in THF:H_2O (1:1) (10mL) was added LiOH.H_2O (0.097g, 2.232 mmol), the reaction mixture was left to stir at ambient temperature over two nights. Reaction progression monitored *via* TLC. The mixture was acidified using 5% aqueous HCl and extracted with ethyl acetate (15mL x 2) and washed with water (10mL x 1) then brine (10mL x1) and dried over Na_2SO_4. Reaction mixture was concentrated under reduced pressure and placed on the high vacuum. The crude mixture was purified using the biotage auto-column on silica with solvent conditions 10 % MeOH: $CHCl_3$ to afford a yellowy oil (0.19g, 35%).^{1}H NMR (400 MHz, chloroform-*d*) 1.26 (d, 1H), 1.33 (m, 2H), 1.42 (s, 9H), 1.51 (m, 2H), 1.76 (m, 1H), 1.91 (m, 1H), 3.17 (m, 2H), 4.54 (m, 1H), 5.08 (br.s, 2H), 5.15 (br.s, 1H), 6.73 (br.s, 1H, NH), 7.36-7.38 (m, 5H).^{13}C NMR (400 MHz, chloroform-*d*) 172.6, 172.1, 156.4, 136.1, 127.9, 128.1, 128.0, 77 (reference peak), 66.1, 60.0, 40.1, 31.5, 28.8, 28.1, 22.0, 21.0, 14.1, 1.0. Mass confirmed by GC/MS, as found 490 $C_{22}H_{33}N_3O_7K$, requires 451 for $C_{23}H_{35}N_3O_7$.

4.2.1.3. Synthesis of triflates

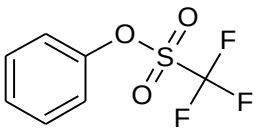

64

A solution of hydroxybenzene (0.5g, 2.3mmol) in DCM (30mL) was prepared and cooled to 0 °C. To this DIEA (0.47mL, 2.7mmol, 1.15eq.) and trifluoromethanesulfonic anhydride (0.44mL, 2.7mmol, 1.15eq.) were added and the reaction was stirred at room temperature for 1.5 hours. The reaction was quenched with water and extracted with DCM. The organic layer was washed with $CuSO_4$(aq) and brine, dried over magnesium sulfate and filtered under gravity and concentrated under vacuum. The crude mixture was purified using flash chromatography on silica gel with mobile phase of hexane: ethylactetate of ratio 7:3 to afford a greeny-white crystalline solid (0.33g, 61%). ^{1}H NMR (400 MHz, chloroform-*d*) 7.39 (m, 2H), 7.32 (m, 1H), 7.2 (m, 2H).^{13}C NMR (100 MHz, chloroform-*d*) 149.33, 129.95, 128.07, 121.02, 53.8. ^{19}F NMR (376 MHz, chloroform-*d*) δ -72.7 (s); GC-MS found 226, requires 226 for $C_7H_5F_3O_3S$.

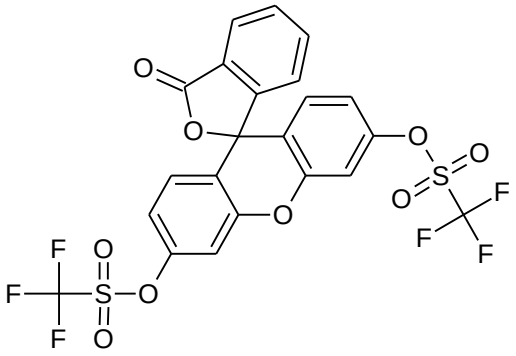

65

A suspension of fluorescein (2.50g, 7.52mmol) in DCM (30mL) was prepared and cooled to 0 °C. To this pyridine (4.87mL, 60.2mmol, 8.0eq) and trifluoromethanesulfonic anhydride (5.06mL, 30.1mmol, 4.0eq) were added and the reaction was stirred a room temperature for 5 hours. The reaction was quenched with water and extracted with DCM. The organic layer was washed with $CuSO_4$(aq) and brine, dried over magnesium sulfate and filtered under gravity and concentrated under vacuum. The crude mixture was purified using flash chromatography on silica gel with mobile phase of hexane: ethylactetate of ratio 7:3 to afford a clear foam (47%).^{1}H NMR (400 MHz, chloroform-*d*) 8.09 – 8.06 (m, 1H), 7.73 (td, *J* = 7.4, 1.4 Hz, 1H), 7.67 (td, *J* = 7.4, 1.2 Hz,1H), 7.36 (d, *J* = 2.4 Hz, 2H), 7.27 – 7.15 (m, 1H), 7.03 (dd, *J* = 8.8, 2.4 Hz, 2H), 6.93 (d, *J* = 8.8 Hz, 2H); ^{13}C NMR(100 MHz, chloroform-*d*) 166.16, 151.9, 151.2,150.5, 135.2, 129.1, 128.9, 124.5,125.1, 122.7, 120.3, 119.8, 118.8, 111.3, 81.2. ^{19}F NMR (376 MHz, chloroform-*d*)
δ -72.9 (s); MS (ESI) found 404.2, requires 403.4 for $C_{22}H_{11}F_6O_9S_2$.

4.2.2. Synthesis of fragment 2.

4.2.2.1. Synthesis of 1-Azido-4-nitrobenzene

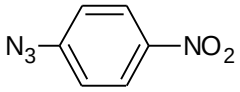

66

pTsOH.H_2O (1.71g, 9mmol, 9eq.) was dissolved in H_2O (11mL). To this solution para nitro aniline (0.138g, 1mmol, 1eq.) was added. To the resulting suspension $NaNO_2$ (0.76g, 18mmol, 9eq.) was slowly added over a period of 10 minutes. The solution was left stirring at room temperature for an hour, then NaN_3 (0.104g, 1.6mmol, 1.6eq) was added. The mixture was filtered under vacuum and washed with H_2O (1 x 50mL), to afford a beige powder (0.15g, 92%). ^{1}H NMR (400 MHz, DMSO-d_6) δ ppm 2.50 (solvent reference peak), 3.33 (H_2O peak), 7.36 (s, 2H), 8.24 (s, 2H).^{13}C NMR (100 MHz, DMSO-d_6) δ ppm 39.7 (solvent reference peak), 120.32, 125.78, 144.27, 146.92. m.p 52.2-52.7°C, literature reference value 52°C.[146]

4.2.2.2. Synthesis of BocGlnAMC – A four step process including deprotection

Synthesis *via* selenocarboxylate/ azide amidation:[1,2]

Part 1)

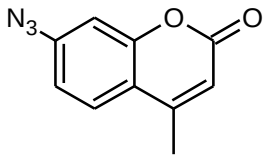

67

pTsOH.H_2O (3.42g, 18mmol, 9eq.) was dissolved in H_2O (18mL). To this solution AMC (0.35g, 2mmol, 1eq.) was added. To the resulting suspension $NaNO_2$ (1.52g, 18 mmol, 9eq.) was slowly added over a period of 10 minutes. The solution was left stirring at room temperature for an hour, then NaN_3 (0.21g, 3.2 mmol, 1.6eq.) was added. The mixture was filtered under vacuum and washed with H_2O (1 x 50mL), to afford a beige powder (0.36g, 89%). ^{1}H NMR (400 MHz, DMSO-d_6) δ ppm 2.41 (d, *J*=1.25 Hz, 3 H), 3.33 (H_2O peak), 6.34 (d, *J*=1.25 Hz, 1 H), 7.09 - 7.16 (m, 2 H), 7.77 (d, *J*=8.53 Hz, 1 H). ^{13}C NMR (100 MHz, DMSO-d_6) δ ppm 17.87, 39.31 (solvent reference peak), 106.59, 112.98, 115.35, 116.54, 126.78, 143.08, 152.73, 153.81, 159.32. m.p 110.4-110.6°C, literature reference 110°C.[147]

Part 2)

Preparation of an isopropanol solution of sodium hydrogen selenide needed for part 3)

To a suspension of degassed isopropanol (10mL) and selenium (93mg) was added sodium borohydride (53mg, 1.4mmol) and left stirring for 45 minutes to get a colourless solution ready for use.

Part 3)

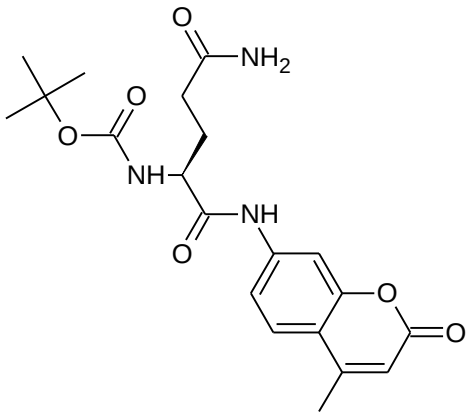

68

Under a nitrogen atmosphere, to a solution of BocGlnOH (0.29g, 1.18mmol, 1.2eq.) and N –methyl piperidine (143µL, 1.18mmol, 1.2eq.) in DMF (5mL) was added isopropylchloroformate (162µL, 1.18mmol, 1.2eq.) at -15°C, the mixture was stirred at -15°C for a further 20 mins. The NaHSe solution prepared in part 2, was added to the mixed anhydride solution *via* cannulation slowly over a period of 5 mins. The reaction mixture was left for a further 30 mins stirring below 10°C, and then a solution of the azide was prepared, azido methyl coumarin (0.2g, 0.98mmol, 1eq.) in DMF (4mL) and cannulated into the reaction mixture. The reaction was left stirring overnight at room temperature. Reaction progression confirmed *via* TLC. The volatile solvents were removed under pressure, redissolved in 30mL of DCM and washed with $NaHCO_3$ (2 x 10mL), water (1 x 9mL) then brine (2 x 9mL) and dried over Na_2SO_4. Reaction mixture was concentrated under reduced pressure and placed on the high vacuum. The crude product was purified using prep TLC (3% MeOH:DCM) to give a white powder (0.0322g, 8%). ^{1}H NMR (400 MHz, methanol-d_4) δ ppm 1.41 (s, 9 H), 1.94 (m, 1 H), 2.11 (m, 1 H), 2.37 (t, 2 H), 2.45 (s, 3 H), 4.21 (m, 1 H), 6.23 (s, 1H), 7.5 (d, 1H), 7.7 (d, 1H) and 7.81 (d, 1H). Grease peaks omitted. ^{13}C NMR (100 MHz, DMSO-d_6) δppm 18.46, 28.63, 29.00, 32.39, 48.84 (solvent reference peak) 56.31, 80.72, 108.03, 113.55, 117.13, 126.66, 130.65, 143.35, 155.2, 155.32, 163.18, 177.64.
IR (ATR) ν_{max} / cm^{-1} 3370, 2976, 2928, 2409, 1640, 1613. TOF MS ES found 404.2, requires 403.4 for $C_{20}H_{25}N_3O_6$.

Part 4)

Boc deprotection to give NH_2GlnAMC**, 69**

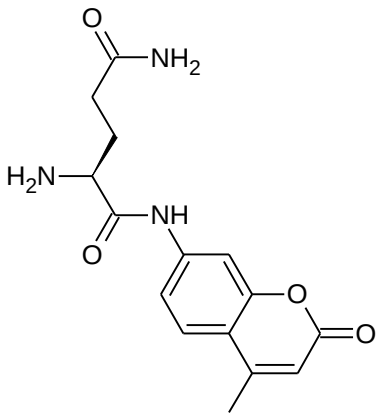

69

The boc protected amino acid (0.0322g, 0.11mmol) was dissolved in DCM (1mL) to this solution TFA (0.2mL) was added and left to stir at room temperature for 1 hour. Reaction completion was detected *via* TLC. The volatile solvents were removed under reduced pressure, diluted with ethyl acetate, neutralised using $NaHCO_3$ and dried over $MgSO_4$. Reaction mixture was concentrated under reduced pressure and placed on the high vacuum. Product afforded as a yellowy smear in flask (0.029g, 87%). TLC used to determine reaction completion no further data was collected.^{1}H NMR (400 MHz, methanol-d_4) δ ppm (grease), 2.19 (m, 1 H), 2.35 (m, 1 H), 2.45 (s, 3H), 2.53 (m, 2H), 4.35 (dd, 2H), 6.35 (s, 1H), 7.52 (dd, 1H), 7.70 (d, 1H), 7.81 (d,1H). ^{13} C NMR (100 MHz, methanol-d_4) δ ppm 18.66, 26.99, 30.63, 49.15 (solvent reference peak), 58.99, 108.26, 113.90, 117.31, 126.93, 131.49, 143.45, 155.34, 155.50, 163.29, 173.62, 181.74.

4.2.2.3. Final peptide coupling to give BocAlaLys(Z)GlnAMC, 70.

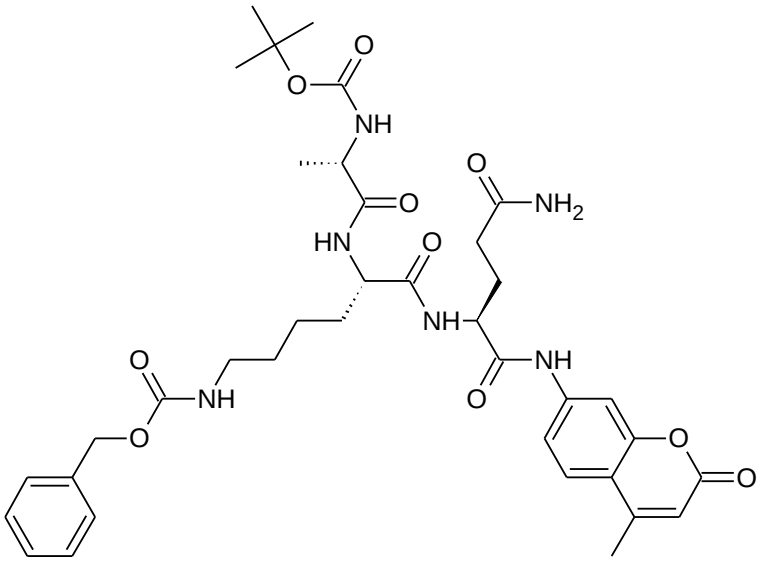

70

Under a nitrogen atmosphere, BocAlaLys(Z)OH (65mg, 0.14mmol, 1.5eq.), NH_2GlnAMC (29mg, 0.96mmol, 1eq.), HATU (72 mg, 0.19 mmol, 2eq.) were dissolved in 1.5ml of anhydrous DMF. To this solution the base) was added DIEA (5.68g, 80µL, 5eq.). The resultant yellow solution was left at 50°C for a week. Reaction progression was monitored *via* TLC. The reaction was quenched with 2mL of water and extracted with 6 mL ethyl acetate and further washed 3 x 2mL with saturated lithium chloride solution and dried over Na_2SO_4. Reaction mixture was concentrated under reduced pressure and placed on the high vacuum. The crude mixture was purified using preparative TLC (6.5% MeOH:DCM) (3mg, 0.4%),^{1}H NMR (400 MHz, methanol-d_4) δ ppm 1.26 - 1.35 (m, 1 H), 1.41 - 1.46 (m, 9 H), 1.47 - 1.51 (m, 1 H), 1.51 - 1.52 (m, 1 H), 1.52 - 1.54 (m, 1 H), 1.88 - 1.90 (m, 1 H), 2.43 - 2.48 (m, 1 H), 2.69 - 2.73 (m, 1 H), 2.91 - 2.93 (m, 1 H), 3.09 - 3.16 (m, 1 H), 3.34 - 3.36 (m, 1 H), 3.45 - 3.50 (m, 1 H), 3.62 - 3.65 (m, 1 H), 5.02 - 5.07 (m, 1 H), 6.21 - 6.26 (m, 1 H), 7.25 - 7.38 (m, 1 H), 7.67 - 7.76 (m, 3 H), 7.85 - 7.87 (m, 1 H), 7.90 - 7.95 (m, 1 H). ES TOF MS found 737.35, requires 736.8 for $C_{37}H_{48}N_6O_{10}$. Molecular formula verified by elemental analysis: C, 60.01; H,6.87; N, 11.37; O, 21.70.

4.2.2.4. Final peptide coupling to give BocAlaLys(Boc)Gln(Trt)AMC, 71.

HATU coupling of tripeptide sequence to the AMC to synthesise BocAlaLys(Boc)Gln(Trt)AMC, **71**

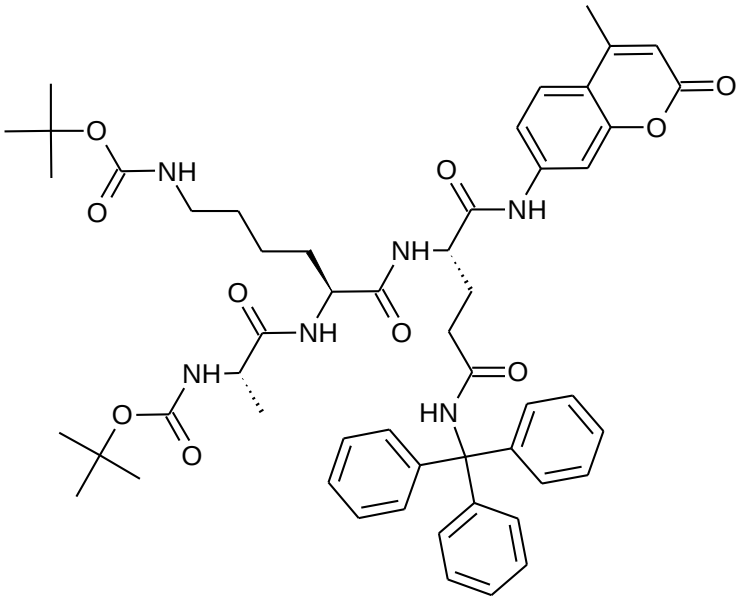

71

Under a nitrogen atmosphere, BocAlaLys(Boc)Gln(Trt)OH (50 mg, 0.0634mmol, 1eq.), AMC (11 mg, 0.0635 mmol, 1eq.), HATU (48 mg, 0.127mmol, 2eq.) were dissolved in 5ml of anhydrous DMF. To this solution the base DIEA (41 mg, 55µL, 5 eq.) was added. The resultant yellow solution was left at 50°C for 3 nights. Reaction progression was monitored *via* TLC. The reaction was quenched with 10mL of water and extracted with 3 x 10mL ethyl acetate and further washed 3 x 8mL with saturated lithium chloride solution and dried over Na_2SO_4. Reaction mixture was concentrated under reduced pressure and placed on the high vacuum. The crude mixture was purified using the preparative TLC with solvent conditions: 5%MeOH:DCM to give BocAlaLys(Boc)Gln(Trt)AMC as a clear oil (10 mg, 15.7%). ^{1}H NMR (400 MHz, methanol-d_4) δ ppm 1.05 - 1.22 (m, 3 H) 1.23 - 1.35 (m, 4 H) 1.37 - 1.53

(m, 18 H) 2.81 (s, 1 H) 2.86 (d, *J*=0.75 Hz, 1 H) 2.96 - 3.08 (m, 2 H) 3.69 (d, *J*=6.78 Hz, 1 H) 3.81 - 4.17 (m, 1 H) 4.34 - 4.51 (m, 1 H) 4.58 - 4.67 (m, 1 H) 4.68 - 4.80 (m, 1 H) 6.22 - 6.25 (m, 1 H) 7.13 - 7.33 (m, 15 H). ^{13}C NMR (100 MHz, methanol-d_4) δ ppm,16.61, 17.31, 18.43, 19.91, 23.10, 27.45, 28.12, 28.41, 29.93, 30.35, 30.83, 31.31, 32.6, 33.24, 33.33, 36.46, 37.10, 38.35, 40.23, 49.05, 49.20, 51.56, 54.27, 111.13, 117.25, 121.35, 122.05, 127.04, 128.18, 128.21, 133.5. Mass confirmed by TOF MS ES as found 967.4595 $C_{53}H_{64}N_6O_{10}Na$, requires 945 for $C_{53}H_{64}N_6O_{10,}$ Molecular formula verified by elemental analysis: C, 67.31; H, 6.87; N, 8.81; O, 16.70.

REFERENCE AND NOTES

REFERENCES AND NOTES

[1]A. B. Zahur, H. Irshad, M. Hussain, R. Anjum, M. Q. Khan. (2006). Transboundary Animal Diseases in Pakistan. *Zoonoses and Public Health*. 53 (s1), p19-22.

[2]N. Knowles, J. He, Y. Shang and D.P. King, *et al.* (2012). Southeast Asian Foot-and-Mouth Disease Viruses in Eastern Asia. *Emerging Infectious Diseases*. 18 (3), p499-501.

[3]Image: https://wellcomecollection.org/works/y9t42evg. Structure of foot-and-mouth disease virus. Credit: David Stuart, Uni. of Oxford. CC BY

[4]E. M. Cottam, D. T. Haydon, D. J. Paton, J. Gloster, J. W. Wilesmith, N. P. Ferris, G. H. Hutchings and D. P. King. (2006). Molecular epidemiology of the FMDV in UK outbreak 2001. *Journal of Virology*. 80, p11274-11282.

[5] S. M. Jamal, G. J. Belsham. (2018). Molecular epidemiology, evolution and phylogeny of FMDV. *Infection, Genetics and Evolution*. 59, p84-98.

[6] F. D-S. Segundo, G. N. Medina, C. Stenfeldt, J. Arzt and T. de los Santos. (2017). Foot-and-mouth disease vaccines. *Veterinary Microbiology*. 206, p102–112.

[7] S. Alexandersen, Z. Zhang, A. I. Donaldson, A. J. M. Garland. (2003). The pathogenesis and diagnosis of foot and mouth disease. *Journal of Comparative Pathology*. 129, p1-36.

[8] N. Longjam, R. Deb, A. K. Sarmah, T. Tayo, V. B. Awachat and V. K. Saxena. (2011). A brief review on diagnosis of foot and disease of livestock: conventional to molecular tools. *Veterinary Medicine International*.p1-17.

[9] Department for Environment, Food & Rural Affairs and Animal and Plant Health Agency DEFRA and PHA. (2014). *Foot and mouth disease: how to spot and report it.* Available: https://www.gov.uk/guidance/foot-and-mouth-disease. Last accessed 1st March 2018

[10]D. J. Paton, S. Gubbins, D. P. King. (2018). Understanding the transmission of FMDV at different scales. *Current opinion in virology*. 28, p85-91.

[11]B. Baxt and M. J. Grubman. (2004). Foot-and-Mouth Disease. *Clinical Microbiology Reviews*, 17(2), p465–493.

[12]F. D-S. Segundo, G. N. Medina, C. Stenfeldt, J. Arzt and T. de los Santos. (2017). Foot and mouth disease vaccines. *Veterinary Microbiology*. 206, p102-112.

[13]OIE/FAO, 2017. In: D. King and M. Henstock (Eds.), Foot-and-Mouth Disease Reference Laboratory Network. OIE/FAO.

[14] D. King. (2017). Chapter 2.1.8 FMD (infection of FMDV).*OIE Terrestrial Manual*.p1-29.

[15] E. L. A. Howson, B. Armson, M. Madi, C. J. Kasanga, S. Kandusi, R. Sallu, E. Chepkwony, A. Siddle, P. Martin, J. Wood, V. Mioulet, D. P. King, T. Limbo, S.Cleaveland, V. L. Fowler. (2017). Evaluation of Two Lyophilized Molecular Assays to Rapidly Detect Foot-and-Mouth Disease Virus Directly from Clinical Samples in Field Settings. *Transboundary and Emerging Diseases*. 64 (3), p861-871.

[16]Image: https://laboratoryinfo.com/wp-content/uploads/2015/03/complement-fixation-test.jpg

[17] Reproduced from: Immunology, Pearson education 2013

[18] M. J. Grubman and B. Baxt. (2004). Foot-and-Mouth Disease. *Clinical Microbiology Reviews*, 17(2), pp.465–493. K. D. Clercq, et al. (2017). Laboratory validation of two real-time RT-PCR methods with 5′-tailed primers for an enhanced detection of foot-and-mouth disease virus. *Journal of Virological Methods*. 246, p90–94.

[19] F. Vandenbussche, D. J. Lefebvre, I. D. Leeuw, S. V. Borm and K. D. Clercq. (2017). Laboratory validation of two real-time RT-PCR methods with 5′-tailed primers for an enhanced detection of foot-and-mouth disease virus. *Journal of Virological Methods*. 246, p90–94.

[20]J. P. Dukes, D. P. King and S. Alexandersen. (2006). Novel reverse transcription loop-mediated isothermal amplification for rapid detection of foot-and-mouth disease virus. *Archives of virology*. 151 (6), p1093.

[21] S. Yang, J. Yang, G. Zhang, X. Wang, S. Qiao, D. Zhao, Y. Zhi, X. Li, G. Xing, J. Luo, J. Fan and D. Bao. (2010). Development of an immunochromatographic strip for the detection of antibodies against foot-and-mouth disease virus serotype O. *Journal of Virological Methods*. 165, p139–144.

[22]A. I. Donaldson, A. Hearps and S. Alexandersen. (2001). Evaluation of a portable, 'real-time' PCR machine for FMD diagnosis. *The Veterinary Record.*149 (14), p430.

[23] M. Madi, A. Hamilton, D. Squirrell, V. Mioulet, P. Evans, M. Lee and D. P. King. (2011). Rapid detection of foot-and-mouth disease virus using a field-portable nucleic acid extraction and real-time PCR amplification platform. *The Veterinary Journal*. 193 (1), p67-72.

[24]Anonymous. (2010). Rapid detection of FMDV by RT-LAMP. *The International Journal of Applied Research in Veterinary Medicine*. 8 (2), p133-142.

[25] T. Notomi, H. Okayama, H. Masubuchi, T. Yonekawa, K. Watanabe, N. Amino and T. Hase. (2000). Loop-mediated isothermal amplification of DNA. *Nucleic Acids Research*. 28 (12), e63.

[26]A. V. Amerongen, J. Veen, H. A. Arends and M. Koets.(2018). Chapter 7 – Lateral Flow Immunoassays. In: S. K. Vashist and J. H.T. Luong, *Handbook of Immunoassay Technologies: Approaches, Performances, and Applications*. Netherlands: Academic Press. p157–182.

[27] M. Sajid, A-N. Kawde and M. Daud. (2016). Designs, formats and applications of lateral flow assay: A literature review. *Journal of Saudi Chemical Society*. 82, p286-306.

[28] N. P. Ferris, A. Nordengrahn, G. H. Hutchings, S. M. Reid, D. P. King, K. Ebert, D. J. Paton, T. Kristersson, E.Brocchi, S. Grazioli and M. Merza. (2009). Development and laboratory validation of a lateral flow device for the detection of foot-and-mouth disease virus in clinical samples. *Journal of Virological Methods.*155, p10–17.

[29]N. P. Ferris, A. Nordengrahn, G. H. Hutchings, D. P. King, D. J. Paton, T. Kristersson, E.Brocchi, S. Grazioli and M. Merza. (2010). Development and laboratory validation of a lateral flow device for the detection of serotype SAT 2 foot-and-mouth disease viruses in clinical samples. *Journal of Virological Methods*. 163, p474-476.

[30] J. K Oem, N. P. Ferris, K-N. Lee, Y-S.Joo, B-H.Hyun and J-H Park. (2009). Simple and rapid lateral-flow assay for the detection of foot-and-mouth disease virus. *Clinical and Vaccine Immunology*. 16, p1660–1664.

[31] T. Jiang, Z. Liang, W. Ren, J. Chen, X. Zhi, G. Qi, Y. Yang, Z. Liu, X. Liu and X. Cai. (2011). Development and validation of a lateral flow immunoassay using colloidal gold for the identification of serotype-specific foot-and-mouth disease virus O, A and Asia 1.*Journal of Virological Methods*. 171, p74-80.

[32] S. Yang, J. Yang, G. Zhang, X. Wang, S. Qiao, D. Zhao, Y. Zhi, X. Li, G. Xing, J. Luo, J. Fan and D. Bao. (2010). Development of an immunochromatographic strip for the detection of antibodies against foot-and-mouth disease virus serotype O. *Journal of Virological Methods*. 165, p139–144.

[33] V. L. Fowler, E. L. A. Howson, M. Madi, V. Mioulet, C. Caiusi, S. J. Pauszek, L. L. Rodriguez and D. P. King. (2016). Development of a reverse transcription loop-mediated isothermalamplification assay for the detection of vesicular stomatitis New Jersey virus: Use of rapid molecular assays to differentiate betweenvesicular disease viruses. *Journal of Virological Methods*. 234, p123-131.

[34] R. A. Waters, V. L. Fowler, B. Armson, N. Nelson, J. Gloster, D. J. Paton and D. P. King. (2014). Preliminary Validation of Direct Detection of Foot-And-Mouth Disease Virus within Clinical Samples Using Reverse Transcription Loop-Mediated Isothermal Amplification Coupled with a Simple Lateral Flow. *PLoS One 9*. e105630.

[35]E. L. A. Howson, B. Armson, M. Madi, C. J. Kasanga, S. Kandusi, R. Sallu,E. Chepkwony, A. Siddle, P. Martin, J. Wood, V. Mioulet, D. P. King, T. Lembo, S. Cleaveland and V. L. Fowler. (2015). Evaluation of Two Lyophilized Molecular Assays to Rapidly Detect Foot-and-Mouth Disease Virus Directly from Clinical Samples in Field Settings. *Transboundary and Emerging Diseases, PLOS ONE*.9 (8), e105630.

[36]A. Romey, A. Relmy, K. Gorna, E. Laloy, S. Zientara, S. Blaise-Boisseau and L. Bakkali Kassimi. (2017). Safe and cost-effective protocol for shipment of samples from Foot-and-Mouth Disease suspected cases for laboratory diagnostic. *Transboundary and Emerging Diseases*. 65, Abstract.

[37]T. J. D Knight-Jones andJ. Rushton. (2013). The economic impacts of foot and mouth disease – What are they, how big are they and where do they occur? *Preventive Veterinary Medicine*. 112 , p161-173.

[38]OIE, animal disease summary information 2018

Available: http://www.oie.int/wahis_2/public/wahid.php/Diseaseinformation/Immsummary.

Last accessed: 11th March 2020.

[39]D. King, OIE, 2017. Infection with foot and mouth disease virus.OIE Terrestrial Animal Health Code. OIE (World Organization for Animal Health), Paris, France (Chapter 8.8).

[40]C. Brown, D. Thompson, P. Muriel,D. Russell,P. Osborne, A. Bromley, M. Rowland and S. Creigh-Tyte. (2002) Economic costs of the foot and mouth disease outbreak in the United Kingdom in 2001. Revue Scientifique et Technique (International Office of Epizootics). 21 (3), p675-687.

[41]Great Britain National Audit Office (2002). *The 2001 outbreak of foot and mouth disease House of Commons papers 2001-02 939.* England: TSO (The Stationery Office). 133 pages.

[42]Anonymous.*At what cost? 2001 and 2007 FMD outbreak UK.*

Available: https://oda.state.ok.us/ais/atwhatcost.pdf.

Last accessed 2nd March 2018.

[43]S. Denver, L. Alban, A. Boklund, H. Houe, S. Mortensen, E. Rattenborg, T. VigTamstorf, H. Zobbe and T. Christensen. (2016). The costs of preventive activities for exotic contagious diseases—A Danish case study of foot and mouth disease and swine fever. *Preventive Veterinary Medicine*. 131, p111-120.

[44] E. M. Cottam, J. Wadsworth, A. E. Shaw, R. J. Rowlands, L. Goatley, S. Maan, N. S. Maan, P. P. C. Mertens, K. Ebert, Y. Li, E. D. Ryan, N. Juleff, N. P. Ferris, J. W. Wilesmith, D. T. Haydon, D. P. King, D. J. Paton and N. J. Knowles. (2008). Transmission Pathways of Foot-and-Mouth Disease Virus in the United Kingdom in 2007. *PLOS Pathogens* 4 (4).

[45]B. P. Brito, L. L. Rodriguez, J. M. Hammond, J. Pinto and A. M. Perez. (2015). Review of the Global Distribution of Foot-and-Mouth Disease Virus from 2007 to 2014.*Transboundary and Emerging Diseases*. 64 (2), p316-332.

[46]T.J.D.Knight-Jones andJ.Rushton. (2013). The economic impacts of foot and mouth disease –What are they, how big are they and where do they occur? *Preventive Veterinary Medicine*, 112, p161-173.

[47]T. J. D. Knight-Jones, L. Robinson, B. Charleston, L. L. Rodriguez, C. G. Gay, K. J. Sumption and W. Vosloo. (2016). Global foot-and-mouth disease research update and gap analysis: 2 epidemiology, wildlife and economics. *Transboundary and Emerging Diseases*. p14–29.

[48] F. D-S. Segundo, G. N. Medina, C. Stenfeldt, J. Arzt and T. de los Santos.(2017).Foot-and-mouth disease vaccines.*Veterinary Microbiology*.206, p102–112.

[49]B. P. Sreenivasa, J. K. Mohapatra, S. J. Pauszek, M. Koster, V. C. Dhanya, R.P.Tamil Selvan, M. Hosamani, P. Saravanan, S. H. Basagoudanavar, T. de los Santos,R. Venkataramanan, L. L. Rodriguez andM. J. Grubman. (2017). Recombinant human adenovirus-5 expressing capsid proteins of Indian vaccine strains of foot-and-mouth disease virus elicits effective antibody response in cattle. *Veterinary Microbiology*. 203, p196-201.

[50] V. L. Fowler, J. B. Bashiruddin, F. F. Maree, P. Mutowembwa, B. Bankowski, D. Gibson, S. Cox, N. Knowles and P. V. Barnett. (2011). Foot-and-mouth disease marker vaccine: Cattle protection with a partial VP1 G–H loop deleted virus antigen. *Vaccine*. 29 (46), p8405-8411.

[51]Å. Uttenthal, S. Parida, T. B. Rasmussen, D. J. Paton, B. Haas and W. G. Dundon. (2010). Strategies for differentiating infection in vaccinated animals (DIVA) for foot-andmouth disease, classical swine fever and avian influenza. *Expert Review of Vaccines*. 9 (1), p73-87.

[52]V. Fowler, L. Robinson, B. Bankowski,S. Cox, S. Parida, C. Lawlor, D. Gibson, F. O'Brien, B. Ellefsen, D. Hannama, H. -H. Takamatsu and P. V. Barnett. (2012). A DNA vaccination regime including protein boost and electroporation protects cattle against foot-and-mouth disease. *Antiviral Research*. 94 (1), p25-34.

[53]R. P. Kitching, A. M. Hutber and M. V. Thrusfield. (2005). A review of foot-and-mouth disease with special consideration for the clinical and epidemiological factors relevant to predictive modelling of the disease.*The Veterinary Journal*. 169 (2), p197-209.

[54]S. S. Hayer, R. Ranjan, J. K. Biswal, S. Subramaniam, J. K. Mohapatra, G. K. Sharma, M. Rout, B. B. Dash, B. Das, B. R. Prusty, A. K. Sharma, C. Stenfeldt, A. Perez, L. L. Rodriguez, B. Pattnaik, K. VanderWaal and J. Arzt. (2018). Quantitative characteristics of the foot-and-mouth disease carrier state under natural conditions in India.*Transboundary and Emerging Diseases*. 65 (1), p253-260.

[55]D. J. Paton, S. Gubbins and D. P. King. (2018). Understanding the transmission of foot and mouth disease virus at different scales. *Current opinion in virology*. 28, p85-91.

[56]The Pirbright Institute. (March 2018). *The Picornavirus Pages.*

Available: http://www.picornaviridae.com/.

Last accessed 19th Mar 2018.

[57]L.Lutwick.(2014).*Picornavirus-Overview.*

Available:https://emedicine.medscape.com/article/225483-overview.

Last accessed 19th Mar 2018.

[58] R. Hunt. (last updated 2016). *Virology– Chapter 10 Picornaviruses - Part One Enteroviruses and general features of picornaviruses.*

Available:http://www.microbiologybook.org/virol/picorna.htm.

Last accessed 19th Mar 2018.

[59]C. Carrillo, E. R. Tulman, G. Delhon, Z. Lu, A. Carreno, A. Vagnozzi, G. F. Kutish, and D. L. Rock.(2005). Comparative Genomics of Foot and Mouth Disease Virus. *Journal of Virology*. 79 (10), p6487-6504.

[60]J. Newman, A. S. Asfor, S. Berryman, T. Jackson, S. Curryand T. J. Tuthill. (2018). The cellular chaperone heat shock protein 90 is required for foot-and-mouth disease virus capsid precursor processing and assembly of capsid pentamers. Journal of Virology. 92: e01415-17.

[61]N. Luz and E. Beck. (1991). Interaction of a cellular 57-kDa protein with the internal translation initiation site of foot-and-mouth disease virus. *Journal of Virology*. 65, p6486-6494.

[62]G. Wang, Y. Wang, Y. Shang, Z. Zhang and X. Liu. (2015). How foot-and-mouth diseasevirus receptor mediates foot-and-mouth disease virus infection. *Virology Journal*.12 (9), p1-7.

[63]E. Fry, R. Acharya and D. Stuart. (1993). Methods used in the structure determination of foot-and-mouth disease virus.Acta Crystallogr, Sect.A 49: p45-55.

[64]N. Malik, A. Kotecha, S. Gold, A. Asfor, J. Ren, J. T. Huiskonen, T. J. Tuthill, E. E. Fry and D. I. Stuart. (2017). Structures of foot and mouth disease virus pentamers: Insight into capsid dissociation and unexpected pentamer reassociation. *PLOS Pathogens* 13(9): e1006607.

[65]A. Sinclair, L. E. Mulcahy, L. Geldeard, S. Malik, M. D. Fielder and A. Le Gresley (2013). Development of an in situ culture-free screening test for the rapid detection of Staphylococcus aureus within healthcare environments. *Organic & Biomolecular Chemistry*, 11(20), p3307–3313.

[66]M. Ford, J.D. Perry, I. Robson, S. Morgan, M.G. Holliday, K.E. Orr and F.K. Gould (1999). Evaluation of tube coagulase and a fluorogenic substrate for rapid detection of methicillin-resistant Staphylococcus aureus from selective enrichment broth in an outbreak of EMRSA 15. *Journal of Hospital Infection*. 41, p133-135.

[67]G. J. Belsham. (2013). Influence of the Leader protein coding region of foot-and-mouth disease virus on virus replication. *Journal of General Virology*. 94, p1486–1495.

[68]P. W. Mason, M. J. Grubman and B. Baxt.(2003). Molecular basis of pathogenesis of FMDV. *Virus Research*. 91, p9-32.

[69]E. Ziegler, A. M. Borman, R. Kirchweger, T. Skern and K. M. Kean. (1995). Foot and mouth disease virus Lb proteinase can stimulate rhinovirus and enterovirus IRES - driven translation and cleave several proteins of cellular and viral origin. *Journal of Virology*. 69, p3465-3474.

[70]D. Wang, L. Fang, P. Li, L. Sun, J. Fan, Q. Zhang, R. Luo, X. Liu, K. Li, H. Chen, Z. Chen and S. Xiao. (2011). Foot and mouth disease virus leader proteinase negatively regulates the procrine interferon pathway by Acting as a Viral Deubiquitinase. *Molecular Immunology*. 49, p407-412.

[71]D. Wang, L Fang, J Bi, Q Chen, L Cao, R Luo, H Chen and S. Xiao. (2011). Foot and mouth disease virus leader proteinase inhibits dsRNA-induced RANTES transcription in PK-15 cells. *Virus Genes*. 42, p388-393.

[72]T. D. L. Santos, F. D-S. Segundo and M. J. Grubman. (2007). Degradation of nuclear factor kappa B during foot and mouth disease virus infection. *Journal of Virology*. 81, p12803-12815.

[73]F. Tulloch, G. A. Luke and M. D. Ryan.(2017). *Foot-and-Mouth Disease Virus Current Research and Emerging Trends*. Norfolk UK: Caister Academic Press. p43-59.

[74] J. Steinberger, I. Grishkovskaya, R. Cencic, L. Juliano, M. A. Juliano and T. Skern. (2014). Foot and mouth disease virus leader proteinase: Structural insights into the mechanism of intermolecular cleavage. *Journal of Virology*. 468-470, p397-408.

[75] M. Wadhawan, N. Singh and S.Rathaur. (2014) Inhibition of cathepsin B by E-64 induces oxidative stress and apoptosis in filarial parasite. PLoS ONE ***9*** e93161

[76] M. Ryan, M. L. L. Donnelly, G. Luke , A. Mehrotra , X. Li , L. E. Hughes and D. Gani. (2001). Analysis of the aphthovirus 2A/2B polyprotein 'cleavage' mechanism indicates not a proteolytic reaction, but a novel translational effect: a putative ribosomal 'skip'. *Journal of General Virology*. 82, p1013-1025.

[77] P. Sharma, F. Yan, V. A. Doronina, H. Escuin-Ordinas, M. D. Ryan and J. D. Brown. (2012). 2A peptides provide distinct solutions to driving stop-carry on translational recoding. *Nucleic Acids Research*. 40 (7), p3143–3151.

[78]J. R. Birtley, S. R. Knox, A. M. Jaulent, P Brick, R. J. Leatherbarrow and S. Curry. (2005). Crystal Structure of Foot-and-Mouth Disease Virus 3C Protease NEW INSIGHTS INTO CATALYTIC MECHANISM AND CLEAVAGE SPECIFICITY. *Journal of Biological Chemistry*. 280, p11520-11527.

[79]T. Kristensen, P. Normann, M. Gullberg, U. Fahnøe, C. Polacek, T. B. Rasmussen and G. J. Belsham. (2017). Determinants of the VP1/2A junction cleavage by the 3C protease in foot-and-mouth disease virus-infected cells. *Journal of General Virology*. 98, p385–395.

[80]P. A. Zunszain, S. R. Knox, T. R. Sweeney, J. Yang, N. Roqué-Rosell, G. J. Belsham, R. J. Leatherbarrow and S. Curry. (2010). Insights into Cleavage Specificity from the Crystal Structure of Foot-and-Mouth Disease Virus 3C Protease Complexed with a Peptide Substrate. *Journal of Molecular Biology*. 395, p357-389.

[81]Anonymous.(2011). *Fluorescence fundamentals.*

Available:https://www.thermofisher.com/uk/en/home/references/molecular-probes-the handbook/introduction-to-fluorescence-techniques.html.

Last accessed 10th Apr 2018.

[82]J. Lakowicz. (2010). *Principles of Fluorescence Spectroscopy*. 3rd ed. New York: Springer. p1-11.

[83]H. C. Hemker et al., (1983). Substrates / Fluorogenic substrates. In: S. Iwanaga et al *Handbook of Synthetic Substrates*. Boston: Martin Nijhoff. p44 and p83.

[84]K. E. Sapsford, L. Berti and I. L. Medintz. (2006). Materials for Fluorescence Resonance Energy Transfer Analysis: Beyond Traditional Donor–Acceptor Combinations. *Angew. Chem. Int. Ed*. 45 (28), p4562-4589.

[85] C. M. Chung, S. Y. Cho, Y. K. Song, J. G. Kim, S. Y. Oh. (2009). Photoconversion of o-hydroxycinnamates to coumarins and its application to fluorescence imaging. *Tetrahedron Letters*. 50 (33), p4769-4772.

[86] P. Greenspan and S. D. Fowler. (1985). Spectrofluorometric studies of the lipid probe, nile red. *Journal of Lipid Research*. 26, p781-789.

[87] A. Minta, J. P. Kao and R. Y. Tsien. (1989). Fluorescent Indicators for Cytosolic Calcium Based on Rhodamine and Fluorescein Chromophore. *Journal of Biological Chemistry*. 264 (14), p8171-8178.

[88] J. B. Grimm, L. M. Heckman, L. D. L. Janelia. (2012). Chapter One - The Chemistry of Small-Molecule Fluorogenic Probes. In: M. C. Morris. *Fluorescence-Based Biosensors: From Concepts to Applications*. USA: Academic Press. p1-27.

[89] S. Orenga, A. L. James, M. Manafi, J. D. Perry and D. H. Pincus. (2009). Enzymatic substrates in microbiology. *Journal of Microbiological Methods*. 79, p139-155.

[90]J. P. Goddard and J. L. Reymond. (2004). Recent advances in enzyme assays. *Trends in Biotechnology*. 22 (7), p363-370.

[91]J. B. Grimm, T. D. Gruber, G. Ortiz, T. A. Brown and L. D. Lavis. (2016). Virginia Orange: A Versatile, Red-Shifted Fluorescein Scaffold for Single- and Dual-Input Fluorogenic Probes. *Bioconjugate Chemistry*. 27, p474-480.

[92]M. J. Smyth, T. Wiltrout, J. A. Trapani, K. S. Ottaway, R. Sowder, L. E. Henderson, C. M. Kam, J. C. Powers, H. A. Young and T. J. Sayers. (1992). Purification and cloning of a novel serine protease, RNK Met-1, from the granules of a rat natural killer cell leukemia. *The Journal of Biological Chemistry*. 267, p24418-24425.

[93] F. Velotti, G. Palmieri, D. D'Ambrosio, M. Piccoli, L. Frati and A. Santoni. (1992). Differential expression of granzyme A and granzyme B proteases and their secretion by fresh rat natural killer cells (NK) and lympokine-activated killer cells with NK phenotype (LAK-NK). *European Journal of Immunology*. 22, p1049-1053.

[94]H. R. Stennicke, M.Renatus, M. Meldal and G. S. Salvesen. (2000). Internally quenched fluorescent peptide substrates disclose the subsite preferences of human caspases 1, 3, 6, 7 and 8. *Journal of Biological Chemistry*. 350, p563–568.

[95] D. Maly, F. Leonetti, B. J. Backes, D. S. Dauber, J. L. Harris, C. S Craik and J. A. Ellman. (2002). Expedient Solid-Phase Synthesis of Fluorogenic Protease Substrates Using the 7-Amino-4-carbamoylmethylcoumarin (ACC) Fluorophore.*Journal of Organic Chemistry*. 67, p910-915.

[96]J. Woelcke and U. Hassiepen. (2010). Fluorescence- based biochemical protease assay formats. In: T. Chen *A Practical Guide to Assay Development and High-Throughput Screening in Drug.* United states: CRC press. p25-35.

[97]S. P.Leytus, L. L.Melhado and W. F.Mangel. (1983). Rhodamine-based compounds as fluorogenic substrates for serine proteinases. *Journal of Biochemistry*. 209 (2), p299 – 307.

[98]S. K. Grant, J. G. Sklar and R. T. Cummings. (2002). Development of Novel Assays for Proteolytic Enzymes Using Rhodamine-Based Fluorogenic Substrates. *Journal of Biomolecular Screening*. 7 (6), p531-540.

[99] L. Bywaters, L. Mulcahy-Ryan, M. Fielder, A. Sinclair and A. L. Gresley. (2017). Synthetic scale-up of a novel fluorescent probe and its biological evaluation for surface detection of Staphylococcus aureus. *Molecular and Cellular Probes*. 36, p1-9.

[100] J. Woelcke and U. Hassiepen., (2010). Fluorescence- based biochemical protease assay formats. In: T. Chen *A Practical Guide to Assay Development and High-Throughput Screening in Drug.* Unites states: CRC press. p25-35.

[101]S. X. Cai, H. Z. Zhang, J. Guastella, J. Drewe, W. Yang and E. Weber. (2001). Design and Synthesis of Rhodamine 110 Derivative and Caspase-3 Substrate for Enzyme and Cell-Based Fluorescent Assay. *Bioorganic& Medicinal Chemistry Letters*. 11, p39-42.

[102] A. Niles et al., (2006). Caspase-3 assay to detect apoptosis. L. K. Minor. *Handbook of Assay Development in Drug Discovery*. : CRC press. p396-399.

[103]D. Zeng, Y. Ma, R. Zhang, Q. Nie, Z. Cui, Y. Wang, L. Shang and Z. Yin. (2016). Synthesis and structure–activity relationship of a-keto amides as enterovirus 71 3C protease inhibitors.*Bioorganic& Medicinal Chemistry Letters*. 26, p1762-1766.

[104]Q. M. Wang, R. B. Johnson, J. D. Cohen, G. T Voy, J. M Richardson and L. N. Jungheim. (1997). Development of a continuous fluorescence assay for rhinovirus 14 3C protease using synthetic peptides.*Antiviral Chemistry & Chemotherapy*. 8 (4), p303-310.

[105]A. M. Prior, Y. Kim, S. Weerasekara, M. Moroze, K. R. Alliston, R. A. Z. Uy, W. C. Groutas, K. Chang and D. H. Hua. (2013). Design, synthesis, and bioevaluation of viral 3C and 3C-like protease inhibitors.*Bioorganic & Medicinal Chemistry Letters*. 23, p6317-6320.

[106]A. M. Jaulent, A. S. Fahy, S. R. Knox, J. R. Birtley, N. Roqué-Rosell, S. Curry and R. J. Leatherbarrow. (2007). A continuous assay for FMDV 3C protease activity.*Analytical Biochemistry*. 368, p130-137.

[107]J. R. Birtley, S. R. Knox, A. M. Jaulent, P Brick, R. J. Leatherbarrow and S. Curry.(2005). Crystal Structure of Foot-and-Mouth Disease Virus 3C Protease NEW INSIGHTS INTO CATALYTIC MECHANISM AND CLEAVAGE SPECIFICITY.*Journal of Biological Chemistry*. 280, p11520-11527.

[108]J. Woelcke and U. Hassiepen. (2010). Fluorescence- based biochemical protease assay formats. In: T. Chen, *A Practical Guide to Assay Development and High-Throughput Screening in Drug* .Unites states: CRC press. p25-35.

[109]A. Sinclair, L. E. Mulcahy, L. Geldeard, S. Malik, M. D. Fielder and A. Le Gresley (2013). Development of an in situ culture-free screening test for the rapid detection of Staphylococcus aureus within healthcare environments. *Organic & Biomolecular Chemistry*, 11(20), p3307–3313.

[110]T. I. Al-Warhi, H. M. A. Al-Hazimi and A. El-Faham.(2012). Recent development in peptide coupling reagents. *Journal of Saudi Chemical Society*, 16 (2), p97–116.

[111] R. B Merrifield, (1963). Solid Phase Peptide Synthesis. I. The Synthesis of. *Journal of the American Chemical Society*, 85 (14), p2149.

[112]J. R. Birtley, S. R. Knox, A. M. Jaulent, P Brick, R. J. Leatherbarrow and S. Curry.(2005). Crystal Structure of Foot-and-Mouth Disease Virus 3C Protease NEW INSIGHTS INTO CATALYTIC MECHANISM AND CLEAVAGE SPECIFICITY.*Journal of Biological Chemistry*. 280, p11520-11527.

[113]L. Bywaters, L. Mulcahy-Ryan, M. Fielder, A. Sinclair and A. L. Gresley. (2017). Synthetic scale-up of a novel fluorescent probe and its biological evaluation for surface detection of Staphylococcus aureus. *Molecular and Cellular Probes*. 36, p1-9.

[114]J. B. Grimm and L. D. Lavis.(2011). Synthesis of Rhodamines from Fluoresceins Using Pd-Catalyzed CN Cross-Coupling. *Organic Letters*.13 (24), p6354-6357.

[115]L. Wysocki and L. D. Lavis. (2011). Advances in the chemistry of small molecule fluorescent probes. *Current Opinion in Chemical Biology*.15 (6), p752-759.

[116]J. B. Grimm and L. D. Lavis.(2011). Synthesis of Rhodamines from Fluoresceins Using Pd-Catalyzed CN Cross-Coupling. *Organic Letters*. 13 (24), p6354-6357.

[117]J. B. Grimm and L. D. Lavis.(2011). Synthesis of Rhodamines from Fluoresceins Using Pd-Catalyzed CN Cross-Coupling. *Organic Letters*. 13 (24), p6354-6357.

[118] X. Wu and L. Hu. (2007). Efficient Amidation from Carboxylic Acids and Azides via Selenocarboxylates: Application to the Coupling of Amino Acids and Peptides with Azides. *Journal of Organic Chemistry*. 72, p765-774.

[119]K. V. Kutonova, M. E, Trusova, P, S, Postnikov, V. D. Filimonov and J. Parello.(2013). A Simple and Effective Synthesis of Aryl Azides via ArenediazoniumTosylates. *Synthesis*.45, p2706-2710.

[120] H. C. Kolb, M. G. Finn and K. B. Sharpless (2001) Click Chemistry: Diverse Chemical Function from a Few Good Reactions, Angew. Chem. Int. Ed., 40, p2004-2021.

[121]S. Bräse, C. Gil, K. Knepper and V. Zimmermann. (2005) Organic Azides: An Exploding Diversity of a Unique Class of Compounds, Angew. Chem. Int. Ed., 44, p5188-5240.

[122] X. Wu and L .Hu. (2011). A novel high-yield synthesis of aminoacyl p-nitroanilines and aminoacyl 7-amino-4-methylcoumarins: Important synthons for the synthesis of chromogenic/ fluorogenic protease substrates. *Beilstein J. Org. Chem*. 7, p1030-1035.

[123]A. Krief. (1995). Selenium. In: E. W. Abel, F. G. A. Stone and G. Wilkinson. *Comprehensive Organometallic Chemistry II*. Great Britain: Elsevier Science. p519.

[124]B. S. Furniss, A. J. Hannaford, P. W. G. Smith and A. R Tatchell. (1989). *Vogel's textbook of practical organic chemistry*. 5th ed. England: Longman Scientific and Technical. p452.

[125]A. Krief and L. Hevesi (1988). *Organoselenium Chemistry I: Functional Group Transformations*. Berlin: Springer-Verlag. p20.

[126]L. Wei, Z. Zhu, Y. Li, L. Yi and Z. Xi.(2015). A highly selective and fast-response fluorescent probe for visualisation of enzymatic hydrogen selenide production in vitro and living cells. *Chem Comm*. 51, p10463-10466.

[127]K. A. Cupp-Sutton and M. T. Ashby.(2016). Biological Chemistry of Hydrogen Selenide. *Antioxidants*. 5 (4), p1-18.

[128]J. Bjerrum, et al. Stability Constants, Chemical Society, London, 1958.pK value quoted from compilation produced in pKa Data by W.P. Jencks, F.H. Westheimer and R. Williams.

[129]P. Bhattacharyya and D. Woollins. (2001). Selenocarbonyl synthesis using Woollins reagent. *Tetrahedron Letters*. 42 (34), p5949-5951.

[130]X. Wu and L. Hu. (2005). Amide bond formation from selenocarboxylates and aromatic azides.*Tetrahedron Letters*. 46 (48), p8401-8405.

[131]P. G. M. Wuts and T. W. Greene. (2007). *Greene's Protective Groups in Organic Synthesis*. 4th ed. New Jersey: John Wiley and sons. p826-827.

[132]A. K. Pathak, V. Pathak, L. E. Seitz, K. N. Tiwari, M. S. Akhtar and R. C. Reynold. (2001). A facile method for deprotection of trityl ethers using column chromatography.*Tetrahedron Letters*. 42, p7755-7757.

[133]P. G. M. Wuts and T. W. Greene.(2007). *Greene's Protective Groups in Organic Synthesis*. 4th ed. New Jersey: John Wiley and sons. p826-827.

[134]T. R. Sweeney, N. Roqué-Rosell, J. R. Birtley, R. J. Leatherbarrow, S. Curry. (2007). 1. Structural and Mutagenic Analysis of Foot-and-Mouth Disease Virus 3C Protease Reveals the Role of the β-Ribbon in Proteolysis. *Journal of Virology*.81 (1), p115-124.

[135]S.Curry, N.Roqué-Rosell, T.R.Sweeney, P.A.Zunszain, R.J.Leatherbarrow. (2007). Structural analysis of foot-and-mouth disease virus 3C protease: A viable target for antiviral drugs? *Transactions* 35 (Pt 3), p594-8.

[136]F. H. Niesen, H. Berglund and M. Vedadi. (2007). The use of differential scanning fluorimetry to detect ligand interactions that promote protein stability. *Nature Protocols*. 2 (9), p2122-p2212.

[137]J. R. Birtley, S. R. Knox, A. M. Jaulent, P. Brick, R. J. Leatherbarrow, and S. Curry. (2004). Crystal Structure of Foot-and-Mouth Disease Virus 3C Protease New insights into catalytic mechanism and cleavage specificity. *The Journal of Biological Chemistry*. 280 (12), p11520-11527.

[138]G. Y. Shinowara. (1966). Human thrombin and fibrinogen the kinetics of their interaction and the preparation of the enzyme.*Biochimica et Biophysica Acta (BBA) - Enzymology and Biological Oxidation*. 113 (2), p359-374.

[139]S. K. Grant, J. G. Sklar and R. T. Cummings. (2002). Development of Novel Assays for Proteolytic Enzymes Using Rhodamine-Based Fluorogenic Substrates. *Journal of Biomolecular Screening*. 7 (6), p531-540.

[140]J. B. Grimm and L. D. Lavis.(2011). Synthesis of Rhodamines from Fluoresceins Using Pd-Catalyzed CN Cross-Coupling.*Organic Letters*.13 (24), p6354-6357.

[141]J. R. Birtley, S. R. Knox, A. M. Jaulent, P Brick, R. J. Leatherbarrow and S. Curry.(2005). Crystal Structure of Foot-and-Mouth Disease Virus 3C Protease NEW INSIGHTS INTO CATALYTIC MECHANISM AND CLEAVAGE SPECIFICITY. *Journal of Biological Chemistry*. 280, p11520-11527.

[142]P.A. Zunszain, S. R. Knox, T. R.Sweeney, J. Yang, N. Roqué-Rosell, G. J. Belsham, R. J. Leatherbarrow, S. Curry. (2010). Insights into Cleavage Specificity from the Crystal Structure of Foot-and-Mouth Disease Virus 3C Protease Complexed with a Peptide Substrate. *Journal of Microbiology*. 395 (2), p375-389.

[143] L. Bywaters and A. Legresley. (2020). Synthesis and Spectral Properties of Novel Singapore Green Analogues for Protease Detection. *Nature Research*. 10 (259).

[144] L. Bywaters and A. Legresley. (2017). Synthetic scale-up of a novel fluorescent probe and its biological evaluation for surface detection of Staphylococcus aureus. *Molecular and Cellular Probes*. 36, 1-9.

[145]Y. H. Ahn, J.S. Lee and Y.T Chang (2007). Combinatorial Rosamine Library and Application to in Vivo Glutathione Probe. *Journal of the American Chemical Society*. 129 (15), 4510 - 4511.

[146] K. V. Kutonova, M. E. Trusova, P. S. Postnikov, V. D. Filimonov and J. Parello. (2013). A Simple and Effective Synthesis of Aryl Azides via Arenediazonium Tosylates. *Synthesis*.45, p2706-2710.

[147] M. K. Thorson, T. Majtan, J. P. Kraus, A. M. Barrios. (2013). Identification of cystathionine β-synthase inhibitors using a hydrogen sulfide selective probe.. *Angewandte Chemie (International ed. in English)*. 52 (17), p4641-4644.